

Double Layer Relaxation in Colloids

CENTRALE LANDBOUWCATALOGUS



0000 0426 3246

Promotor: dr. J. Lyklema
hoogleraar in de fysische chemie, met bijzondere
aandacht voor de grensvlak- en kolloidchemie

Co-promotor: dr. H. P. van Leeuwen
universitair hoofddocent bij de vakgroep Fysisische en
Kolloidchemie

NN 08201, 1571

Johan Kijlstra

Double Layer Relaxation in Colloids

Proefschrift

ter verkrijging van de graad van
doctor in de landbouw- en milieuwetenschappen
op gezag van de rector magnificus,
dr. H. C. van der Plas,
in het openbaar te verdedigen
op dinsdag 15 december 1992
des namiddags te vier uur in de aula
van de Landbouwuniversiteit te Wageningen

CIP-GEGEVENS KONINKLIJKE BIBLIOTHEEK, DEN HAAG

Kijlstra, Johan

Double layer relaxation in colloids / Johan Kijlstra.-
[S.l.: s.n.].-11l.

Proefschrift Wageningen.- Met lit. opg.- Met
samenvatting in het Nederlands.

ISBN 90-5485-045-0

Trefw.: colloïdchemie.

BIBLIOTHEEK
LANDBOUWUNIVERSITEIT
WAGENINGEN

STELLINGEN

I

Het verschijnsel van 'oppervlaktegeleiding binnen het afschuifvlak' heeft een belangrijke invloed op de elektrokinetische eigenschappen van een grote groep kolloiden. Enkel door combinatie van zulke eigenschappen kan men deze invloed vaststellen en de karakteristieke dubbellaagparameters, waaronder de ζ -potentiaal, bepalen.

Dit proefschrift, hoofdstuk 3-5.

II

Voor licht geaggregeerde kolloiden geven schattingen van de deeltjesstraal op basis van de frequentie-afhankelijkheid van de geleidbaarheid van het kolloïd een beter resultaat dan die op basis van de frequentie-afhankelijkheid van de permittiviteit.

Dit proefschrift, hoofdstuk 4.

III

De interaktietijd tussen twee kolloïdale deeltjes neemt af als de hoogte van de energiebarrière, die de deeltjes moeten overwinnen om te aggereren, toeneemt.

Dit proefschrift, hoofdstuk 7.

IV

Met hun theory voor de elektroforese van biologische cellen voorspellen Ohshima en Kondo dat onder bepaalde omstandigheden de elektroforetische beweeglijkheid ongelijk aan nul kan zijn bij een oppervlaktepotentiaal gelijk aan nul. Deze voorspelling is enkel het gevolg van hun ongebruikelijke definitie van het oppervlak, dat zij buiten het afschuifvlak plaatsen.

H. Ohshima and T. Kondo, Biophysical Chemistry, 39 (1991) 191-198.

V

De discussie over het mechanisme van de biologische aktiviteit van toxische stoffen, aangaande de vraag of deze een invloed uitoefenen op de lipid-structuur van het membraan dan wel op de eigenschappen van de membraaneiwitten, gaat voorbij aan de spontane vorming van het complete membraan.

N. P. Franks and W. R. Lieb, Nature 300 (1982) 487-493.

A Nelson et al., Biochimica et Biophysica Acta 1021 (1990) 205-216.

VI

De relatie tussen kracht, dipoolmoment en elektrisch veld, die gebruikt wordt om elektro-rotatie (1) en dielektoforese (2) van cellen en bacteriën te verklaren, is alleen van toepassing op systemen in het iso-elektrisch punt of op systemen met een zeer lage geleiding van het oplosmiddel.

1 W. M. Arnold and U. Zimmermann, *J. Electrostatics* 21 (1988) 151-191.

2 K. V. I. S. Kaler and T. B. Jones, *Biophys. J.* 57 (1990) 173-182.

VII

Een GAA-rijke sequentie, aanwezig in het alternatieve exon, maakt deel uit van een algemeen positief cis-acting element in de alternatieve processing van pre-mRNA's.

C. C. M. van Oers et al. (1992), *in preparation*.

VIII

De viering van 'Orange Day' door protestanten in Noord-Ierland is geen kompliment aan het Nederlandse volk.

IX

De opschudding die recentelijk werd veroorzaakt door de oprichting van islamitische scholen in Nederland onderschrijft nog eens extra de oude leus 'Onverdeeld naar het Openbaar Onderwijs'.

X

Het feit dat veel Nederlanders denken wijn te moeten drinken bij het nuttigen van een pizza geeft blijk van hun gebrekkige kennis van de Italiaanse cultuur.

XI

Bij balsporten geeft een statisch veld doorgaans aanleiding tot een oscillerende respons.

Stellingen behorende bij het proefschrift "**Double Layer Relaxation in Colloids**".

Johan Kijlstra, Wageningen, 15 december 1992.

Chapter 3: accepted for publication in *Journal of the Chemical Society, Faraday Transactions 2* (J. Kijlstra, H. P. van Leeuwen and J. Lyklema).

Chapter 4: submitted for publication in *Langmuir* (J. Kijlstra, H. P. van Leeuwen and J. Lyklema).

Chapter 5: submitted for publication in *Bioelectrochemistry and Bioenergetics* (J. Kijlstra and A. van der Wal).

Chapter 6: *Journal of Colloid and Interface Science* in press (J. Kijlstra).

Chapter 7: submitted for publication in *Journal of Colloid and Interface Science* (J. Kijlstra and H. P. van Leeuwen).

Contents

1 Introduction

General background	1
Dielectric spectroscopy	1
Colloid stability	3
Aim and outline of this study	4
References	5

2 Dielectric Spectrometer for Sols

Abstract	7
Introduction	7
General definitions	9
The instrument	10
Electrical network	11
Data analysis	12
Results	14
Conclusions	19
References	19

3 Effects of Surface Conduction on the Electrokinetic Properties of Colloids

Abstract	21
Introduction	21
Theory	24
General equations	25
Spherical particles	29
Induced dipole coefficient and complex conductivity	32
Results and discussion	33
Effects of surface conduction	35

Comparison between theory and experiment	39
Conclusions	43
Appendix A	43
Appendix B	44
References	45

4 Low-frequency Dielectric Relaxation of Hematite and Silica Sols

Abstract	47
Introduction	47
Experimental section	50
Theoretical background	52
Kramers-Kronig relations	54
Classical electrokinetic theory	55
Surface conduction	57
Fitting procedures	58
Results and discussion	59
Accuracy and reproducability	60
General features	63
Comparison between $\Delta\epsilon_r$ and $\Delta\sigma$	64
Influence of aggregates	67
Comparison with mobilities	71
Conclusions	75
References	76

5 Electrokinetic Properties of Bacterial Suspensions

Short communication

Introduction	79
Results and discussion	80
References	84

6 Polarizability Effects in the Electrostatic Repulsion between Charged Colloidal Particles

Abstract	85
Introduction	85
Theory	88
Derjaguin approximation	92
Results and conclusions	93
References	96

7 Surface Charge Relaxation during Coagulation

Abstract	99
Introduction	99
Basic principles	102
Smoluchowski-Fuchs theory	103
Interaction energy	105
Double layer dynamics	109
method 1	110
method 2	113
Results and discussion	113
Simple statistical analysis	117
Conclusions	120
Appendix A	120
Appendix B	121
References	123
Summary	125
Samenvatting	129
Curriculum Vitae	135
Nawoord	137

Chapter 1

Introduction

General background

In most hydrophobic colloids, the particles carry a charge. This charge, which often is largely located at the surface, will be compensated for and screened by ions in solution, giving rise to an electrical double layer. The existence of such a double layer has important consequences for the sol properties. For example, it affects the properties of the particles as adsorbent and their stability against coagulation, two well-known phenomena. Therefore, it is not surprising that much attention has been paid to the investigation of the double layer structure. The vast majority of these studies involved double layers at rest, i.e. the equilibrium structure was studied. However, when the double layer is perturbed, its structure will change. Such perturbations occur under dynamic conditions, for example when colloidal particles coagulate or under conditions of electrokinetic experiments. These experiments are devised to measure the response of a colloid to an externally applied field and they are widely used to characterize colloids, especially microelectrophoresis. Coagulation in relation to colloid stability is of course important for their applications. Obviously, perturbations of the equilibrium double layer structure lead to relaxation processes. To understand the dynamic properties of a sol, a basic knowledge of these processes and the pertaining relaxation times is required.

Dielectric spectroscopy

One approach to study relaxation of double layers around charged particles is to apply dielectric spectroscopy to dilute colloids. This technique involves the measurement of the dielectric response of a sol

as a function of the frequency of an applied electric field. The dielectric response represents the conductive and the capacitive parts of the electric current flowing through the sol. As mentioned, the electric field will distort the ionic atmospheres around the particles so that the double layers become polarized. The extent of this polarization can be quantified by an induced dipole moment, which, in its turn, can be relatively simply related to the dielectric response (1, 2). The induced dipole moment itself is very sensitive to the ionic current flows around the particle, which are strongly dependent on the equilibrium double layer structure. Therefore, dielectric spectroscopy in the proper frequency range enables us to study relaxation processes in the double layer as well as its equilibrium structure.

Obviously, phenomena such as electrophoresis, static conductivity and dielectric response are related and therefore they share a common physical basis. In order to describe these phenomena, one has to solve the equations which govern the flow of ions and solvent around the particle. Solutions of these equations, which encompass the polarization of the double layer, have been given by a number of people (1-9). Dielectric measurements in the low-frequency range of approximately $10^2 - 10^5$ Hz have been performed on latices by Springer et al. (10). Comparison of their results with the theory of Dukhin et al. (1, 4) did not show good agreement in all respects; especially the experimental dielectric increment was much too high as compared to theoretical expectation (6, 11). The theory of Dukhin et al. is based on polarization of the diffuse part of the double layer and more recent (numerical) work has shown that it is basically correct (5, 9). Consequently, Lyklema et al. (11) concluded that latices are not ideal model colloids. Recently, the anomalous dielectric behaviour of latices has been confirmed by the work of Rosen and Saville (12, 13). They compared their dielectric data to electrophoretic results and again, large inconsistencies were found. Similar inconsistencies were also obtained in the comparison between electrophoresis and static conductivity data (14, 15).

The comparisons between different electrokinetic properties provide good tests of the classical theories, which are based on the polarization of the diffuse part of the double layer *only*. The corresponding models have just one experimental unknown parameter:

the ζ potential at the plane of shear. Therefore, if these models apply, different electrokinetic properties should yield the same value for the ζ potential. However, the interrelationships between the different electrokinetic quantities will change if the non-diffuse part of the double layer contributes to the relaxation processes in the double layer. One of these processes that has to be considered is surface conduction, as far as it occurs behind the slip plane. Indeed, the abovementioned investigations indicate that this type of conduction also occur in latices.

Colloid stability

In Fuchs' theory for the stability of colloids, the coagulation rate is determined by the interaction energy between two particles (16). This energy can be calculated with the DLVO (Derjaguin-Landau-Verwey-Overbeek) theory, in which it is described as the net result of attractive Van der Waals and repulsive electrostatic forces. The calculation of the electrostatic forces is usually based on equilibrium thermodynamics. However, coagulation of colloids is a dynamic process. During an encounter between particles, double layer overlap occurs. Since the equilibrium double layer structure changes with the interparticle distance, the double layer will tend to adjust itself during the collision. Therefore, the justification of the use of equilibrium thermodynamics in calculating the electrostatic force depends on the time scales of the relevant relaxation processes in the double layer relative to that of an encounter. According to Overbeek (17) and Lyklema (18), the latter is much larger than the relaxation time of most of the relaxation processes in the double layer. Consequently, these processes can be regarded as being in equilibrium during the encounter. However, this is not necessarily true for the adjustment of the surface charge density. Estimates for the corresponding relaxation times vary by orders of magnitude, depending on the type of colloid, and they can be well of the same order or much larger then the time scale of interaction. The first attempts to incorporate the disequilibration of the double layer into the theory of slow coagulation has been made by Dukhin and Lyklema (19, 20). They developed a perturbation theory which is appropriate only for small deviations from the equilibrium structure.

Aim and outline of this study

In the light of the difficulties involved in interpreting dielectric and other electrokinetic properties of latices, the availability of low-frequency dielectric data on well-defined inorganic colloids is highly desirable. Preferably, these data should be supplemented by those obtained electrophoretically. In principle, the influence of surface conduction on the electrokinetic properties can then be distinguished. In connection with this, the present study will be aimed first at achieving the following objectives:

- (i) construction of a dielectric spectrometer, suitable for obtaining sufficiently accurate data in the low-frequency range,
- (ii) theoretical investigation of the influence of surface conduction on electrokinetic properties and
- (iii) experimental investigation of the dielectric behaviour of inorganic colloids, comparison with electrophoretic behaviour and theory.

Regarding (iii), experiments will be performed with hematite and silica colloids. For these systems, recipes are available for the synthesis of homodisperse (nearly) spherical particles in sufficiently large amounts. The advantage of having spherical particles is that the theories are best developed for that particular geometry. Point (i) will be dealt with in **chapter 2**, (ii) in **chapter 3** and (iii) in **chapter 4**. In **chapter 5**, it will be shown how the experimental and theoretical framework developed in the previous chapters can be of help in elucidating the electric properties of bacterial surfaces.

The second aim of this thesis is to investigate the occurrence of transient deviations in the equilibrium structure of the double layer during a particle interaction. As mentioned, the theory of Dukhin and Lyklema is appropriate only for small deviations from the equilibrium structure. Since the magnitude of these deviations is generally expected to vary in a wider range, it is of interest to develop a more rigorous approach. The last two chapters will be devoted to colloid stability. **Chapter 6** discusses the influence of the polarizability of the particles themselves on their (equilibrium) electrostatic interaction. This can be of relevance when during a particle encounter the double layer is

disequilibrated, giving rise to a potential variation along the surface and, hence, an electric field inside the particles. The influence of transient deviations from the equilibrium surface charge density during the interaction of colloidal particles will be discussed in **chapter 7**.

References

- (1) Dukhin, S. S. and Shilov, V. N., "Dielectric Phenomena and the Double Layer in Disperse Systems and Polyelectrolytes", Wiley, New York, 1974.
- (2) DeLacey, E. H. B. and White, L. R., *J. Chem. Soc., Faraday Trans. 2* **77**, 2007 (1981).
- (3) Wiersema, P. H., Loeb, A. L. and Overbeek, J. T. G., *J. Colloid Interface Sci.* **22**, 78 (1966).
- (4) Dukhin, S. S. and Derjaguin, B. V., in "Surface and Colloid Science" (E. Matijevic, Ed.), p. 273. Wiley, New York, 1974.
- (5) Fixman, M., *J. Chem. Phys.* **78**, 1483 (1983).
- (6) Lyklema, J., Dukhin, S. S. and Shilov, V. N., *J. Electroanal. Chem.* **143**, 1 (1983).
- (7) O'Brien, R. W. and White, L. R., *J. Chem. Soc., Faraday Trans. 2* **74**, 1607 (1978).
- (8) O'Brien, R. W., *J. Colloid Interface Sci.* **81**, 234 (1981).
- (9) O'Brien, R. W. and Hunter, R. J., *Canad. J. Chem.* **59**, 1878 (1981).
- (10) Springer, M. M., Korteweg, A. and Lyklema, J., *J. Electroanal. Chem.* **153**, 55 (1983).
- (11) Lyklema, J., Springer, M. M., Shilov, V. N. and Dukhin, S. S., *J. Electroanal. Chem.* **198**, 19 (1986).
- (12) Rosen, L. A. and Saville, D. A., *J. Colloid Interface Sci.* **149**, 542 (1992).
- (13) Rosen, L. A. and Saville, D. A., *Langmuir* **7**, 36 (1991).
- (14) Zukoski IV, C. F. and Saville, D. A., *J. Colloid Interface Sci.* **107**, 322 (1985).
- (15) O'Brien, R. W. and Perrins, W. T., *J. Colloid Interface Sci.* **99**, 20 (1984).
- (16) Fuchs, N., *Z. Physik* **89**, 736 (1934).
- (17) Overbeek, J. T. G., *J. Colloid Interface Sci.* **58**, 408 (1977).
- (18) Lyklema, J., *Pure & Appl. Chem.* **52**, 1221 (1980).
- (19) Dukhin, S. S. and Lyklema, J., *Langmuir* **3**, 94 (1987).
- (20) Dukhin, S. S. and Lyklema, J., *Faraday Discuss. Chem. Soc.* **90**, 261 (1990).

Chapter 2

Dielectric Spectrometer for Sols

Abstract

A description is given of a four-electrode dielectric spectrometer, designed to measure the complex admittance (or dielectric response) of sols in the frequency range of approximately 500 Hz to 500 kHz. The instrument consists of a dielectric cell connected to a signal processing unit, both home-built, and a commercial automatic frequency response analyzer. The four-electrode design is developed to avoid problems related to electrode polarization and, at the same time, to enable the use of the automatic frequency response analyzer. The device is suitable for fast and accurate data acquisition, the measurement of one complete spectrum taking a few minutes only. The home-built components of the instrument and the data analysis are described in detail. The present set-up is especially made to measure relatively small differences between the complex admittances of a sample and that of a blank. Several tests of the instrument show that the obtained data are reliable.

Introduction

This chapter contains a concise description of the experimental set-up we have used to measure the complex admittance (or dielectric response) of aqueous sols. The contents are restricted to relevant technical information and no attempt has been made to give a comprehensive historical overview of the developments in this area.

If a sol is subjected to an alternating electric field, then a current will flow through it. Generally, this current will not run in phase with the applied field. It is well accepted that the electric properties of a conducting solution can be described by an equivalent circuit of an resistance R parallel placed to a capacitance C (1, 2). However, a sol does not behave like an ideal RC circuit; the values of its components will vary with the frequency. This is called dielectric dispersion and it is

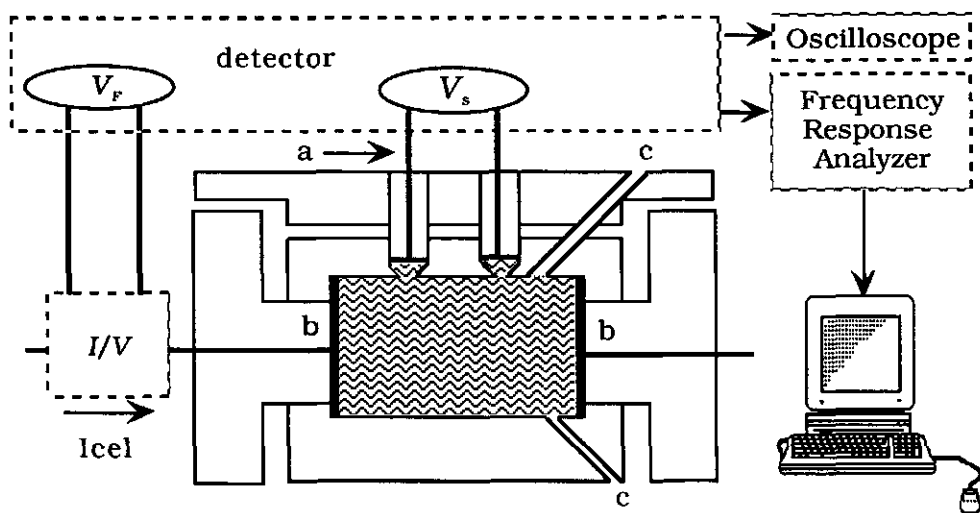


Figure 1. The instrument. a sensor electrodes, b current supply electrodes, c filling openings.

related to relaxation processes inside and outside the electric double layer associated with the colloidal particles. In subsequent chapters, it will be shown that these processes cause a dispersion at frequencies less than 1 MHz, the so-called low-frequency dielectric dispersion. Its characteristic relaxation frequency is determined by the particle size and the diffusion coefficient of the ions in solution. The aim of the newly developed instrument is to accurately measure this low-frequency dispersion of dilute sols.

The measurement of the dielectric behaviour of dilute suspensions is not trivial. First, the signal-to-noise ratio is inherently low since the suspension is dilute. Hence, changes in the response due to temperature fluctuations should be minimized by temperature control down to $\pm 0.05^\circ\text{C}$. Furthermore, as will be shown, the unfavourable ratio between the resistive and the capacitive current requires an extremely sensitive detector to accurately determine both components. Second, there are the interfering problems related to electrode polarization. This especially occurs at frequencies lower than 1 kHz. Previously, two-electrode set-ups have been used in combination with a manual impedance bridge (1-3). However, in this way, one does not measure the impedance of the suspension, but the impedance of the complete

cell, including a contribution due to electrode polarization. By measuring the impedance as a function of the electrode distance, one could separate the suspension impedance from the electrode impedance. Hence, the major disadvantage of this method is that it is very laborious and time-consuming.

In the four-electrode set-up, problems related to electrode polarization have vanished since the electrode functions are separated; two electrodes are used as current suppliers, while the other two are sensor electrodes. The sensor electrodes are used to measure the voltage drop in the solution. This voltage measurement is not complicated by electrode polarization since no current passes through these electrodes. However, until recently, the four-electrode set-up has hardly been used, due to the complexity of the required electronic circuits. The present instrument shows how these problems can be solved by the use of new precise electronic components. Similar instruments, which also have been used to study sols, have been discussed in literature recently (4, 5). Previously, four-electrode set-ups have also been used to investigate the dielectric behaviour of solutions of polyelectrolytes (6-11), for a review see ref. (12).

General definitions

The dielectric spectrometer is designed to measure a voltage drop V_s in the solution and the current I_{cell} passing through the cell. The admittance Y_s can then be written as

$$Y_s = \frac{I_{cell}}{V_s} = G_s + i\omega C_s \quad [1]$$

with G_s the conductance and C_s the capacitance. The admittance Y_s is the inverse of the complex impedance Z_s and linearly related to the complex conductivity K^*

$$Y_s = \frac{1}{Z_s} = cK^* \quad [2]$$

with c the cell constant and

$$K^* = \sigma + i\omega\epsilon_0\epsilon_r \quad [3]$$

where σ is the conductivity, ϵ_0 is the permittivity of vacuum and ϵ_r the relative permittivity. For a pure electrolyte solution, these three parameters are considered as frequency-independent constants in the frequency range of interest (1). The phase angle δ is defined by

$$\tan \delta = \frac{G_s}{\omega C_s} = \frac{\sigma}{\omega\epsilon_0\epsilon_r} \quad [4]$$

The Instrument

A general picture of the instrument is given in Figure 1. The cylindrical cell is made of transparent polycarbonate and has four electrodes, two current supply electrodes and two sensor electrodes. The circular supply and sensor electrodes have radii of 1.0 cm and 0.3 mm, respectively, and the total volume of the cell is approximately 16 cm³. The sensor electrodes are placed in a conical hole in the wall of the cell. The opening in the cell wall, the sensor opening, has a diameter of approximately 2 mm. All electrodes are made of blank platinum foil; blackening the electrodes had no effect on the results. The current I_{cell} is determined with an I/V converter, which produces the voltage drop V_F . The voltage drop V_s between the sensor electrodes and V_F are treated by the detector. The resulting signals are fed into the frequency response analyzer (Solartron 1255 HF Frequency Response Analyzer), which is connected to a personal computer for controlling the experimental procedure, data storage and analysis. An oscilloscope is used to calibrate the instrument and to monitor the process. The function of the detector is crucial, because the response analyzer is not capable to directly measure V_F and V_s sufficiently accurately. This is due to the unfavourable phase angle of δ of sols (very close to 90 degrees).

Two openings in the cell wall enable filling of the (flow-through) cell from either of the two storage bottles by a tube pump. Usually, one storage bottle contains the suspension, the other the blank solution, i.e. an electrolyte solution with the pH and ionic strength adjusted to that of the sample. Two taps allow the cell to be alternatingly filled with the

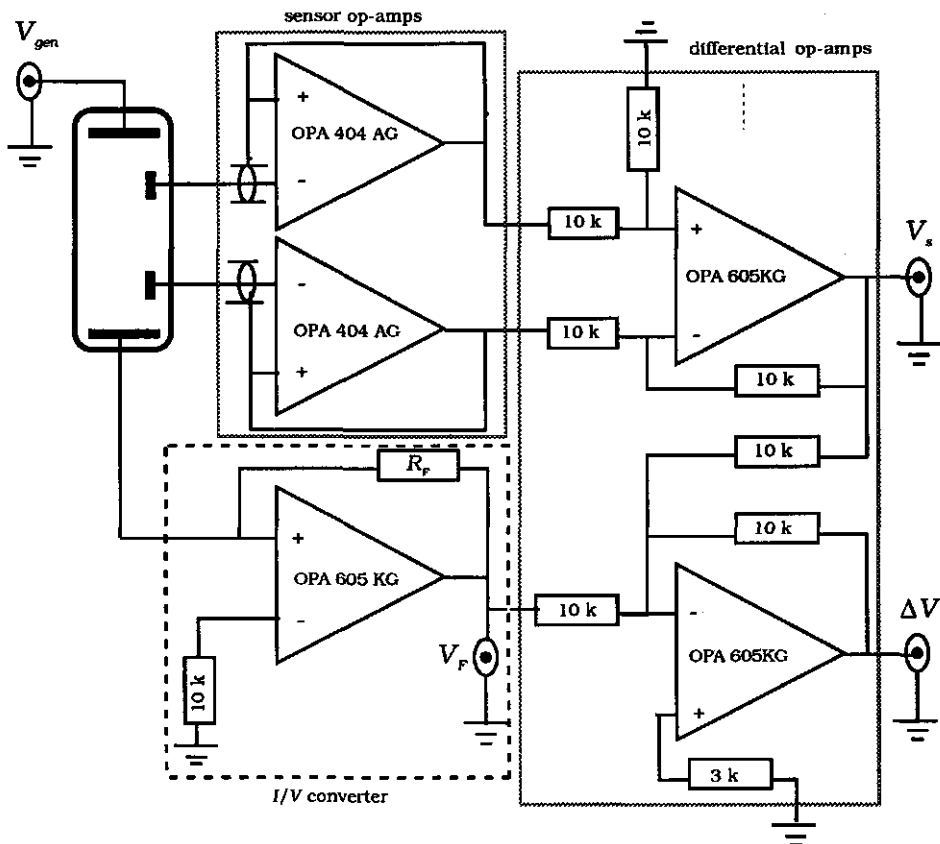


Figure 2. Simplified electronic scheme of the detector. Explanation in the text.

sample and blank without changing the set-up otherwise. If desired, the liquid in the storage bottles can be mixed by a stirrer and purged with nitrogen. The pH can be measured by introducing a combined glass electrode (Ingold) through an opening in the cap of the bottle. The cell and storage bottles are placed in a temperature controlled air stream (usually 25.00 ± 0.05 °C).

Electrical network

The function of the detector, including the *I/V* converter, is to create a voltage difference $\Delta V = V_s - V_F$, which can be handled by the response analyzer. The voltages ΔV and V_F are fed to the analyzer.

which determines the ratio $\Delta V/V_F$. A simplified block diagram of the detector is given in Figure 2. The feedback resistance R_F is manually adjustable. The I/V converter has an optimal phase response when $R_F = R_s$ and its output V_F equals $I_{cel}R_F$. Therefore, by perfectly matching R_F to the resistance R_s of the suspension, the voltage ratio $\Delta V/V_F$ becomes, at not too high frequencies when $\omega C_s R_s \ll 1$, purely imaginary. In practice, the matching will be less perfect. Nevertheless, the real and imaginary parts of $\Delta V/V_F$ will be of the same order, enabling accurate measurement by the response analyzer. Consequently, the complex conductivity K^* follows from $\Delta V/V_F$ and the value of the matched resistance R_F .

To minimize residual capacitance effects, the detector is placed directly on top of the cell. The two sensor operational amplifiers OPA 404 AG have a high input impedance ($10^{10}\text{ k}\Omega$) and low input capacitance (less than 1 pF). Both op-amps are emitter followers and placed in one package. Therefore, drift in the response of these op-amps due to temperature fluctuations is automatically compensated for. One differential amplifier is used to subtract the signal of one sensor amplifier from the other, giving V_s . The second differential amplifier subtracts the output of the I/V converter V_F from V_s , giving ΔV . All resistances used have a low temperature coefficient. Some of them are matched within 1 promille, in order to ensure that the differential amplifiers have a gain of exactly 1. To measure accurately in the high-frequency range, all op-amps must be very fast in reaction (slew rate $35\text{ V}/\mu\text{s}$), since phase accuracy is crucial.

Data analysis

The simplified equivalent electronic circuit of the dielectric cell for data analysis is shown in Figure 3. The sensor electrodes detect only the impedance of the solution between them. The remaining part of the impedance of the dielectric cell, including the contribution of the electrodes, is represented by the impedances Z_{el} . The capacitance C_{ex} is optional but useful in the analysis. First, it illustrates the influence of stray capacitances. Second, a known capacitance C_{ex} can be included into the circuit in order to test the electronic design. The applied

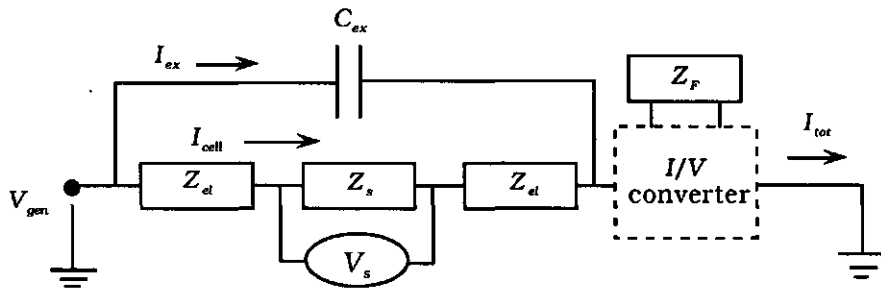


Figure 3. Simplified electrical representation of cell for data analysis

generator voltage is designated as V_{gen} and I_{ex} is the current through C_{ex} . The different current densities I_{cell} , I_{ex} and I_{tot} are indicated in Fig. 3.

Given the values for ΔV and V_F , ϵ and σ can be computed as follows. Application of Kirchoff's laws gives

$$\Delta V = V_s - V_F = (I_{tot} - I_{ex})Z_s - I_{tot}Z_F \quad [5]$$

since $V_s = I_{cel}Z_s$. We have also used $V_F = I_{tot}Z_F$, since the feedback resistance R_F might have a small capacitance C_F as well. Hence, the impedance Z_F is defined by

$$\frac{1}{Z_F} = \frac{1}{R_F} + i\omega C_F \quad [6]$$

By taking the ratio $\Delta V/V_F$, Z_s can be written as

$$Z_s = Z_F \left(\frac{\Delta V}{V_F} + 1 \right) \left(1 - i\omega C_{ex} Z_F \frac{V_{gen}}{V_F} \right)^{-1} \quad [7]$$

where we have also used $I_{ex} = i\omega C_{ex} V_{gen}$.

The inverse of the impedance Z_s gives the admittance Y_s

$$Y_s = \frac{1}{Z_s} = \frac{1}{Z_F} \left(\frac{\Delta V}{V_F} + 1 \right)^{-1} \left(1 - i\omega C_{ex} Z_F \frac{V_{gen}}{V_F} \right) \quad [8]$$

To separate Y_s into its real and imaginary components, it is convenient to define

$$\left(\frac{\Delta V}{V_F} + 1 \right)^{-1} = r' + i r'' \quad [9]$$

and

$$\frac{V_{gen}}{V_F} = v' + i v'' \quad [10]$$

If we substitute Eqs [9] and [10] into Eq. [8], then we obtain the following equations for C_s and G_s

$$C_s = \frac{1}{\omega R_F} r'' + C_F r' - C_{ex} (v' r' - v'' r'') \quad [11]$$

and

$$G_s = \frac{1}{R_F} r' - \omega C_F r'' + \omega C_{ex} (v'' r' + v' r'') \quad [12]$$

Hence, the admittance is expressed in measurable quantities and ϵ and σ immediately follow from the above equations once the cell constant is known. Note that if the capacitance C_{ex} could be only placed parallel to impedance Z_s instead of parallel to the sum of Z_s and Z_{el} , then by definition $v' r' - v'' r'' = 1$ and $v'' r' + v' r'' = 0$.

Results

The electrical network has been tested using electronic RC circuits instead of the dielectric cell. These tests proved that the electronic design worked excellently. Furthermore, tests have been performed with the dielectric cell, containing pure electrolyte and suspensions with different volume fractions of the particles. The applied voltage was 0.5V, low enough to avoid electrolysis, resulting in a field strength of approximately 13V/m. The cell constant c has been determined with electrolyte solutions of known conductivity. One complete frequency scan from 90 Hz til 500 kHz took less than about 2

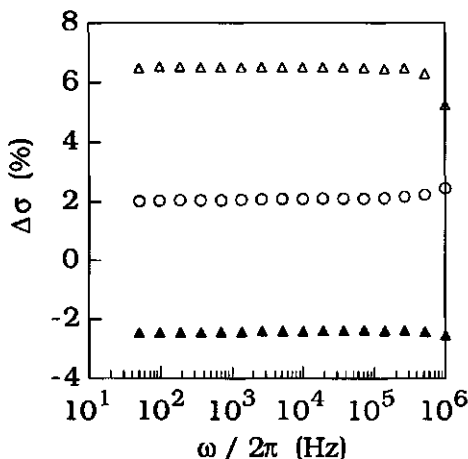


Figure 4. Relative conductivity difference $\Delta\sigma_{rel}$ as function of frequency, explanation see text. (○) $\sigma_1 \approx 1.5 \cdot 10^{-2}$, (△) $\sigma_1 \approx 2 \cdot 10^{-3}$, (▲) $\sigma_1 \approx 4 \cdot 10^{-2}$, with σ_1 in S/m.

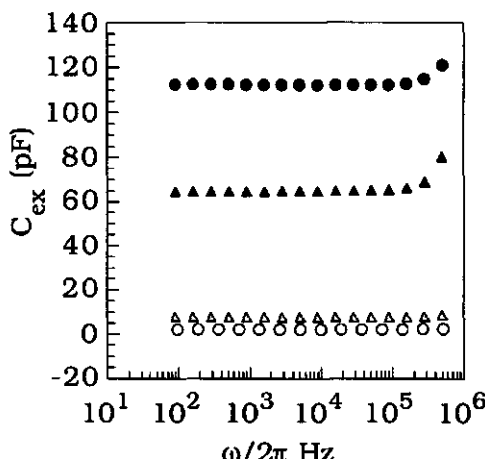


Figure 5. Measured value for different values external capacitance C_{ex} as function of frequency, explanation see text. C_{ex} in pF: (○) 2 pF, (△) 8, (▲) 65, (●) 113.

minutes and therefore problems related to temperature drift and, hence, conductivity drift could be avoided.

Our primary aim is to measure the dielectric dispersion of sols. Therefore, it is of interest to see if reliable difference spectra could be obtained. Such a spectrum is the difference between the spectrum of a sol and that of a blank, for example a suitable electrolyte solution. Hence, the spectrum of the blank functions as the baseline. This method could be tested by changing either the permittivity or the conductivity by a certain frequency-independent amount and measuring the change in the response. For the conductivity this can be easily done by adjusting the electrolyte concentration. Figure 4 displays the relative difference $\Delta\sigma_{rel}$ in the conductivity for three sets of electrolyte solutions. The $\Delta\sigma_{rel}$ is defined by

$$\Delta\sigma_{rel} = (\sigma_1 - \sigma_2)/\sigma_1(50\text{Hz.})$$

[13]

with the indices indicating the different solutions in each set. The difference between the conductivities of each set is large. In contrast, the relative conductivity difference $\Delta\sigma_{rel}$ of each set is small, being of the same order as found for the relative change of the conductivity of sols versus frequency. The obtained values for $\Delta\sigma_{rel}$ are remarkably constant; only at frequencies larger than 500 kHz do some small deviations occur.

No easy similar test could be carried out for the capacitance. The permittivity of the electrolyte solution can be changed by mixing it with an inorganic liquid. Unfortunately, the conductivity will then also change, affecting the stray effects. Another test is to connect an external capacitance C_{ex} parallel to the cell, as shown in Fig. 3. By measuring the response with and without C_{ex} , its value can be calculated with Eqs. [11] and [12]. This is done for several capacitances C_{ex} placed parallel to the dielectric cell filled with a 1 mM KCl solution. The results are shown in Figure 5. Excellent results are obtained. The calculated value for C_{ex} is perfectly constant at frequencies smaller than 500 kHz, above which again some deviation occurs.

In the frequency range applied, the capacitance and conductivity of a KCl solution ought to be constant (1). Figure 6 shows the response of a KCl solution with a concentration and static conductivity of approximately 1.3 mM and $2 \cdot 10^{-2}$ S/m respectively. The capacitance, estimated on the basis of the geometry of the cell and the permittivity of water, the latter being negligibly different from that of dilute electrolyte solutions (1), is approximately 20 pF. However, Fig. 6 shows a significant frequency dependence of both the capacitance and the conductivity. The frequency dependence of the conductivity became more pronounced with decreasing electrolyte concentration, while the dependence of the capacitance appeared to be sensitive to stray effects, it was a function of the conductivity, pH and size of the sensor openings. These stray effects could be influenced by placing a special guard outside the dielectric cell near the sensor electrodes, see Fig. 6. This guard had no influence on the conductivity results. In conclusion, the present dielectric cell is not suitable to determine absolute values of the permittivity and conductivity.

The results given so far indicate that the present set-up is suitable to measure difference spectra. However, one important condition has to

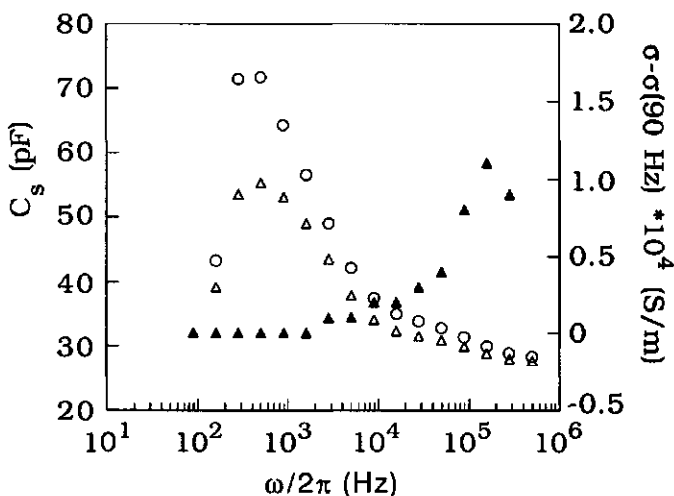


Figure 6. Response dielectric cell filled with KCl solution, static conductivity approximately $2 \cdot 10^{-3}$ S/m. (○) and (△) capacitance for different guards, (▲) conductivity increment $\sigma - \sigma(90\text{Hz})$.

be satisfied: stray effects should be kept under control and must be identical for the blank and the measuring solution. In practice, this is done by matching the conductivities (within 1%) and pH values of the suspension and the blank.

The final test is to measure the difference spectra for a dilute sol as a function of its volume fraction ϕ of the particles. According to the theoretical prediction for dilute suspensions, the dielectric dispersion should be a linear function of ϕ . The dielectric dispersion can be represented by the dielectric increment $\Delta\epsilon_r$, and the conductivity increment $\Delta\sigma$, calculated by

$$\Delta\epsilon_r = \frac{1}{c\epsilon_0} [(C_{s,sol} - C_{s,sol}^{\max}) - (C_{s,blank} - C_{s,blank}^{\max})] \quad [15]$$

and

$$\Delta\sigma = \frac{1}{c} [(G_{s,sol} - G_{s,sol}^{\min}) - (G_{s,blank} - G_{s,blank}^{\min})] \quad [16]$$

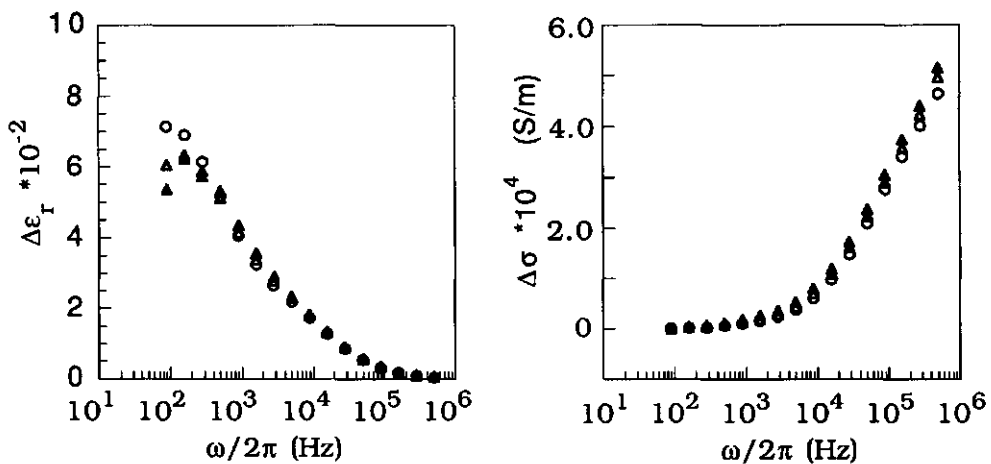


Figure 7. Dispersion of $\Delta\epsilon_r$ and $\Delta\sigma$ for hematite sols in KCl of 3 different volume fractions. $[KCl] \approx 1.3$ mM, $\sigma(90\text{Hz}) \approx 1.9 \cdot 10^{-2}$ S/m and ϕ : (○) 4%, (△) 3%, (▲) 2%. The increments of the last mentioned two sols are recalculated to $\phi=4\%$, see text.

respectively, where the subscripts "sol" and "blank" speak for themselves while the superscripts "min" and "max" refer to the lowest and highest measurement frequency respectively.

Figure 7 shows the increments for a hematite suspension with a volume fraction of approximately 4%. This suspension has been diluted twice and the corresponding results are incorporated into these figures as well. The lowest volume fraction was approximately 2%. Note that the increments of the diluted suspensions are recalculated to the volume fraction of the suspension with $\phi \approx 4\%$. As expected, the three curves in each plot merge, confirming the linear relation between the increments $\Delta\epsilon_r$ and $\Delta\sigma$ and ϕ . Some scatter is observed in $\Delta\epsilon_r$ at low frequencies. This reflects the fact that the baseline is most sensitive to stray effects at low frequencies. Moreover, $\tan\delta$ increases with decreasing frequency, which limits the measurement in the lower frequency range. For example, the value of δ for the most concentrated suspension at 100 Hz is approximately $\delta \approx 89.986^\circ$ ($\tan\delta \approx 4 \cdot 10^3$). The same calculation for the blank gives $\delta \approx 89.998^\circ$ ($\tan\delta \approx 2.5 \cdot 10^4$). Hence,

these values clearly indicate the necessity of high experimental accuracy, especially at high electrolyte concentrations!

The required experimental accuracy increases with growing electrolyte concentration. Therefore it was not possible to study solutions with conductivities higher than that of approximately 2 mM KCl. Obviously, the lowest frequency at which the permittivity ϵ_r can still be measured depends on the response of the suspension itself. Usually, the lower limit of the frequency is located near 500 Hz. Similar measurements have been carried out with latex and silica suspensions too, and in all cases the same linear relation has been found.

Conclusions

A four-electrode dielectric spectrometer has been developed to measure the dielectric dispersion of dilute sols. The instrument is suitable to investigate the dielectric behaviour of sols at frequencies less than 500 kHz. The lower limit of the frequency range is determined by the signal-to-noise ratio and is usually near 500 Hz. The signal-to-noise ratio decreases with the conductivity of the suspension, which is therefore limited to values less than that of approximately 2 mM KCl. Stray effects hamper the measurement of the absolute permittivity and conductivity of the suspensions but they can be eliminated by taking difference spectra. The obtained response for dilute sols is linearly dependent on the volume fraction of the particles, in accordance with theoretical prediction.

References

- (1) Springer, M. M., Ph. D. Thesis, 1979.
- (2) Springer, M. M., Korteweg, A. and Lyklema, J., *J. Electroanal. Chem.* **153**, 55 (1983).
- (3) Blom, J., *J. Phys. E: Sci. Instrum.* **12**, 889 (1979).
- (4) Meyers, D. F. and Saville, D. A., *J. Colloid Interface Sci.* **131**, 448 (1989).
- (5) Sauer, B., Stock, R. S., Lim, K. and Ray, W. H., *J. Appl. Polymer Sci.* **39**, 2419 (1990).
- (6) Berberian, J. G. and Cole, R. H., *Rev. Sci. Instrum.* **40**, 811 (1969).

- (7) Hayakawa, R., Kanda, H., Sakamoto, M. and Wada, Y., *Jap. J. Appl. Phys.* **14**, 2039 (1975).
- (8) Sakamoto, M., Kanda, H., Hayakawa, R. and Wada, Y., *Biopolymers* **15**, 879 (1976).
- (9) Tung, M. S., Molinari, R. J., Cole, R. H. and Gibbs, J. H., *Biopolymers* **16**, 2653 (1977).
- (10) Sakamoto, M., Hayawaka, R. and Wada, Y., *Biopolymers* **17**, 1507 (1978).
- (11) Umemura, S., Sakamoto, M., Hayakawa, R. and Wada, Y., *Biopolymers* **18**, 25 (1979).
- (12) Mandel, M. and Odijk, T., *Ann. Rev. Phys. Chem.* **35**, 75 (1984).

Chapter 3

Effects of Surface Conduction on the Electrokinetic Properties of Colloids

Abstract

To quantify the effects of surface conduction behind the slip plane on the electrokinetic transport properties of colloids, we have extended the thin double layer theory of Fixman for dilute sols of spherical particles. The computations show that it causes the static conductivity and the low-frequency dielectric response of the sol to increase and the mobility of the particles to decrease. Hence, the occurrence of surface conduction significantly changes the relationships between the different electrokinetic properties. Therefore, for a rigorous interpretation of experimental results taking possible effects of surface conduction adequate into account, it is imperative to collect data with more than one electrokinetic technique. For polystyrene latices, a comparison between theory and experiment has been made. The mobility and static conductivity data can be well reconciled if surface conduction is accounted for. The corresponding estimates of surface charge densities agree very well with values obtained by independent measurements. However, the extreme dielectric behaviour of latex colloids cannot be attributed to surface conduction.

Introduction

Electrokinetic measurements on charged colloids are widely used to gain information about the electrical double layer at the particle/solution interface. However, despite many investigations in this area, interpretation of the transport properties of dilute colloids (sols) in a weak electric field is still a matter of discussion (1-4). Commonly measured properties are the electrophoretic mobility and the sol conductivity in a static electric field, and the low-frequency dielectric response of sols in an alternating electric field. The interpretation of

these properties in terms of double layer parameters is the subject of this paper.

For the interpretation of electrokinetic properties of colloids, a model for the electric double layer around the colloidal particle has to be invoked. In the classical models, particles are considered as solid spheres surrounded by a diffuse double layer. The slip plane is assumed to coincide with the particle surface and, hence, a possible conduction contribution by ions within the slip plane is neglected. This model has been elaborated upon several studies where the polarization of the double layer is accounted for.

Important work has been done by Dukhin (5-7), who presented a theory for the electrophoretic mobility and the dielectric response for the case of particles with thin double layers ($\kappa a \gg 1$, with κ^{-1} the Debye length and a particle radius). Simplified versions of this theory were later given by Fixman (8,9) and O'Brien and Hunter (10). One of the main results of these theories is that the mobility as a function of the ζ potential exhibits a maximum. The appearance of this maximum is a consequence of the polarization of the double layer, which can be considerable even at reasonably high κa values. These results were in agreement with the numerical calculations of Wiersema et al. (11,12), who already suggested the presence of this maximum. Unambiguous proof of its existence was later given by the numerical work of O'Brien and White (13). By comparison with exact numerical results, O'Brien and Hunter (10) as well as Fixman (9) showed that the thin double layer approximation works very well. According to Fixman, for systems with KCl as the indifferent electrolyte, the difference between analytical and numerical results for the mobility is only 10% at $\kappa a = 10$; the corresponding difference for the dielectric response is negligible for systems with $\kappa a > 20$ and a ζ potential lower than roughly 100 mV. The first exact numerical calculations for the dielectric response were given by DeLacey and White (14).

Despite the theoretical developments in this area, a satisfactory quantitative explanation of many experimental data has not been given yet. For example, interpretation with the classical model of data on latices, obtained with different techniques, resulted in different values of the ζ potential (3,4). At the same time, the existence of the so-called

surface conduction, here defined as the excess conduction due to the ions *within* the plane of shear, has been experimentally demonstrated by the behaviour of the streaming potential of plugs of latices and silica particles (15,16). Moreover, for silica it is well-known that estimates of the surface charge density from the electrophoretic mobilities are much smaller than the values found by potentiometric titration (17). Hence, it can be concluded that the classical electrokinetic model, with its simple double layer model containing only two characteristic parameters (ζ and κa), is not applicable to a number of systems.

Again Dukhin and his co-workers (18) were the first to incorporate the effects of surface conduction into the thin double layer theory. They assumed that even inside the stagnant layer between surface and slip plane the ions are mobile and that the potential profile in this layer is also governed by the Poisson-Boltzmann equation. Consequently, besides the ζ potential, the surface (or Stern) potential also shows up in their equations. Generally, surface conduction leads to a lowering of the electrophoretic mobility; using classical theory ζ is underestimated. Unfortunately, Dukhin et al. presented no results which illustrate the influence of surface conduction on other electrokinetic properties. After the efforts of Dukhin and co-workers, it took nearly twenty years before the phenomenon of surface conduction had been incorporated into numerical methods. Examples are the work of Zukoski and Saville (4,19) and, more recently, that of Mangelsdorf and White (20). Their results support Dukhin's conclusion that, at given ζ potential, the occurrence of surface conduction reduces the mobility and they show that it also causes the static conductivity to increase.

In all these studies, a specific model for the surface conduction within the plane of shear has been used. However, the distribution and mobility of ions inside the stagnant layer are expected to differ greatly from system to system. It is this variability which complicates the development of a general model, covering all types of surface conduction. For example, the notion of Stern-layer conduction applied by Mangelsdorf and White, where tangential movement of ions inside the Stern-layer is allowed, has quite a different physical origin than the type of surface conduction which is likely to occur in systems with adsorbed polymer on the particle surface. It is well-known that the

hydrodynamic radius of a particle with adsorbed polymer is mainly due to polymer tails, protruding into the solution (21). These protruding tails effectively shift the plane of shear outward, while the polymer density behind the slip plane can be still very low. Therefore, it is reasonable to expect that movement of ions in this stagnant layer is, to a certain extent, still possible. Hence, the adsorption of non-ionic polymers on a charged surface is expected to cause a decrease of the ζ potential and an increase of the surface conductivity.

Considering the quality of the thin double layer theory in the absence of surface conduction, it seems useful to find out if this theory can be extended with a surface conductivity contribution without making detailed assumptions about the structure of the stagnant layer. It appears that the work of Fixman (8,9) is very suitable as a starter. The general formulation of the extended model makes it very attractive to test it on systems like latices or bacterial sols, i.e. systems in which a certain surface conduction may take place.

In this paper, the theoretical predictions of the consequences of surface conduction for the electrophoretic mobility, the static conductivity and the dielectric response of sols are discussed. A comparison between theory and experiment has been made for latices, with the experimental data being taken from the literature. The nomenclature will partially follow that in Fixman's papers, to which the reader is referred for an intensive discussion of the basic equations and approximations. In a subsequent paper, experimental results on the dielectric response of hematite and silica sols of spherical particles will be presented and discussed.

Theory

We shall discuss the electrokinetic properties of dilute colloids in a weak applied electric field under conditions where it is sufficient to consider only one particle embedded in an electrolyte solution. Only static and low-frequency properties will be discussed. Hence, the frequencies of interest are well below those corresponding to the high frequency or Maxwell-Wagner relaxation regime. In Fixman's linear thin double layer theory, two types of fields are considered, i.e. the fields

inside and those outside the double layer. The latter are long range fields and designated as the "far fields". The fields are related to the local perturbations in the electrostatic potential, the electrolyte concentration and the fluid flow, as resulting from the externally applied field. Outside the double layer the space charge density is supposed to be zero and consequently the "far fields" will be governed by relatively simple differential equations for which the general solutions are known. The specific solutions of these equations have to be determined by matching the general solutions of the "far fields" with the fields inside the double layer. One way to accomplish this, as will be shown below, is to solve the equations for the "far fields", given certain boundary conditions. The boundary conditions will be derived from the flux balances of ions and the fluid flow inside the double layer. In the thin double layer approximation, these conditions are independent of the particle geometry as, in this model, the double layer is assumed to be locally flat. Consequently, the particle geometry only enters the equations for the "far fields". All relevant electrokinetic quantities can be inferred from the "far field" solutions.

General equations

Consider an isolated charged particle immersed in an electrolyte solution with the thickness of its double layer small compared to the local radii of curvature of the particle surface. The distances from the particle surface to the slip plane and to the outer boundary of the double layer are designated by B_1 and B_2 , respectively. The outer boundary B_2 can be arbitrarily taken as located several Debye lengths from the particle surface. The knowledge of its exact position is, however, not necessary, as will be shown below. Between the particle surface and the slip plane, i.e. inside the stagnant layer, movement of ions is allowed. It is also assumed that the fluid is incompressible and that the potential profile outside the plane of shear obeys the Poisson-Boltzmann equation. The set of equations governing the flow of solvent and the displacement of the ions around the isolated particle has to be solved. The thin double layer theory, extended with the effects of surface conduction, now runs as follows.

The conservation equation for the ions of type i gives

$$\frac{\partial c_i}{\partial t} = -\nabla \cdot c_i \mathbf{v}_i = -\nabla \cdot c_i^e \mathbf{v}_i \quad [1]$$

with c_i the local electrolyte concentration, superscript "e" indicating equilibrium values and ∇ the differential operator. The second step in [1] is allowed in the linear response regime of interest. The drift velocity vector \mathbf{v}_i of ion type i can be written as

$$\mathbf{v}_i = \mathbf{v} - \frac{kT}{\beta_i} \nabla \mu_i \quad [2]$$

with \mathbf{v} the solvent velocity vector, k the Boltzmann constant, T the absolute temperature and β_i the friction coefficient, which, in principle, could be a function of position. The electrochemical potential μ_i is given as

$$\mu_i = h_i + \frac{z_i e}{kT} \Phi \quad [3]$$

with z_i the valency of ion i , e the unit charge and the potentials h_i and Φ defined as

$$h_i = \ln c_i - \ln c_i^e \quad [4]$$

and

$$\Phi = \psi - \psi^e \quad [5]$$

, respectively, with ψ the electrostatic potential. The gradient of the electrochemical potential μ_i represents the net force on an ion i due to the perturbations in the electrostatic and osmotic forces. Combination of equations [1] and [2] gives

$$\frac{\partial c_i}{\partial t} = -\nabla \cdot c_i^e \left[\mathbf{v} - \frac{kT}{\beta_i} \nabla \mu_i \right] \quad [6]$$

Outside the double layer, the perturbations are governed by the "far fields", which will be indicated by the superscript " f ". In this region the values for the friction coefficients and the equilibrium electrolyte

concentrations reduce to their bulk values, β_i^∞ and c_i^∞ , respectively. Eq. [6] then becomes

$$\frac{\partial c_i^f}{\partial t} = -\nabla \cdot c_i^\infty \left[\mathbf{v} - \frac{kT}{\beta_i^\infty} \nabla \mu_i^f \right] \quad [7]$$

with \mathbf{v}^f replaced by \mathbf{v} , which is allowed due to the incompressibility of the solvent. Subtracting [7] from [6] and integration over the double layer gives the net rate of change of the excess ion surface concentration per unit area. By splitting the divergence into its locally normal and tangential components, we get

$$\int_0^{B_2} \frac{\partial(c_i - c_i^f)}{\partial t} db = - \int_{B_1}^{B_2} (c_i^e - c_i^\infty) \nabla_t \cdot \mathbf{v}_i db + \frac{kT}{\beta_i^\infty} \left[c_i^\infty \frac{\partial \mu_i^f}{\partial b} \Big|_{b=0} + \int_0^{B_2} \left(\frac{\beta_i^\infty}{\beta_i} c_i^e \nabla_t \cdot \nabla_t \mu_i - c_i^\infty \nabla_t \cdot \nabla_t \mu_i^f \right) db \right] \quad [8]$$

with b the local cartesian coordinate normal to the surface (with $b=0$ on the surface) and ∇_t the tangential part of the divergence. Due to the facts that (i) fluid flow only takes place outside the plane of shear, (ii) the particle surface is impenetrable and (iii) the electrochemical potentials μ and μ_i^f are identical at the outer boundary of the double layer, several terms have cancelled in obtaining [8]. The difference between our [8] and [2.12] of Fixman is the range of integration, which in our case includes a stagnant part in the double layer ($0 < b < B_1$).

At this point, two assumptions will be made. The first assumption is that the double layer adjusts itself instantaneously to changes in the electrolyte concentration outside the double layer. The argumentation behind this approximation is that non-stationary currents in solution have decayed on time scales larger than the Maxwell-Wagner relaxation time. This time is of the order of $\beta/kT\kappa^2$, which for 10^{-3} M KCl is approximately 10^{-7} s. Hence, if processes are studied on a time scale much longer than the Maxwell-Wagner relaxation time, it is allowed to neglect the time derivative in [8].

The occurrence of slow relaxation processes in our system is related to the development of approximately neutral electrolyte gradients outside the double layer, which relax by diffusion processes. The development of these concentration gradients is a consequence of the fact that the current inside the double layer is mainly carried by the counterions, whereas outside the double layer the contributions of the counter- and co-ions to the current are equally important. This unbalance of charge carriers in different regions causes the particle with its double layer to act effectively as a source of neutral electrolyte at one side of the particle and as a sink at the other side. The extension of the concentration gradients into the solution will depend on the rate of diffusion, the particle size and of course on the frequency of the applied electric field.

The second assumption identifies $\nabla_t \mu_i^f$ with $\nabla_b \mu_i$ inside the double layer, where this quantity is supposed to be constant. This assumption is a local equilibrium approximation and based on the fact that the leading term of μ_i is independent of b . It follows from the conservation equation [6] and the observation that the divergence of the tangential flux is small and of the order of μ_i/a^2 . The reasonability of this approximation has been confirmed by the exact numerical calculations of Fixman (9). By using dimensionless quantities, with distances normalized on κ^{-1} , [8] can now be reduced to

$$-\gamma_i \int_{\kappa b}^{\kappa B_i} (f_i - 1) \nabla_t \cdot \mathbf{V}_t dZ + \partial \mu_i^f / \partial Z + (I_i^e + I_i^s) \nabla_t^2 \mu_i^f = 0 \quad [9]$$

with \mathbf{V}_t the tangential solvent velocity normalized on $2(kT)^2 \epsilon_0 \epsilon_r \kappa / 3\eta e^2$, $Z = \kappa b$, η the solvent viscosity, ϵ_0 and ϵ_r the permittivity of vacuum and the relative solvent permittivity, respectively, and f_i and the dimensionless ionic drag coefficient γ_i defined by respectively

$$c_i^e = f_i c_i^\infty \quad [10]$$

and

$$\gamma_i = \frac{2kT\epsilon_0\epsilon_r}{3\eta e^2} \beta_i^\infty \quad [11]$$

The integrals I_i^s and I_i^e in [9] are given by

$$I_i^s = \int_0^{kB_1} \left(\frac{\beta_i^\infty}{\beta_i} f_i - 1 \right) dZ \quad [12]$$

and

$$I_i^e = \int_{kB_1}^{kB_2} (f_i - 1) dZ \quad [13]$$

where the integration boundaries, as in [9], are in normalized distances. In obtaining [13], we have assumed that the ion friction coefficients in the diffuse part of the double layer are identical to their bulk values. Apart from a constant factor, the integral I_i^s equals the contribution of ion i to the effective electrokinetic charge density inside the stagnant layer.

Surface conduction can now be expressed in terms of $\sum_i z_i I_i^s$. Its occurrence can lead to some interesting consequences. For example in an extreme case, it could cause a particle to show a large dielectric response at negligible electrophoretic mobility. If in the stagnant layer $\beta \rightarrow \infty$, then the influence of the integral I_i^s is equivalent to an increase of the particle radius with the thickness of the stagnant layer, as is shown in appendix B. The next step is to solve the equations for the "far fields", with the specific solutions being determined by the boundary conditions, among which [9] and the particle geometry.

Spherical particles

The set of equations will be elaborated for a spherical particle of radius a in a symmetrical electrolyte ($z_1 = -z_2 = z$). It is assumed that both types of ions have the same friction constant, i.e. $\beta_i = \beta$ and $\gamma_i = \gamma$. Outside the double layer the charge density is supposed to be zero, i.e. there $h_i = h$, and the Laplace equation is applicable

$$\nabla^2 \Phi^f = 0 \quad [14]$$

Consequently, outside the double layer the electrolyte concentration will be governed by the following ordinary diffusion equation

$$\frac{\partial h}{\partial t} = \frac{kT}{\beta^\infty} \nabla^2 h \quad [15]$$

while the fluid flow will be governed by the Navier-Stokes equation without the inertial (low Reynolds number) and the electrostatic body force terms. The solution will be given for an alternating sinusoidal field, i.e. $E_0 = |E_0|e^{i\omega t}$, with ω the angular velocity and $\sqrt{i} = -1$. Consequently, the time derivative in [15] can be written as $i\omega h$. The boundary conditions for the "far field" expressions at the particle surface follow from [9] and the properties of the fluid flow inside the double layer. It appears that $\nabla_t \mathbf{V}$ can be written in terms of μ_i^f , which can be used to calculate the first term in [9], representing the convective contribution to the flow of ions inside the double layer, and the slip velocity. The slip velocity is defined as the tangential fluid velocity at the outer boundary of the double layer and serves as a boundary condition for the "far field" fluid velocity, formally applied at the particle surface itself. The flow field around the particle then follows from the assumption that the normal component of \mathbf{V} at the particle surface vanishes and that far from the particle the fluid flow relative to the particle approaches $-v_{el}$, with v_{el} the electrophoretic velocity.

The general solution of the Laplace equation [14] is well-known and given by

$$\Phi^f = -E_0 r \cos \theta + E_0 C_0 \frac{a^3}{r^2} \cos \theta \quad [16]$$

with r and θ the usual spherical coordinates and E_0 the applied field. In an alternating field, the dimensionless induced dipole coefficient C_0 is generally a complex quantity, i.e. $C_0 = C'_0 + iC''_0$. The induced dipole moment itself is given by $4\pi\epsilon_0\epsilon_r a^3 C_0 E_0$. According to Fixman (9), the solution to the set of equations governing the far field components of the electric ([14]) and concentration fields (Eq [15]) can be given in terms of

$$C_0 = (L_1 H_2 - L_2 H_1) / \Delta \quad [17]$$

$$W = (L_2 J_1 - L_1 J_2) / \Delta \quad [18]$$

$$\Delta = J_1 H_2 - J_2 H_1 \quad [19]$$

where

$$H_i = \frac{1}{\kappa a} (2 + 2x + x^2) + \frac{2}{(\kappa a)^2} (1+x) \sum_{j=1}^2 A_j \quad [20]$$

$$J_i = -2z_i - \frac{2}{\kappa a} \sum_{j=1}^2 z_j A_j \quad [21]$$

$$L_i = z_i - \frac{2}{\kappa a} \sum_{j=1}^2 z_j A_j \quad [22]$$

with

$$x = (1+i)\sqrt{\tau\omega}, \quad \tau = \frac{\beta^* a^2}{2kT} \quad [23]$$

Analytical expressions for the integrals A_j are given in appendix A. These integrals are functions of I_i^e and I_i^s and therefore sensitive to the charge distribution in the double layer. The sol conductivity and the complex dielectric response can be deduced from C_0 , which also appears, together with the quantity W , in Fixman's equation for the dimensionless mobility U_{el}

$$\begin{aligned} U_{el} &= \frac{3\eta e}{2kT\epsilon_0\epsilon_r} u_{el} = (1-C_0) \sum_{i=1}^2 \frac{z_i}{2z^2} I_i^u + \frac{W}{\kappa a} \sum_{i=1}^2 \frac{1}{2z^2} I_i^u \\ &= (1-C_0)\zeta + \frac{W}{\kappa a} \sum_{i=1}^2 \frac{1}{2z^2} I_i^u \end{aligned} \quad [24]$$

where $u_{el} = v_{el}/E_0$ is the mobility in physical units and ζ is the potential at the slip plane normalized on kT/e . The quantity W is closely related to the concentration perturbation h . For analytical expressions for the integrals I_i^u , see again appendix A.

Eq. [24] will be compared to the final equation for the electrophoretic mobility from the thin double layer theory of O'Brien and Hunter (10)

$$U_{el}^{OBH} = \frac{3}{2}\zeta - \frac{3}{2}\frac{\alpha}{1+\alpha} \left[\zeta - \frac{2\ln 2}{z_c} (1 - e^{-z_c\zeta}) \right] \quad [25]$$

where

$$\alpha = \frac{2}{\kappa a} \left(1 + \frac{3\gamma}{z_c^2} \right) e^{-z_c\zeta/2} \quad [26]$$

and z_c the co-ion valency. The first term in [25] is the Smoluchowski expression for the mobility of particles with thin double layers. The effects of double layer polarization are reflected by the second term, which is written as a function of the ζ potential only. This implies that a surface conduction contribution is not taken into account in [25]. Eq. [24] also reduces to the Smoluchowski expression if the polarization of the double layer is negligible. In that case, $C_0 = -0.5$ while the second term in [24] vanishes. According to [24], the mobility U_{el} is sensitive to surface conductivity, as μ and W are functions of I_i^s .

Induced dipole coefficient and complex conductivity

The complex conductivity increment ΔK^* of a sol is defined by

$$\Delta K^* = K_{sol}^* - K_\infty^* \quad [27]$$

where for any K^*

$$K^* = \sigma + i\omega\epsilon_0\epsilon_r \quad [28]$$

with the subscript " ∞ " indicating the background electrolyte quantity. The real part σ of K^* represents the resistive part of the complex conductivity; the imaginary part $i\omega\epsilon_0\epsilon_r$ represents the capacitive component. For dilute colloids of spherical particles and finite frequencies, a simple relation exists between the induced dipole coefficient and the complex conductivity (7,14)

$$\Delta K^* = 3\phi C_0 K_\infty^* \quad [29]$$

where ϕ is the volume fraction of the particles. Eq. [29] can be derived in two ways, i.e. by directly calculating the contribution of the induced

dipole moments to the total electric field (7) or by calculating the volume averages of the electric current and the electric field (14).

As shown by O'Brien (22), [29] is also suitable to calculate the conductivity increment $\Delta\sigma_{stat} = \sigma_{sol} - \sigma_\infty$ in a static field, on the condition that the friction coefficients of all types of ions in the system are equal. Although in this paper the systems under consideration are assumed to satisfy this condition, it may be stated that [29] can also be used to determine $\Delta\sigma_{stat}$ in systems with different types of ions having different friction coefficients. In this case, instead of the induced dipole coefficient in a static field $C_{0,stat}$, one has to use the limiting dipole coefficient $\lim_{\omega \rightarrow 0} C_0$ in [29]. These two types of dipole coefficients are not the same due to the fact that at finite frequencies the different types of ions react to the varying field with different rates. Consequently, a finite charge density outside the double layer will be generated, and this also contributes to the dipole moment (23,24). According to Teubner (24), who proved it for a binary electrolyte, this long range charge density vanishes pointwise for $\omega \rightarrow 0$, whereas its contribution to C_0 remains finite.

Results and discussion

From the derivation of [9] it is clear that in our picture the distribution of the charge density perturbation inside the double layer does not enter the equations of the thin double layer approximation. Hence, processes, which only affect this distribution but do not alter the flux balance equation [9], have no influence on the final results. Examples of such processes are polarization of the interior of the particle, conduction inside the particle (provided that charge transfer across the particle/solution interface is impossible) and the tangential movement of bound ions which are not able to desorb. This conclusion is in accordance with O'Brien and White's proof that, in general, the electrophoretic mobility is independent of these processes, provided that the applied field is weak (13).

The occurrence of double layer polarization sometimes leads to violation of conclusions. For example, the theoretical prediction of Henry (25) that the mobility should approach zero if the conductivity

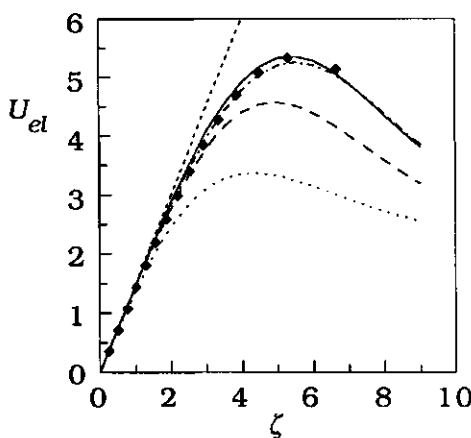


Figure 1. Influence of surface conduction on mobility U_{el} as function of ζ potential. $\kappa a = 50$, (----) Smoluchowski, (—) $\Theta = 0$, (---) $\Theta = 1$, (.....) $\Theta = 5$, (----) $\Theta = 0$ and according to O'Brien and Hunter ([25]), (\diamond) numerical values for $\Theta = 0$.

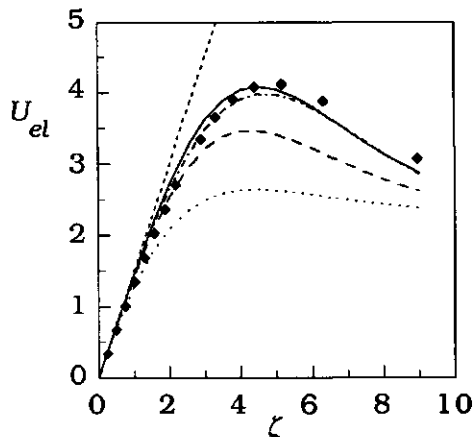


Figure 2. Influence of surface conduction on mobility U_{el} as function of ζ potential. $\kappa a = 20$, (----) Smoluchowski, (—) $\Theta = 0$, (---) $\Theta = 1$, (.....) $\Theta = 5$, (----) $\Theta = 0$ and according to O'Brien and Hunter ([25]), (\diamond) numerical values for $\Theta = 0$.

inside the particle becomes infinitely high, is a consequence of neglecting the double layer polarization, see also ref. (6).

A second example is the paper of Lyklema et. al. (1), in which two types of double layer polarization are compared, i.e. the polarization of the diffuse part of the double layer and the polarization of the distribution of bound ions. To quantify the effects of the polarization of bound ions, a generalized version of Schwartz's model (26) was developed. However, a quantitative comparison based on the thin double layer approximation, as given in ref. (1), is inappropriate when the two mechanisms simultaneously operate. The generalized version of Schwartz's model considers the polarization of the layer of bound ions and these are unable to affect boundary equation [9]. Although this conclusion is again based on the thin double layer theory, it is expected that the influence of the bound ions on the dielectric dispersion is relatively small, like the influence of the value of the dielectric constant

of the particle. In exact numerical calculations, the latter is reported to affect the dielectric response only slightly (9).

Effects of surface conduction

The influence of surface conduction on the electrokinetic properties will be shown for spherical particles in a KCl electrolyte solution with both ion mobilities approximated by $\gamma = 0.1715$. In order to illustrate the frequency dependence of the dielectric response, we plot the dielectric increment $\Delta\epsilon_r$,

$$\Delta\epsilon_r = \epsilon_r(\omega) - \epsilon_r(\omega_r^e) \quad [30]$$

and the conductivity increment $\Delta\sigma$

$$\Delta\sigma = \sigma(\omega) - \sigma(\omega_r^\sigma) \quad [31]$$

The reference frequency ω_r^e is chosen in the high frequency limit of the low-frequency dispersion, i.e. $\omega_r^e \gg \tau^{-1}$ (in our case $\omega_r^e = 2\pi \cdot 1\text{MHz}$), and ω_r^σ is chosen in the low frequency limit, i.e. $\omega_r^\sigma \ll \tau^{-1}$ ($\omega_r^\sigma = 2\pi \cdot 1\text{Hz}$).

The calculation of the electrokinetic properties now requires, besides the usual parameters ζ and κa , the two extra parameters I_1^s and I_2^s . Simplification is possible if the potential in the stagnant layer is sufficiently high. Then the surface conductivity is mainly determined by the counterions whereas the contribution of the co-ions in this region may become negligible small. In order to keep the number of parameters minimum, the contribution of the co-ions to the surface conductivity will also be neglected at low surface potentials. Although the reasonability of this approximation decreases with decreasing surface potential, it generally does not affect the qualitative meaning of the results. A convenient parameter characterizing the surface conductivity is Θ , defined as

$$\Theta = I^s / I^\varepsilon \quad [32]$$

with I^s and I^ε the excess integrals of the counterions, defined by [12] and [13].

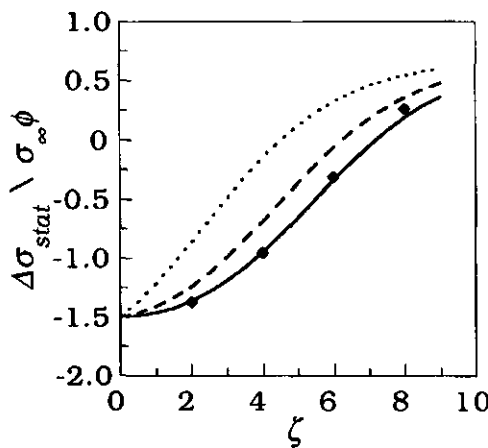


Figure 3. Influence of surface conduction on static conductivity increment $\Delta\sigma_{\text{stat}}/\phi\sigma_\infty$ as function of ζ potential. $\kappa a = 50$, (—) $\Theta = 0$, (---) $\Theta = 1$, (----) $\Theta = 5$, (•) numerical values for $\Theta = 0$.

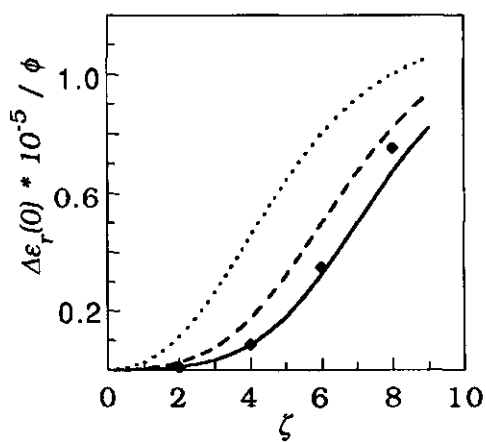


Figure 4. Influence of surface conduction on low frequency limit dielectric increment $\Delta\epsilon_r(0)/\phi$ as function of ζ potential. $\kappa a = 50$, (—) $\Theta = 0$, (---) $\Theta = 1$, (----) $\Theta = 5$, (•) numerical values for $\Theta = 0$.

Figures 1-4 show the influence of surface conduction on the mobility, static conductivity and the dielectric response versus ζ potential. The low frequency limit of the dielectric increment $\Delta\epsilon_r(0)$, defined as $\Delta\epsilon_r(0) = \lim_{\omega \rightarrow 0} \Delta\epsilon_r(\omega)$, is plotted in Fig. 4.

In the absence of surface conduction, the thin double layer theories of Fixman and O'Brien/Hunter give approximately the same results for the electrophoretic mobility. Moreover, even for κa values as low as 20, these agree very well with numerical computations according to the computer programme of O'Brien and White (13).

The maximum in the mobility as a function of the ζ potential is due to the fact that the increase of the electrophoretic retardation force with increasing ζ potential is stronger than that for the driving force. To a first approximation, the driving force for particle movement is proportional to the counter charge outside the slip plane, or in other words, it is related to the ζ potential. The electrophoretic retardation force due to the polarization of the double layer is determined by the

total mobile counter charge inside the double layer. Consequently, if at a fixed ζ potential the surface conduction increases, the retardation force does so too, causing the mobility to decrease. Marked is the fact that the mobility maximum slowly disappears with increasing surface conductivity.

As shown in Figs. 3 and 4, the static conductivity increment $\Delta\sigma_{stat}$ and the dielectric increment $\Delta\epsilon_r(0)$ are both monotonously increasing functions of ζ and Θ . The behaviour of $\Delta\sigma_{stat}$ is readily explained by the contribution of the counterions inside the stagnant layer to the conductivity. The fact that $\Delta\sigma_{stat}/\phi\sigma_\infty = -1.5$ for a colloid of uncharged particles follows from [29] and by realizing that the dipole coefficient C_0 of an uncharged particle with a permittivity much smaller than that of the surrounding solvent is equal to $-1/2$. Our results agree, at least qualitatively, with the numerical calculations by Mangelsdorf and White on the effects of surface conduction on the electrophoretic mobility and the static sol conductivity.

In order to explain the sensitivity of the dielectric increment $\Delta\epsilon_r(0)$ to ζ and Θ , it is instructive to study the frequency dependence of the induced dipole coefficient and the corresponding dielectric response, as shown in Figures 5 and 6. At low frequencies, the real part of the induced dipole coefficient C'_0 is approximately constant; it starts to grow for frequencies beyond $1/\tau$. This frequency dependence of C'_0 reflects the occurrence of the diffusion layers or electrolyte clouds outside the double layer at low frequencies, which at higher frequencies do not have the chance to develop to full extent.

At those frequencies where the diffusion layers are absent, non-stationary fluxes of ions around the particle are prevented by the development of a dipole moment. The induced dipole moment acts as a brake on the flow of ions (mainly counterions) inside the double layer and hence, it compensates for the difference in local conductivity inside and outside the double layer. However, the development of the concentration gradients at low frequencies has a marked effect on the induced dipole moment. These gradients create an entropic force, which, in addition to the dipole field, slows down the current flow inside the double layer. Therefore, the presence of this entropic force affects the current balance and in order not to violate the condition of

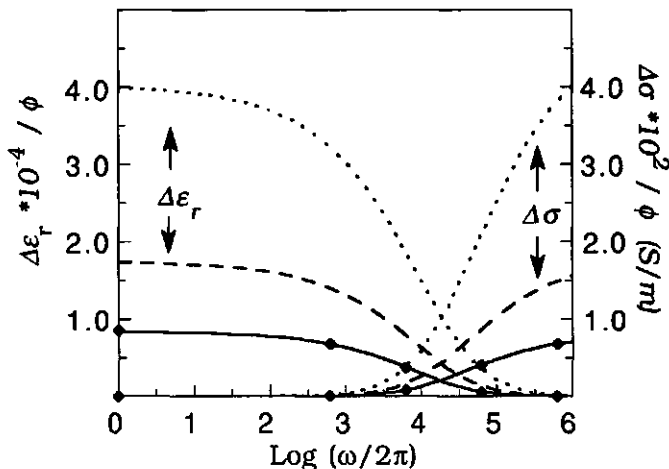


Figure 5. Influence of surface conduction on frequency dependence dielectric increment $\Delta\epsilon_r/\phi$ and conductivity increment $\Delta\sigma/\phi$. $\zeta=4$, $a=200\text{nm}$, $\kappa a=50$, (—) $\Theta=0$, (---) $\Theta=1$, (···) $\Theta=5$, (♦) numerical values for $\Theta=0$.

stationary currents, the dipole moment has to decrease when the concentration gradients develop.

As mentioned before, the long range concentration gradients originate from the fact that the particle and its double layer acts as a source of neutral electrolyte at one side of the particle and as a sink at the other side. From the diffusion equation it follows that at the frequency $\omega=1/\tau$ these gradients extend a distance into the solution of the order of the particle radius. Therefore, overlap of the "sink" and "source" gradients start to occur roughly at $\tau\omega=1$ and for $\tau\omega \ll 1$ the dipole coefficient is approximately constant, as can be seen in Fig. 5.

It can be shown that the conductivity increment $\Delta\sigma(\omega)$ of colloids of charged particles is mainly determined by the real part of the induced dipole coefficient C'_0 and, consequently, $\Delta\sigma(\omega)$ is a monotonously increasing function of the frequency. It can also be deduced that $\Delta\epsilon_r(\omega)$ contains a term which is proportional to the quotient C''_0/ω . The rate of adjustment of the dipole moment to the changing electric field is controlled by relatively slow diffusion processes. Hence, even at very low frequencies, there will be a non-zero

imaginary part of the dipole coefficient, C_0'' , running out of phase with the applied field. From the diffusion equation it follows that at low frequencies C_0'' scales with ω , which explains the finite low frequency limit of the dielectric increment, see Fig. 6.

From the above discussion it is clear that a strong frequency dependence of C_0' and C_0'' exists, and hence, of $\Delta\sigma(\omega)$ and $\Delta\epsilon_r(\omega)$, if processes are present which may give rise to relatively large long range concentration gradients at low frequencies. These gradients are caused by the unequal distribution of charge carriers inside and outside the double layer. Since these differences increase with growing ζ and Θ , the dielectric dispersion is bound to do the same. As shown, surface conduction decelerates the electrophoretic mobility and, at the same time, enhances the dielectric response and the static conductivity increment. This enables experimental determination of ζ and Θ , once the mobility and either the dielectric dispersion or the static conductivity of the sol are known.

Comparison between theory and experiment

The first comparison between theory and experiment has been carried out with the experimental data of Van Der Put for dilute polystyrene latices (27). In his thesis, data are presented for the electrophoretic mobility and the sol conductivity (corrected for negative adsorption) as a function of the electrolyte concentration (KCl), as well as for the (negative) surface charge density σ_0 , as obtained by conductometric titration. For convenience, only the absolute values of charges and potentials will be considered.

If surface conduction may be neglected, then estimates for the potential at the slip plane ζ can be obtained from the electrophoretic mobility u_{el} , i.e. ζ_{el}^{num} and ζ_{el} , and from the static conductivity increment $\Delta\sigma_{stat}/\phi\sigma_\infty$, i.e. ζ_σ . The potential ζ_{el}^{num} is calculated with the programme of O'Brien and White (13), whereas the potentials ζ_{el} and ζ_σ follow from the thin double layer theory. On the other hand, if surface conduction occurs, Θ and ζ_{comb} are obtained by simultaneously fitting the electrophoretic mobility and the static conductivity increment.

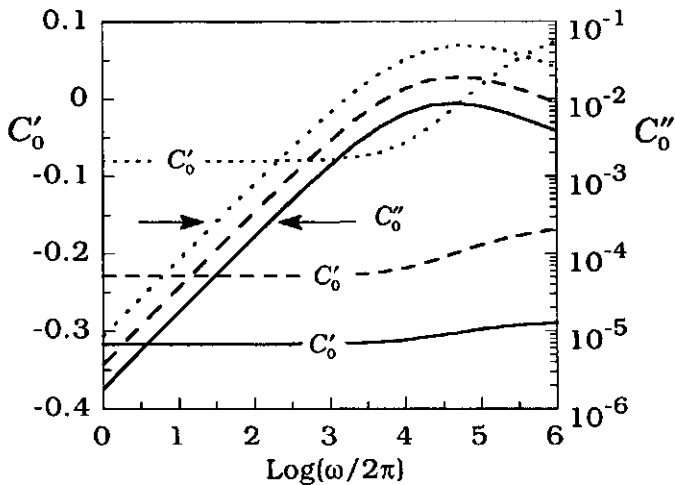


Figure 6. Influence of surface conduction on frequency dependence real part C'_0 and imaginary part C''_0 of induced dipole coefficient, $\alpha = 200\text{nm}$, $\zeta = 4$, $\kappa\alpha = 50$, (—) $\Theta = 0$, (---) $\Theta = 1$, (···) $\Theta = 5$.

The results are listed in Table 1 for three type of colloids, denoted as H, M and L. Also listed are the equilibrium charge densities in the stagnant part and in the diffuse part of the double layer, i.e. σ_d and σ_s respectively, which follow from the values of the fitting parameters ζ_{comb} and Θ and the relations $\sigma_s = I^s c^* F / \kappa$ and $\sigma_d = (I_1^s + I_2^s) c^* F / \kappa$, with F Faraday's constant. Note that, given the assumptions, both σ_s and σ_d represent the total (mobile) charge in each pertaining region.

Apart from two sols of sample L, all sols have in common that the ζ potential obtained from only the mobility is much smaller than the one obtained from only the static conductivity increment, i.e. $\zeta_{el} < \zeta_\sigma$. Moreover, the relative small differences between the electrophoretically obtained ζ potentials do not suggest the existence of a large variation in the surface charge density σ_0 between the three different colloids. This is in contrast to the variation in the ζ potentials obtained from the conductivities.

It is clear from Table 1 that the mobility and conductivity data can be readily reconciled if a significant surface conductivity is accounted for. This is reflected by the relatively high values of the parameter Θ . It is gratifying that the sum of the charge densities in the stagnant part

and in the diffuse part of the double layer, i.e. $(\sigma_s + \sigma_d)$, correlates well with the conductometric surface charge density σ_0 . At the lowest electrolyte concentrations, the agreement is nearly perfect for all three colloids, even though the variation in the surface charge density is as high as one order of magnitude! At higher electrolyte concentrations the agreement is less perfect, but the correlation persists. However, it is reasonable to expect that inside the stagnant layer $\beta \geq \beta^*$ and, hence, the situation with $\sigma_s + \sigma_d < \sigma_0$ is not in contradiction with the model. This is supported by the experimental data of Midmore and Hunter on the high frequency dielectric response of latices (28). They found that for relatively highly charged latices ($\sigma_0 > 10 \mu C/cm^2$) the surface charges estimated from these measurements are much lower than those obtained by conductometric titration, indicating that within the shear plane $\beta \geq \beta^*$. Better agreement was obtained for lower values of σ_0 ($\sigma_0 = 5 \mu C/cm^2$). The two sets of data for sample L, with $\zeta_{el} > \zeta_{comb}$, cannot be reconciled by taking surface conduction into account.

Interpretation of the double layer parameters ζ_{comb} and Θ in terms of a specific structure of the stagnant layer and the distribution of ions within it, will not be considered this paper. In the "dynamic model of the Stern layer" of Zukoski and Saville (4,19) such assumptions about these factors have been made. Their experimental data for the mobility and conductivity of dilute polystyrene latex colloids also lead to $\zeta_{el} < \zeta_\sigma$, corroborating the occurrence of surface conduction.

A second comparison between theory and experiment has been made using Springer's data of the dielectric behaviour of dilute polystyrene latices (2). The frequency dependence of the dielectric increments is in reasonable agreement with theoretical prediction; estimates of particle sizes from $\Delta\epsilon_r(\omega)$ differed less than 15% from values obtained by electron microscopy. However, the absolute size of $\Delta\epsilon_r(\omega)$ is too large to be explained by the present theory, whatever the choice for ζ and Θ . Lyklema et al. (29) arrived at similar conclusions when interpreting the same data. This extreme dielectric behaviour of

Table 1.

Sample H: $\alpha = 290\text{nm}$.

$$\sigma_0 = 9.2 \mu\text{C}/\text{cm}^2, \text{KCl}$$

κa	u_{el}	$\frac{\Delta\sigma_{stat}}{\phi\sigma_\infty}$	ζ_{el}^{num}	ζ_{el}	ζ_σ	ζ_{comb}	Θ	σ_d	σ_s
21	3.98	0.33	2.4	2.2	7.7	6.3	1.8	3.0	5.1
30	4.52	-0.07	2.7	2.6	6.1	4.4	2.5	1.6	3.6
67	5.33	-0.87	3.0	2.9	4.7	3.3	2.0	2.1	3.5

Sample M: $\alpha = 305\text{nm}$.

$$\sigma_0 = 4.0 \mu\text{C}/\text{cm}^2, \text{KCl}$$

κa	u_{el}	$\frac{\Delta\sigma_{stat}}{\phi\sigma_\infty}$	ζ_{el}^{num}	ζ_{el}	ζ_σ	ζ_{comb}	Θ	σ_d	σ_s
32	4.76	-0.23	2.9	2.7	5.6	4.1	2.0	1.4	2.6
71	5.14	-1.15	2.8	2.7	3.7	2.9	1.0	1.7	1.3

Sample L: $\alpha = 253\text{nm}$.

$$\sigma_0 = 0.9 \mu\text{C}/\text{cm}^2, \text{KCl}$$

κa	u_{el}	$\frac{\Delta\sigma_{stat}}{\phi\sigma_\infty}$	ζ_{el}^{num}	ζ_{el}	ζ_σ	ζ_{comb}	Θ	σ_d	σ_s
19	4.26	-0.58	2.7	2.5	3.8	3.0	1.0	0.6	0.4
26	5.49	-1.04	3.8	3.5	2.9	-	-	-	-
59	5.35	-1.36	3.0	2.9	2.2	-	-	-	-

Note. The values for ζ_{el}^{num} and ζ_{el} have been deduced from u_{el} , the ζ_σ from $\Delta\sigma_{stat}/\phi\sigma_\infty$, all without taking surface conductance into account. The ζ_{el}^{num} follows from the theory of O'Brien and White; ζ_{el} and ζ_σ follow from the thin double layer theory. Values of ζ_{comb} and Θ are obtained from the thin double layer theory by fitting on u_{el} and $\Delta\sigma_{stat}/\phi\sigma_\infty$ simultaneously. The charge densities σ_d and σ_s are in $\mu\text{C}/\text{cm}^2$, u_{el} in $10^{-8} \cdot \text{m}^2/\text{Vs}$ and the ion mobility is approximated by $\gamma = 0.1715$. The absolute values of charge densities and potentials are given.

latex colloids has also been observed by Rosen and Saville (30). Moreover, according to their results (31), this extreme behaviour largely disappears if the latices are subjected to a high temperature heat treatment which probably modifies the surface structure. However, the large dielectric response of untreated latices still remains a challenging problem to be solved.

Conclusions

It has been shown that Fixman's linear thin double layer theory for the electrokinetic properties of dilute colloids can be easily extended to include surface conduction, i.e. the conduction by ions behind the slip plane. The formulation is general in the sense that neither restrictions are imposed upon the structure of the layer in which the surface conduction occurs nor upon the ion distribution within it. The computations show that the occurrence of surface conduction leads to a reduction of the electrophoretic mobility and to an increase of the static sol conductivity and the dielectric response. The theoretical results show that an unambiguous interpretation of only one type of electrokinetic data, for example the electrophoretic mobility, is impossible if surface conduction occurs. To assess whether such conduction does take place, one is bound to also measure either the static conductivity or the dielectric response of the sol.

Comparison between theory and experiment shows that the present model is able to provide a consistent explanation for the mobility and static conductivity data of Van Der Put (27) for polystyrene latices. On the basis of these data, estimates have been made for the surface charge densities, which agree very well with values obtained by independent measurements. However, the extreme dielectric behaviour of latex colloids, as measured by Springer (2), cannot be attributed to surface conduction.

Appendix A

The integrals A_y used in [20] are defined by

$$A_y = (I_i^s + I_i^\varepsilon) \delta_y - \frac{3\gamma_i}{4Z_1^2} I_y \quad [A.1]$$

The analytical expressions for the different given integrals are obtained by using the solution of the Poisson-Boltzmann equation, i.e. $f_i = e^{-z_i \psi^*}$, for a single flat unperturbed double layer. Let ζ be the scaled electrostatic potential at the plane of shear and

$$K_i \equiv \tanh(z_i \zeta / 4) \quad [A.2]$$

then we have

$$I_i^\varepsilon = -4K_i / (1 + K_i) \quad [A.3]$$

$$I_y = -8 \ln(1 - K_i^2), \quad i \neq j \quad [A.4]$$

$$I_u = 16 \left[K_i (1 + K_i)^{-1} - \ln(1 + K_i) \right] \quad [A.5]$$

The term I_i^u , used in [24] is defined by

$$I_i^u = 4 \ln(1 + K_i) \quad [A.6]$$

No analytical expression has been given for the integral I_i^s , because no general assumptions can be made about the structure of the double layer in the stagnant layer. We suggest to determine this integral experimentally.

Appendix B

If the friction coefficient of the ions inside the stagnant layer is infinitely high, then the effect of the integrals I_i^s should be equivalent to the effect of increasing the particle radius by the thickness of the stagnant layer. To demonstrate this, we consider an uncharged particle of radius a with a stagnant layer with normalized thickness κB_1 . Inside the stagnant layer $\beta \rightarrow \infty$, which gives, according to [12], $I_i^s = -\kappa B_1$. In this particular case $I_i^\varepsilon = I_y = 0$ and hence [A.1] reduces to $A_u = -\kappa B_1$. This result together with [17] gives the induced dipole coefficient

$$C_0 = -\frac{1}{2} \left[1 + 3 \left(\frac{a}{B_1} - 1 \right)^{-1} \right] \quad [B.1]$$

From [29] the complex conductivity follows as

$$\Delta K^* \propto -\frac{1}{2} \left[1 + 3 \left(\frac{a}{B_1} - 1 \right)^{-1} \right] a^3 \quad [B.2]$$

However, this result should be equal to the complex conductivity for a sol of uncharged particles with an effective radius of $a_{eff} = a + B_1$, which can be given as

$$\Delta K^* \propto -\frac{1}{2} (a + B_1)^3 \quad [B.3]$$

By writing [B.2] as a binomial series it can be shown that the difference between [B.2] and [B.3] is of $O[(B_1/a)^3]$, which is, within the thin double layer approximation, negligibly small.

References

- (1) Lyklema, J., Dukhin, S. S., Shilov, V. N., *J. Electroanal. Chem.* **143**, 1-21 (1983).
- (2) Springer, M. M., Korteweg, A., Lyklema, J., *J. Electroanal. Chem.* **153**, 55-66 (1983).
- (3) O'Brien, R. W., Perrins, W. T., *J. Colloid Interface Sci.* **99**, 20-31 (1984).
- (4) Zukoski IV, C. F., Saville, D. A., *J. Colloid Interface Sci.* **114**, 45-53 (1986).
- (5) Dukhin, S. S., Semenikhin, N. M., *Kolloidn. Zh.* **32**, 360-368 (1970).
- (6) Dukhin, S. S., Derjaguin, B. V., in "Surface Colloid Science" (E. Matijevic, Ed.), Wiley, New York, 1974.
- (7) Dukhin, S. S., Shilov, V. N., "Dielectric Phenomena and the Double Layer in Disperse Systems and Polyelectrolytes", Wiley, New York, 1974.
- (8) Fixman, M., *J. Chem. Phys.* **72**, 5177-5186 (1980).
- (9) Fixman, M., *J. Chem. Phys.* **78**, 1483-1491 (1983).
- (10) O'Brien, R. W., Hunter, R. J., *Canad. J. Chem.* **59**, 1878 (1981).
- (11) Wiersema, P. H., Ph. D Thesis, Utrecht University, 1964.
- (12) Wiersema, P. H., Loeb, A. L., Overbeek, J. T. G., *J. Colloid Interface Sci.* **22**, 78-99 (1966).

- (13) O'Brien, R. W., White, L. R., *J. Chem. Soc., Faraday Trans. 2* **74**, 1607-1626 (1978).
- (14) DeLacey, E. H. B., White, L. R., *J. Chem. Soc., Faraday Trans. 2* **77**, 2007-2039 (1981).
- (15) Put v. d., A. G., Bijsterbosch, B. H., *J. Colloid Interface Sci.* **92**, 499-507 (1983).
- (16) Linde v. d., A. J., Bijsterbosch, B. H., *Croatica Chem. Acta* **63**, 455-465 (1990).
- (17) Tadros, T. F., Lyklema, J., *J. Electroanal. Chem.* **17**, 267-275 (1968).
- (18) Shilov, V. N., Dukhin, S. S., *Kolloidn. Zh.* **32**, 117-123 (1970).
- (19) Zukoski IV, C. F., Saville, D. A., *J. Colloid Interface Sci.* **114**, 32-44 (1986).
- (20) Mangelsdorf, C. S., White, L. R., *J. Chem. Soc. Faraday Trans.* **86**, 2859-2870 (1990).
- (21) Cohen Stuart, M. A., Waaje, F. H. W. H., Cosgrove, T., Vincent, B., Crowley, T. L., *Macromolecules* **17**, 1825-1830 (1984).
- (22) O'Brien, R. W., *J. Colloid Interface Sci.* **81**, 234-248 (1981).
- (23) O'Brien, R. W., *Adv. Colloid Interface Sci.* **16**, 281-320 (1982).
- (24) Teubner, M., *J. Colloid Interface Sci.* **92**, 284-286 (1983).
- (25) Henry, D. C., *Proc. R. Soc. Ser. A* **133**, 106-129 (1931).
- (26) Schwartz, G., *J. Phys. Chem.* **66**, 2636 (1962).
- (27) Put v. d., A. G., Ph. D. Thesis, Wageningen University, 1980.
- (28) Midmore, B. R., Hunter, R. J., *J. Colloid Interface Sci.* **122**, 521-529 (1988).
- (29) Lyklema, J., Springer, M. M., Shilov, V. N., Dukhin, S. S., *J. Electroanal. Chem.* **198**, 19-26 (1986).
- (30) Rosen, L. A., Saville, D. A., *Langmuir* **7**, 36-42 (1991).
- (31) Rosen, L. A., Saville, D. A., *J. Colloid Interface Sci.* **149**, 542-552 (1992).

Chapter 4

Low-Frequency Dielectric Relaxation of Hematite and Silica Sols

Abstract

The low-frequency dielectric response of dilute aqueous hematite and silica sols has been measured as a function of pH, ionic strength and particle size. Results are obtained by applying a four-electrode technique. The response of both sols is pH-dependent and, hence, determined by the surface charge density. The particle size dependence of the characteristic relaxation frequency is in fair agreement with theoretical prediction. Moreover, the magnitude of the response of both sols can be well explained by classical electrokinetic theory, yielding reasonable values for the ζ potentials. However, these values are systematically higher than those obtained electrophoretically. This can be explained if surface conduction within the slip plane occurs, a type of conduction which is not included into the classical theory. Using an extended theory, the surface conductivity has been determined from a combination of electrophoresis and dielectric data. For both hematite and silica, the results show that a large fraction of the (mobile) counter charge is located within the slip plane. This fraction increases with increasing surface charge density.

Introduction

Electrokinetic techniques such as microelectrophoresis are widely used to characterize sols. Nevertheless, the number of rigorous experimental tests of the classical electrokinetic theory are relatively small. In addition, nearly all these tests have been carried out on latices, showing clearly that these systems are not ideal; in several respects their behaviour is not in accordance with the predictions of the classical theory (1-7).

The classical electrokinetic theory is best developed for dilute sols of solid spherical particles (8-10). In this theory, the electric double layer is assumed to be completely diffuse with its potential profile governed by the Poisson-Boltzmann equation. The only experimental unknown parameter in this theory is the ζ potential at the slip plane. Therefore, if the theoretical picture is correct, different electrokinetic methods should yield the same ζ potential. Besides electrophoresis, examples of elektrokinetic properties are the static conductivity and the low- and high-frequency dielectric response of sols. Consequently, at least two different electrokinetic properties should be known for a rigorous test of the classical theory.

In this respect, low-frequency dielectric spectroscopy is a valuable technique. Experiments on latices have proven that the dielectric response is very sensitive to the sol properties (see below). Moreover, the amplitude and the frequency dependence of the response are related to transport processes around the particle, which, in their turn, depend on the double layer structure and the particle shape. Hence, in principle, dielectric spectroscopy in the low-frequency range provides more information than static field measurements of the electrophoretic mobility or the conductivity.

The existence of a limited number of rigorous tests is probably due to a combination of theoretical and experimental difficulties. First, measurement of the sol properties requires a sufficient amount of sol. Preferably, this should be a homodisperse sol of spherical particles to satisfy theoretical assumptions. Second, low-frequency dielectric spectroscopy involves major technical problems related to electrode polarization in combination with unfavourable phase angles of the sol impedance (2, 3). Fortunately, the application of a four-electrode technique (11) seemed to circumvent this problem. Measurement of the static conductivity does not suffer from such technical problems. However, extra care has to be taken with the experimental procedure since the interpretation of the static conductivity increment requires a very accurate knowledge of the composition of the suspending electrolyte solution (12, 13). The first condition can be easily satisfied

by using latices. Hence, these systems have been subject of most previous elektrokinetic studies.

The picture, emerging from the numerous electrokinetic data on latices, makes one thing very clear: difficulties are still involved. Well-known is the issue of the maximum in the electrophoretic mobility of latex particles versus ionic strength (5, 14-16). Hairiness of the latex particle as well as competitive adsorption of both counterions and co-ions onto the particle surface have been suggested as possible explanations. The presence of polymeric hairs on the surface has two consequences. First, the hairs affect the position of the slip plane and second, they probably enable surface conduction, i.e. conduction by ions within the plane of shear. This concept alone has been shown to be adequate in explaining data of Van Der Put on the electrophoretic mobility and the static conductivity of surfactant-free polystyrene latices (6, 7). However, no theoretical foundation has been found yet which satisfactorily explains the large low-frequency dielectric increments of latices, as observed by Springer et. al. (2, 3, 17) and, more recently, by Rosen and Saville (18, 19).

Clearly, the dielectric response is very sensitive to the properties of the particle surface and/or its double layer. This has been illustrated by the recent work of Rosen and Saville (20), who subjected their latices to a high-temperature heat treatment which probably modifies the (hairy) surface structure. In comparison with untreated latices, the heat-treated latices showed a greatly reduced dielectric increment and the resulting ζ potentials agree much better with those obtained electrophoretically. Nevertheless, hairiness cannot explain all their experimental data. Therefore Rosen and Saville suggested that ion binding might also occur.

Although ion binding has been invoked several times to explain the electrophoretic behaviour of latices (4, 15, 21, 22), other investigations are not very supportive towards this idea. For example, Van Der Put (6) found, by non-electrokinetic means, negligible adsorption of chloride ions onto polystyrene latices in KCl solutions with concentrations below $2 \cdot 10^{-2} M$. In addition, the insensitivity to the

nature of the co-ion of the electrophoretic mobility and the high-frequency dielectric response of polystyrene latices, as obtained by Midmore and Hunter (16), sheds doubt on the mechanism of co-ion binding. The fact that mobility curves obtained with different co-ions differ very little has also been found by Goff and Luner (23). Moreover, the ion-binding concept itself provides no full explanation for the dielectric behaviour of polystyrene latices, which have not undergone a high-temperature heat treatment (7, 17, 20).

In the light of the difficulties involved in interpreting the electrokinetic properties of latices, the availability of data on dilute inorganic sols concerning different electrokinetic properties is highly desirable. Therefore, we present data on the low-frequency dielectric response of hematite and silica sols as a function of pH, ionic strength and the particle size. Some of these data are compared to electrophoretic mobilities, using a thin double layer theory (7) which accounts for surface conduction. For hematite and silica, recipes are known for the synthesis of homodisperse (nearly) spherical particles in sufficient large amounts (24, 25). The surface charge density of oxides is pH-dependent, which enables us to study the influence of the surface charge density on the dielectric response at constant ionic strength. The dielectric data are obtained by using a four-electrode spectrometer.

Experimental section

Silica and hematite. Colloidal silica and hematite were prepared according to the methods of Stöber (24) and Penners (25), respectively. The reaction conditions were chosen in order to obtain the desired particle sizes, which were determined by transmission electron microscopy. Isolated silica particles appeared spherical in the electron micrographs, while the nearly spherical hematite particles had slightly cubic shapes. The particle radii were for silica: 80, 132 and 184 nm and for hematite: 100, 184, 257 and 335 nm. The ratio of the weight average to the number average of the particle radius was for most samples smaller than 1.01. For two samples we found higher values, viz. 1.02 (hematite, 100nm) and 1.13 (silica 80 nm). Extensive washing cycles were carried out by centrifuging and resuspending the sol in de-ionized water

adjusted to varying pH values and finally at neutral pH. This procedure was followed in order to remove impurities and to reduce the ionic strength. Sols of high volume fraction and low conductivity (approximately equivalent to 10^{-4} M KCl solution) obtained in this way were diluted with de-ionized water and the pH and ionic strength adjusted to the desired values prior to the measurement of the dielectric response. The electrophoretic mobility was measured with the Zetasizer III of Malvern Instruments Limited. The water used was deionized and purified by a Millipore Super Q system.

Dielectric spectroscopy. A four-electrode technique, in principal similar to the one described by Myers and Saville (26), was used to measure the complex conductivity of the sols in the frequency range of 100Hz-500kHz. Their method was designed to measure frequency-difference spectra and therefore they applied a composite current to their cell by summing two sine waves; one at measuring frequency ω and the second at reference frequency ω_r . Unlike their approach, we applied one frequency at a time. The time needed for one complete frequency scan took less than about 2 minutes and therefore problems connected to the drift in the conductivity were avoided. A home-built signal-processing circuit was connected to the cell which allowed the use of a commercial frequency response analyzer (Solartron 1255 HF Frequency Response Analyzer) to interpret the signals. The temperature was maintained at 25 ± 0.05 °C by a temperature-controlled air stream. All the electrodes used were made of blank platinum foil; blackening the electrodes had no effects on the results. The amplitude of the applied field strength was approximately $13V/m$.

The cell was constructed in such a way that relaxation spectra in a wide frequency range could be obtained. This objective appeared to conflict with the accuracy of the absolute permittivity values, probably due to effects of stray capacitances. Although, in the frequency range applied, the capacitance of an electrolyte solution ought to be constant (2), our results showed a clear frequency dependence. This dependence, which became troubling especially at frequencies lower than 800 Hz, could to a certain extent be influenced by the changing the shielding of the cell. Moreover, it was a function of the pH and the ionic strength of the solution. By subtracting the spectrum of an appropriate blank, i.e. an electrolyte solution with the pH and ionic strength adjusted to that of the sample, the spectrum was corrected for this non-ideality.

The cylindrical flow-through cell could be, without changing the experimental set-up, alternatively filled by a tube pump with sample and blank from two supply bottles. During the course of the experiment, this set-up allowed us to adjust easily the pH or ionic strength, the former was adjusted with KOH and/or HCl, the latter with KCl. The values of the pH and the ionic strength ($[KCl] \leq 2 \cdot 10^{-3} M$) were chosen within a certain range in order to keep the signal to noise ratio sufficiently high. The choice of KCl as the indifferent electrolyte has been made since the small difference between the friction coefficients of K^+ and Cl^- simplifies the theoretical interpretation. At least during two hours prior to the measurement, the sample in the supply bottle was continuously purged with nitrogen.

In most cases, the complex conductivity was measured as a function of the volume fraction ϕ of the particles by adding blank to the sample. Volume fractions up to 6% were studied and no non-linear effects with ϕ were observed. These fractions were calculated from the weight fractions by assuming certain values for the density of the particles. Like Rosen and Saville (19), the density of silica was taken to be 2.0 g/ml, a value assuming 10% porosity. The density of hematite was taken as 5.0 g/ml, which is roughly 5% smaller than the reported value of 5.24% of crystalline hematite (27). For a detailed description of the dielectric spectrometer, see ref. (28).

Theoretical background

Dielectric spectroscopy involves the measurement of the frequency dependence of the complex conductivity K^* of a system, defined by

$$I = K^* E \quad [1]$$

where $I = I_0 e^{i\omega t}$ is the macroscopic current density, $E = E_0 e^{i\omega t}$ the macroscopic applied electric field strength and ω the angular frequency of the field. Formally, K^* can be written as

$$K^* = \sigma + i\omega\epsilon_0\epsilon_r \quad [2]$$

The complex dielectric constant ϵ^* is simply related to K^* by $\epsilon^* = K^*/i\omega$. Here, σ is the conductivity, ϵ_0 and ϵ_r the absolute and relative permittivity, respectively, and $i = \sqrt{-1}$. Dielectric dispersion occurs, i.e.

σ and ϵ_r become frequency dependent, when relaxation mechanisms are present in the system which react at a finite rate to the alternating electric field.

In sols, the relaxation mechanism of interest is the polarization of the electric double layer. The applied field causes the centre of the counter charge in the double layer to displace from the centre of the surface charge. The electric field arising from this charge redistribution can be described by the induced dipole moment and it determines the dielectric response. Moreover, it will retard the electrophoretic mobility u_{el} . The dipole coefficient C_0 contains information about the double layer structure. For dilute sols, theoretical analyses (10, 29) have shown that C_0 can be quite simply related to the complex conductivity increment ΔK^*

$$\Delta K^* \equiv K_{sol}^* - K_\infty^* = 3\phi C_0 K_\infty^* \quad [3]$$

where the subscript " ∞ " indicates the background electrolyte quantity and ϕ the volume fraction of the particles.

Convenient parameters to describe the frequency dependence of the response are the conductivity increment $\Delta\sigma$ and the dielectric increment $\Delta\epsilon_r$, defined by

$$\Delta\sigma = \sigma(\omega) - \sigma(\omega^0) \quad [4]$$

$$\Delta\epsilon_r = \epsilon_r(\omega) - \epsilon_r(\omega^\infty) \quad [5]$$

where ω^0 represents the lowest measurement frequency and ω^∞ the highest.

The quantities $\Delta\sigma$ and $\Delta\epsilon_r$ can be determined by measuring the response at different frequencies. Their determination does not require any knowledge about the composition of the background electrolyte solution. In contrast, a very accurate knowledge of the conductivity σ_∞ of the background solution is necessary to determine the static conductivity increment $\Delta\sigma_{stat} = (\sigma_{susp} - \sigma_\infty)/\phi\sigma_\infty$ (6, 30). Consequently, the

interpretation of $\Delta\sigma_{stat}$ is much more sensitive to small errors in the knowledge of σ_{∞} than the interpretation of the dielectric increments.

Kramers-Kronig relations

Although in the field of colloid chemistry the term "dielectric relaxation" is commonly used to describe the frequency dependence of the increments $\Delta\epsilon_r$ and $\Delta\sigma_r$, one could argue that the term "conductivity relaxation" might be more appropriate. In physical terms, dielectric relaxation refers to the behaviour of orientational polarization of molecules in a time-dependent field, whereas processes concerning translations of charged particles are attributed to a conductivity K_v^* (31). When it takes a certain time for the "translational" current to adjust to a time-variant electric field, this quantity becomes complex. In our frequency range of interest, relaxation of the orientational polarization of individual molecules is absent. Hence, $\Delta\epsilon_r$ in colloids is a consequence of conduction processes. Therefore, we can write

$$K_v^* = \sigma + i\omega\epsilon_0\Delta\epsilon_r \quad [6]$$

As the frequency dependence of the real and imaginary part of K_v^* are determined by one and the same physical process, general relations exist between the two of them: the Kramers-Kronig equations (32, 33). These equations permit one to calculate either part of K_v^* at any frequency if the other part is known at all frequencies. However, the complicated nature of the numerical analyses and, in most cases, the restricted amount of experimental data prevent wide application of these relations. Nevertheless, the numerical complications (partially) disappear if one is merely interested in calculating the difference in the plateau values of one increment from the dispersion curve of the other. In our case, the Kramers-Kronig relations then reduce to

$$\lim_{\omega \rightarrow 0} \Delta\epsilon_r \equiv \Delta\epsilon_r(0) = \frac{2}{\pi\epsilon_0} \int_0^\infty \frac{\Delta\sigma}{\omega^2} d\omega \quad [7]$$

and

$$\Delta\sigma(\omega^\infty) = \frac{2\epsilon_0}{\pi} \int_0^{\omega^\infty} \Delta\epsilon_r d\omega \quad [8]$$

where the upper boundary of the integration ω^∞ is a frequency in the high-frequency limit of the low-frequency dispersion regime. If sufficient experimental data are at hand, these relations can be used as a model-independent check for their internal consistency.

Classical electrokinetic theory

Interpretation of the complex dipole coefficient C_0 in terms of intrinsic sol parameters has been the subject of many studies (10, 29, 34-37). In dilute sols with thin double layers, i.e. $\kappa a \gg 1$ with κ^{-1} the Debye length and a the particle radius, two dispersion regimes can be distinguished: the low-frequency and the high-frequency dielectric dispersion (34). The former occurs at frequencies of order $kT/\beta^\infty a^2$, i.e. for particles of colloidal size approximately in the range of $10^2 - 10^5$ Hz. Here, β^∞ is the ion friction coefficient in the background electrolyte solution, k the Boltzmann constant and T the absolute temperature.

The high-frequency dispersion occurs at frequencies of order $kT\kappa^2/\beta^\infty$, i.e. for 10^{-3} M KCl at approximately 10^7 Hz. It can be described by the model of O'Konski (38), which is a Maxwell-Wagner type of theory which accounts for the excess conduction inside the double layer. In the high-frequency range, long-range perturbations in the electrolyte density outside the double layer may be neglected (34). However, long-range concentration gradients do occur at low frequencies, affecting the polarization state of the double layer. The frequency-dependence of their magnitude creates the low-frequency dispersion (29). With decreasing κa , the two dispersion regimes will gradually merge. The remainder of this section will be restricted to the low-frequency dispersion of dilute sols.

The first numerical calculations for the low-frequency dielectric response using the classical electrokinetic model have been given by DeLacey and White (10). The clear distinction between the two dispersion regimes for sols with thin double layers also lead to

significant analytical progress. Dukhin et al. (29, 39, 40) and, more recently, Fixman (36, 37) presented a thin double layer theory for dilute sols. Both theories are based on a local equilibrium approximation and are restricted to symmetrical electrolytes with both types of ions having the same friction coefficient. Comparison between these analytical and the numerical results showed good agreement (7, 37). From Fixman's theory, one can, to a good approximation, deduce for the frequency dependencies of $\Delta\epsilon_r$ and $\Delta\sigma$

$$\Delta\epsilon_r = f \frac{1}{(1 + \omega\tau)(1 + \sqrt{\omega\tau})} \quad [9]$$

and

$$\Delta\sigma = g \frac{\omega\tau\sqrt{\omega\tau}}{(1 + \omega\tau)(1 + \sqrt{\omega\tau})} \quad [10]$$

where $\tau = \beta a^2 / 2kT$. The absolute values of these increments are determined by f and g , which are both functions of the equilibrium double layer structure, the types of ions in the system and κa .

As mentioned, the low-frequency dispersion is governed by relaxation processes which are diffusion controlled and which do not obey an exponential decay. Previous investigations (41, 42) used the empirical Cole-Cole equation (43) to interpret the relaxation behaviour of latices. However, the Cole-Cole equation is devised to describe systems with a distribution of relaxation times, all of them representing a relaxation mechanism with an exponential decay function. For the case of a single relaxation time, the Cole-Cole equation reduces to the following pair of Debye equations

$$\Delta\epsilon_r \propto \frac{1}{1 + \omega^2\tau^2}, \quad \Delta\sigma \propto \frac{\omega\tau}{1 + \omega^2\tau^2} \quad [11]$$

It is evident that the graphs for [9] and [10] are much more extended with respect to the frequency axis than those for [11]. The presence of a distribution of relaxation times flattens the graphs.

Consequently, interpretation of dielectric data with the Cole-Cole equation always leads to the conclusion that the system contains a distribution of relaxation times. Clearly, no large relevance should be assigned to this conclusion, since some diffusion process may be operative.

Surface conduction

In a previous paper (7), we have extended the theory of Fixman to incorporate surface conduction. As shown theoretically, the influence of this transport mechanism on the electrophoretic mobility and the dielectric response can be quite large. For example, at given ζ potential, it leads to a reduction of u_{el} and to an increase of $\Delta\epsilon_r$ and $\Delta\sigma$. The extension of the theory with surface conduction is accompanied by the introduction of two new parameters I_1^s and I_2^s , defined by

$$I_i^s = \kappa \int_0^{B_1} \left(\frac{\beta_i^\infty c_i}{\beta_i c_i} - 1 \right) dx \quad [12]$$

whereby c_i and β_i are the local concentration and the local friction coefficient of ion i , respectively, and the superscript " ∞ " indicates the corresponding values in the bulk solution. The integration is carried out across the stagnant layer from the particle surface ($x=0$) to the position of the slip plane ($x=B_1$). The diffuse part of the double layer is located beyond this plane. Hence, I_i^s represents the contribution of ion i to the surface conductivity. Since the extended model applies to sols with thin double layers, the frequency dependence of the increments $\Delta\epsilon_r$ and $\Delta\sigma$, as given by [9] and [10], is retained.

The number of unknown parameters can be reduced if the surface conductivity is dominated by the excess amount of counterions within the slip plane, for example, when approximately $\zeta > 50\text{mV}$. The resulting set of parameters determining the electrokinetic response can then be given by β , κa , τ , ζ and Θ . Here, Θ equals the ratio between the excess charge density of counterions within the plane of shear σ_s and that in the diffuse part of the double layer $\sigma_{d,1}$.

$$\Theta = \sigma_s / \sigma_{d,i}$$

[13]

The charge density σ_s is linearly related to I_1^s . In principle, β , κa and τ are under experimental control, leaving only two unknown parameters characterizing the system. These parameters can be determined from a combination of electrophoresis and dielectric response data.

Fitting procedures

Two fitting procedures are used. The first procedure fits the increments $\Delta\epsilon_r$ and $\Delta\sigma$ to Fixman's theory, with ζ and τ as adjustable parameters. The parameters β and κa are supposed to be known, as they immediately follow from the electrolyte concentration and the particle radius $a(EM)$, as obtained by electron microscopy. The resulting values are designated by $\zeta(\Delta\epsilon_r)$, $\tau(\Delta\epsilon_r)$, $\zeta(\Delta\sigma)$ and $\tau(\Delta\sigma)$.

In principle, β and $a(EM)$ also determine the value of τ . Hence, the use of τ as an adjustable parameter requires some justification. Obviously, no problems appear if theory and experiment perfectly agree; the fitted value for τ will be consistent with the known values for β and $a(EM)$. However, in practice, the adjustability of τ appeared to be necessary to optimize the fit in a number of cases. A possible explanation could be that the effective particle size does not equal $a(EM)$, for example due to the presence of aggregates. To obtain a more consistent fit, the particle size or its distribution could be chosen instead of τ as a fitting parameter. Nevertheless, this approach was not pursued as no theory for systems with aggregates exists.

Clearly, by fitting either of the increments, the fitting procedure provides theoretical values for both types of increments. In the particular case that, for example, $\Delta\sigma$ is fitted, the obtained values for the dielectric increment will be designated as $\Delta\epsilon_r(\Delta\sigma)$. A comparison between $\Delta\epsilon_r(\Delta\sigma)$ and $\Delta\epsilon_r$ provides a check of the applicability of the theory.

The second procedure simultaneously fits the electrophoretic mobility and either the dielectric or the conductivity increment. It applies the extended theory of Fixman with ζ , Θ and τ as adjustable

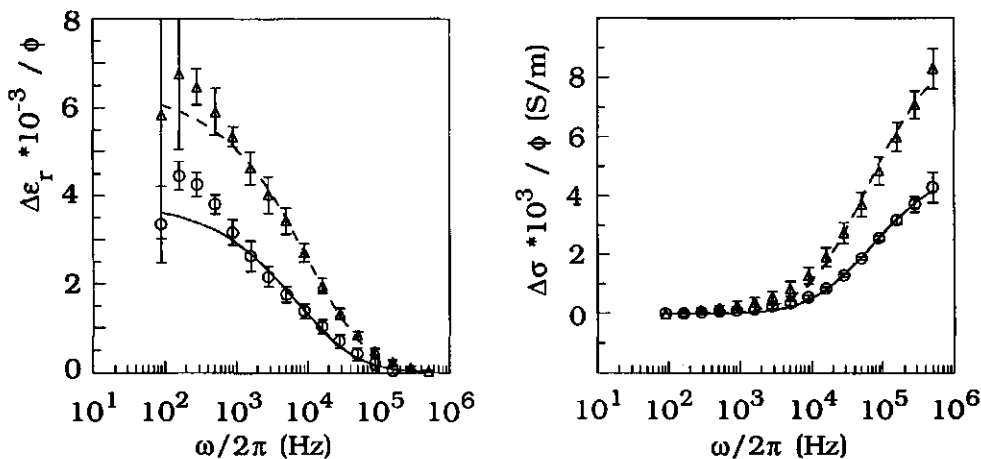


Figure 1. Dispersion of normalized dielectric increment $\Delta\epsilon_r/\phi$ and conductivity increment $\Delta\sigma/\phi$ for hematite sols in KCl as a function of κa . $a=100\text{nm}$, (\circ) $\text{pH}=6.0$, $\kappa a=6$, (Δ) $\text{pH}=6.1$, $\kappa a=12$. Drawn and dashed lines are fitted curves. Explanation see text.

parameters. The resulting value for ζ is denoted as ζ_{comb} . In all other aspects, this procedure resembles the previous one.

Results and discussion

The influence of κa and the pH on the normalized increments $\Delta\epsilon_r/\phi$ and $\Delta\sigma/\phi$ of the hematite and silica sols are displayed in Figures 1-8. In some of the figures, error bars indicate the standard deviation. Most graphs also contain fitted curves, obtained according to the first fitting procedure. The fitted values $\tau(\Delta\epsilon_r)$ and $\tau(\Delta\sigma)$ are displayed as function of $a(\text{EM})$ in Figure 9. No non-linearities in the dependence on ϕ were observed, which justifies the interpretation of the data using a theory for dilute sols.

According to the theory, the particle radius a follows from the fitted value for τ and the ion friction coefficient. In all the calculations, this coefficient is taken as $\beta^*=2.055 \cdot 10^{-12}$, which is an appropriate figure for KCl at 25°C. The resulting values for $a(\Delta\epsilon_r)$ and $a(\Delta\sigma)$ are

listed in Table 1. This table also lists values for ζ and σ_d , as obtained from the first fitting procedure. Here, σ_d represents the total charge density in the diffuse part of the double layer which immediately follows from ζ .

Accuracy and reproducibility

To illustrate the required accuracy of the signal processing circuit, we consider a hematite sol from Fig. 1 with $\phi = 5\%$ and $\kappa a = 12$. At 500 Hz, we have $\epsilon_r = 350$ and $\sigma \approx 2 \cdot 10^{-2}$ S/m, giving a phase angle $\delta = \arctan(\sigma/\omega\epsilon_0\epsilon_r) \approx 89.97^\circ$. Hence, the accuracy should be within approximately $(3 \cdot 10^{-3})^\circ$ for an uncertainty in $\Delta\epsilon_r$ of less than 10%. In this particular case, the maximum value of $\Delta\sigma$ (at $\omega^* = 5 \cdot 10^5$ Hz) only contributes 2% to the total current density.

For silica and at frequencies smaller than 800 Hz, no well reproducible results could be obtained for the dielectric increment $\Delta\epsilon_r$. This problem occurred when the signal-to-noise ratio became extremely small and is probably due to a systematic error. Therefore the theoretical curves for $\Delta\epsilon_r/\phi$ were determined by fitting the experimental data at frequencies higher than 800 Hz. For convenience, this procedure has also been applied to the hematite sols. No similar problems occurred for the conductivity dispersion. Hence the theoretical curves for $\Delta\sigma/\phi$ were obtained by fitting the complete conductivity spectra. In the frequency ranges of the fits, the standard deviations of the increments create an uncertainty in the fitted parameters of approximately less than 5%.

A systematic error in the ζ potential exists due to the uncertainty of the specific density of the particles which is necessary to calculate the volume fraction. Fortunately, the dielectric response is much more sensitive to changes in the ζ potential than to changes in the volume fraction. For example, for sols with $\zeta = 3$, a 25% error in the volume fraction leads to an error in the ζ potential of less than 10%. Relatively, this error decreases with increasing potential.

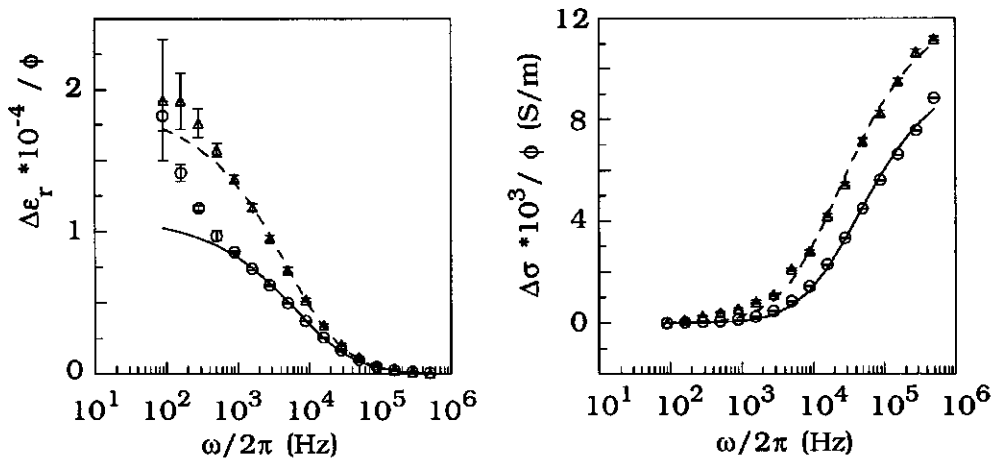


Figure 2. As Fig. 1 but for hematite sols with $a=257\text{nm}$, (\circ) $\text{pH}=4.9$, $\kappa a=15$, (Δ) $\text{pH}=5.0$, $\kappa a=31$.

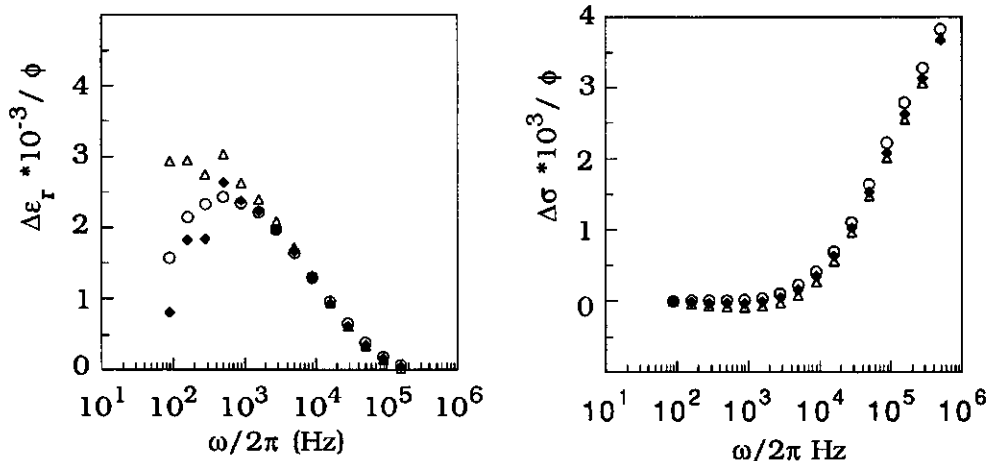


Figure 3. As Fig. 1 but for silica sols with $a=257\text{nm}$, $\text{pH}=7.5$, (\circ) $\kappa a=8$, (Δ), $\kappa a=14$, (\blacklozenge) $\kappa a=17$.

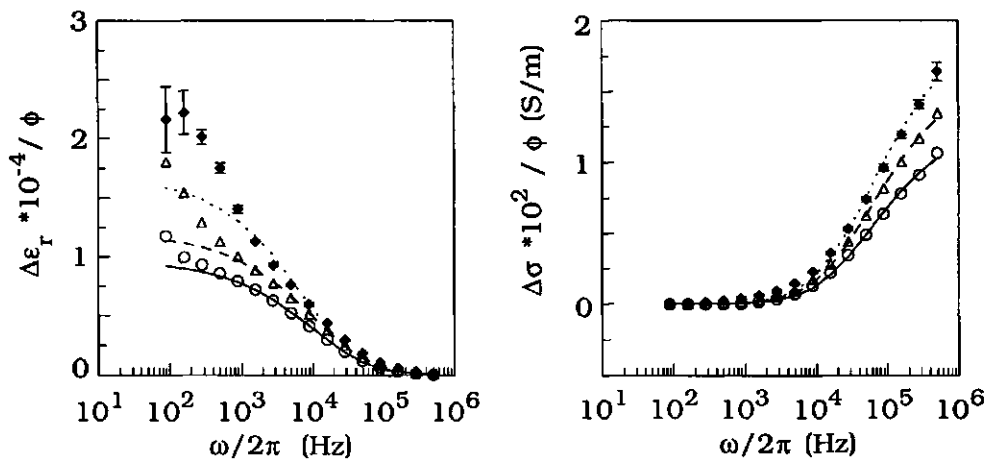


Figure 4. Dispersion of normalized dielectric increment $\Delta\epsilon_r/\phi$ and conductivity increment $\Delta\sigma/\phi$ for hematite sols in KCl as a function of pH. $a=184\text{nm}$, $\kappa a=22$, (○) pH=5.7, (Δ), pH=5.2, (♦) pH=4.3.

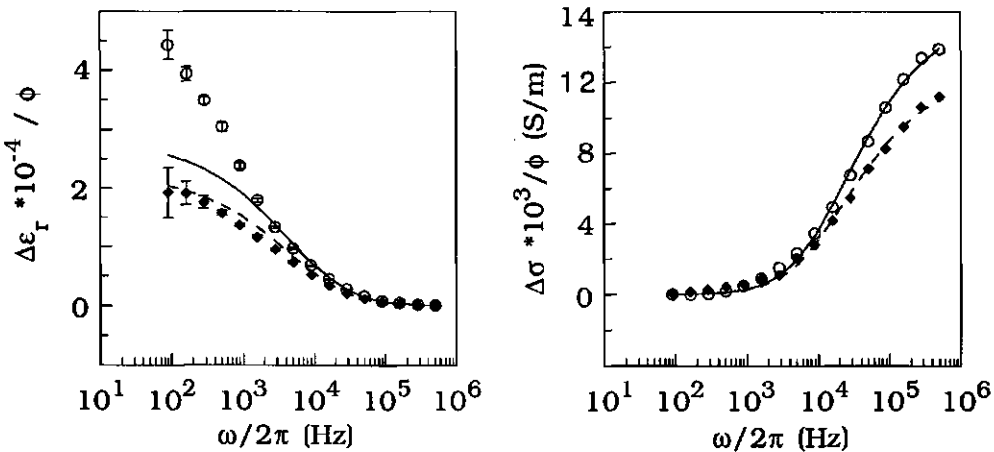


Figure 5. As Fig. 4 but for hematite sols with $a=257\text{nm}$, $\kappa a=31$, (○) pH=4.1, (♦), pH=5.0. In $\Delta\epsilon_r/\phi$ graph: (—) $\Delta\epsilon_r(\Delta\sigma)$, pH=4.1, (---) $\Delta\epsilon_r(\Delta\sigma)$, pH=5.0. Lines in $\Delta\sigma/\phi$ graph are corresponding fits, see text.

General features

As shown in the dispersion graphs, the experimental data of $\Delta\epsilon_r$ and $\Delta\sigma$ can be fitted well in the frequency range of the fitting procedure. Deviations occur between experimental and theoretical values for $\Delta\epsilon_r$, at frequencies smaller than 800 Hz. For silica, as mentioned, these deviations are experimental artefacts due to the low signal-to-noise ratio. However, for the hematite sols, this ratio was generally higher. Moreover, even for frequencies lower than 800 Hz, the dielectric increments $\Delta\epsilon_r$ of hematite appeared to be linearly dependent on the volume fraction. Hence, these deviations for hematite seem to be real and no technical artefacts. Both for silica and hematite, the fit of $\Delta\sigma$ was in most cases excellent over the complete frequency range.

A first glance at the results tells us that indeed the pH, κa and the particle radius are characteristic parameters. Figs. 1 and 2 show that, at constant pH, both $\Delta\epsilon_r$ and $\Delta\sigma$ of the hematite sols increase with κa . This in contrast with the increments of silica, which seem to be hardly affected by the value of κa , see Fig. 3. Quantitatively, both observations could be simply explained. An increase of the ionic strength leads to an increase of κa but, at the same time, it can lead to a decrease of the ζ potential. According to the classical theory, the former effect causes the dielectric response to increase, whereas the latter leads to a decrease. Experimentally, these two effects can be separated by adjusting the pH at constant ionic strength.

Figs. 4-8 show that, for both type of sols, the dielectric response always increases with increasing surface charge density. As for silica the pH values chosen are well above the i.e.p., the dielectric response increases with increasing the pH. This behaviour is clearly reflected in the obtained ζ potentials, which grow with increasing pH. For hematite, the pH values are lower than the i.e.p. and, hence, the dielectric response reduces with increasing pH. Indeed, the potentials $\zeta(\Delta\sigma)$ always increase with decreasing pH. However, this is not always true for the potentials $\zeta(\Delta\epsilon_r)$. According to Table 1, this behaviour is accompanied by large differences in the fitted values for $a(\Delta\epsilon_r)$ at the

different pH values. This is related to the fact that generally $a(\Delta\epsilon_r) > a(\Delta\sigma)$ and $\zeta(\Delta\epsilon_r) < \zeta(\Delta\sigma)$, a phenomenon which will be explained in the next section. For now, we only state that the values obtained from $\Delta\sigma$ better represent the single particle behaviour than those from $\Delta\epsilon_r$. Accepting this for the moment, Fig. 9 shows that $\tau(\Delta\epsilon_r)$ and especially $\tau(\Delta\sigma)$ strongly correlate with the square of $a(EM)$, as the theory predicts.

For latices, the influence of the particle size on the dielectric response has been shown before (41, 42). However, to the authors' knowledge, this is the first time that the influence of the surface charge density on the dielectric response has been observed without simultaneously changing other system parameters. Furthermore, in contrast with the results on latices, it is possible to explain the dielectric response of silica and hematite sols by assuming reasonable values for the ζ potential. In the subsequent sections, comparisons will be made between the parameter values obtained from $\Delta\epsilon_r$, $\Delta\sigma$ and those obtained electrophoretically.

Comparison between $\Delta\epsilon_r$ and $\Delta\sigma$

The Kramers-Kronig relations say that $\Delta\epsilon_r$ and $\Delta\sigma$ contain identical information about the intrinsic properties of the sol. Consequently, validity of the classical model would then imply that $\zeta(\Delta\epsilon_r) = \zeta(\Delta\sigma)$ and $a(\Delta\epsilon_r) = a(\Delta\sigma)$. Although in some cases this is approximately true, it is found in general that $a(\Delta\epsilon_r) > a(\Delta\sigma)$ and $\zeta(\Delta\epsilon_r) < \zeta(\Delta\sigma)$. At issue is now whether or not this is an experimental artefact or caused by a defect in the theory.

Let us first consider the experiments. Clearly, the standard deviation of the increments did not provide enough room to match $\zeta(\Delta\epsilon_r)$ and $\zeta(\Delta\sigma)$ on the one hand and $a(\Delta\epsilon_r)$ and $a(\Delta\sigma)$ on the other. Roughly, the standard deviations created an uncertainty in the fitted parameters too small to explain the observed differences. Further, for the hematite sols, a significant difference generally exists between the experimental data for $\Delta\epsilon_r$ and the fitted curves at frequencies lower

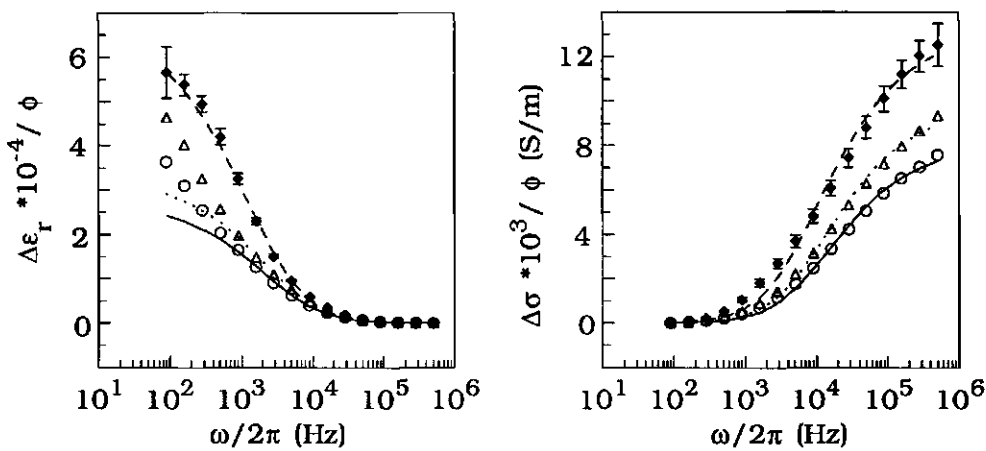


Figure 6. As Fig. 4 but for hematite sols with $a=336\text{nm}$, $\kappa a=40$, (o) pH=5.0, (Δ) pH=4.7, (\blacklozenge) pH=3.7.

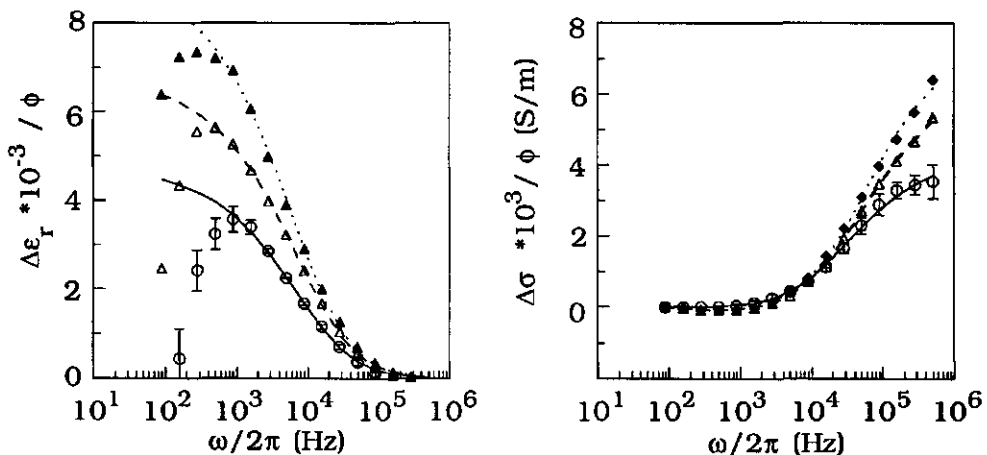


Figure 7. As Fig. 4 but for silica sols with $a=184\text{nm}$, $\kappa a=19$, (o) pH=7.5, (Δ) pH=8.2, (\blacklozenge) pH=8.6.

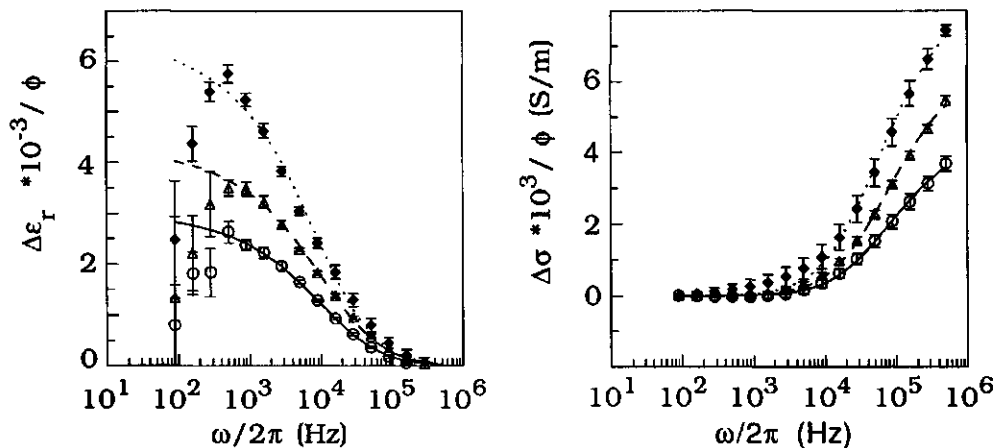


Figure 8. As Fig. 4 for silica sols with $a=132\text{nm}$, $\kappa a=17$, (○) pH=7.5, (△) pH=8.0, (◆) pH=8.6.

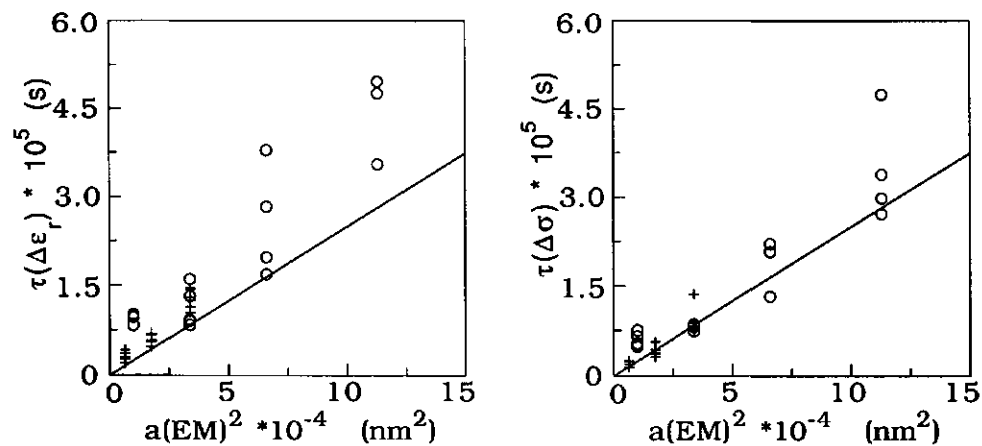


Figure 9. Dependence of τ on square particle radius $a(\text{EM})$; τ obtained from dispersion dielectric increment $\Delta\epsilon_r$ and conductivity increment $\Delta\sigma$ of hematite and silica sols. $\Delta\sigma$, (○) hematite, (+) silica, (—) theoretical prediction.

than approximately 1 kHz. A similar difference appears if the data for $\Delta\epsilon_r$ are compared to the theoretical values $\Delta\epsilon_r(\Delta\sigma)$, following from the fit of $\Delta\sigma$. This is illustrated for the hematite sol at pH=4.1 in Fig. 5. However, the same figure shows that reasonable agreement is obtained between $\Delta\epsilon_r$ and $\Delta\epsilon_r(\Delta\sigma)$ for the hematite sol at pH=5.0, indicating that the experimental data themselves are reliable.

The most rigorous test of the reliability of the experimental data is to check whether or not they obey the Kramers-Kronig equations [7] and [8]. In practice, this appeared not to be a very appropriate approach. Besides the fact that the experimental data only were available over a limited frequency window, the standard deviation of the results played a disturbing role. In particular, the integral of [7] is not dominated by the data of $\Delta\sigma$ with the relative highest accuracy. Consequently, the calculated values for $\Delta\epsilon_r(0)$ were quite meaningless. The evaluation of the integral of [8] suffered less from this problem; the calculated values for $\Delta\sigma(\omega^n)$ were, within approximately 15%, in agreement with the experimental ones. Here, we have another indication that the experimental data are consistent.

At this moment, it can be concluded that the theory for the electrokinetic behaviour of *homodisperse* sols fails to explain all our results. In fact, despite the narrow particle size distribution, the sols were not always homodisperse. In some cases, the presence of aggregates in the sol was observed, even for low pH values where the surface charge density is expected to be high. One possible explanation is that the formation of these aggregates is induced by the tube pump used to fill the dielectric cell.

Influence of aggregates

The theory for sols of solid spherical particles can be used to predict the dielectric behaviour of sols containing aggregates, by simulating them as large solid spheres. Hence, the response of such a sol follows from linear superposition of the increments of the various particle fractions. Figure 10 displays theoretical results for the

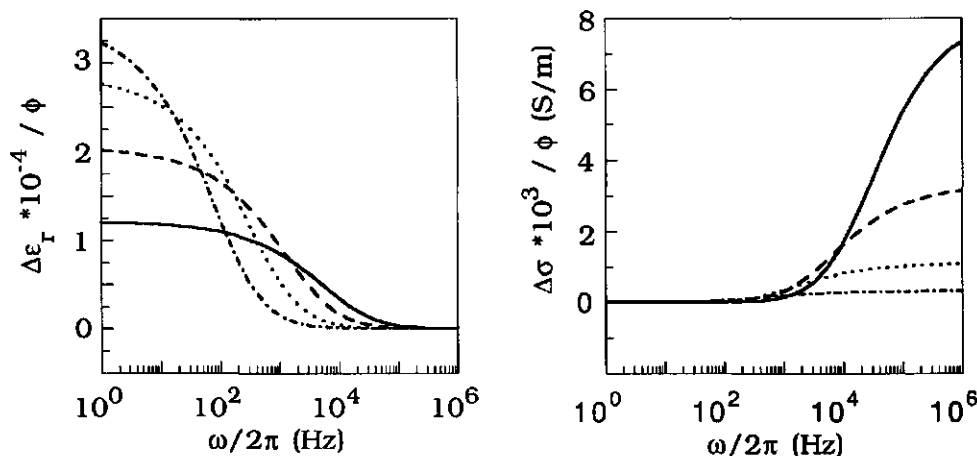


Figure 10. Computed dispersion of $\Delta\epsilon_r/\phi$ and $\Delta\sigma/\phi$ of homodisperse sols in KCl as a function of particle radius at constant ionic strength, results obtained with unmodified theory of Fixman. $\zeta=5$, (—) $a=250\text{nm}$, $\kappa a=30$, (---) $a=500\text{nm}$, $\kappa a=60$, (· · ·) $a=1\mu\text{m}$, $\kappa a=120$, (- · -) $a=2\mu\text{m}$, $\kappa a=240$.

dielectric increment $\Delta\epsilon_r$ and conductivity increment $\Delta\sigma$ as a function of the frequency for four different particle sizes. The ζ potential and the ionic strength are fixed to values which roughly agree with the experimental conditions for the hematite sample at pH=4.1 in Fig. 5: $\zeta=5$ and $\kappa a=30$ for $a=250\text{nm}$. In the high-frequency range where its particle size dependence is most significant, $\Delta\sigma$ increases with decreasing particle radius. At low frequencies, $\Delta\epsilon_r$ increases with growing particle radius whereas it does the opposite at high frequencies. Therefore, the increments of a heterodisperse sol are complicated weighted averages; the weighting factor is a sensitive function of the volume fraction, particle radius and frequency and it is very much different for $\Delta\epsilon_r$ and $\Delta\sigma$.

At issue is now what the fitting procedure would give if the sols were heterodisperse. Figure 11a shows the computed response of a half and half mixture of the two sols with $a=250\text{nm}$ and $a=1\mu\text{m}$ considered in Fig. 10. The fitted curves in Fig. 11 follow from the same fitting

procedure as that applied to the experimental data. In Fig. 11b the comparison between $\Delta\epsilon_r$ and $\Delta\epsilon_r(\Delta\sigma)$ as well as that between $\Delta\sigma$ and $\Delta\sigma(\Delta\epsilon_r)$ is made. The values obtained for the fitting parameters are: $\zeta(\Delta\epsilon_r) = 3.6$, $\zeta(\Delta\sigma) = 4.1$, $a(\Delta\epsilon_r) = 437\text{nm}$ and $a(\Delta\sigma) = 286\text{nm}$. Despite the simplicity of this model, its qualitative behaviour is strikingly in agreement with the experimental results. First, the same differences are found between the actual and fitted values for $\Delta\epsilon_r$ at low frequencies. Second, this deviation is also retrieved in the comparison between $\Delta\epsilon_r$ and $\Delta\epsilon_r(\Delta\sigma)$, see Fig. 5a. Third, the values for the fitting parameters obtained for the theoretical mixture agree with the experimental fact that generally $a(\Delta\epsilon_r) > a(\Delta\sigma)$ and $\zeta(\Delta\epsilon_r) < \zeta(\Delta\sigma)$.

The following conclusions can now be drawn. The apparent inconsistency between the experimental data for $\Delta\epsilon_r$ and $\Delta\sigma$ is probably caused by the presence of aggregates. Hence, the spread in the data for $a(\Delta\epsilon_r)$ and $a(\Delta\sigma)$, as shown in Fig. 9, likely follows from the fact that the extent of aggregation was not sufficiently under experimental control. If aggregates are present, both $a(\Delta\epsilon_r)$ and $a(\Delta\sigma)$ are too high whereas $\zeta(\Delta\epsilon_r)$ and $\zeta(\Delta\sigma)$ are too low. The mutual differences between these estimates provides information about the extent to which the aggregates thwarts the interpretation. For heterodisperse sols, the dispersion of $\Delta\sigma$ is especially dominated by the smallest particles in the system. This leads to the fact that $a(\Delta\sigma)$ and $\zeta(\Delta\sigma)$ provide better estimates for the single particle radius and the ζ potential than $a(\Delta\epsilon_r)$ and $\zeta(\Delta\epsilon_r)$, respectively, a conclusion that we already used before.

In some previous investigations on the dielectric response of latices, a discrepancy between the experimental and theoretical values for the characteristic frequency was observed (11, 19). This may also be caused by a certain extent of aggregation. Unfortunately, these publications neither provide information about possible aggregation nor give a detailed comparison between $\Delta\epsilon_r$ and $\Delta\sigma$. However, for latices such discrepancy is not always found. Apart from the magnitude of the response, which was too large to be adequately explained, Springer et al. (3) and Lyklema et al. (17) obtained reasonable agreement between the experimental and theoretical values for the characteristic frequency.

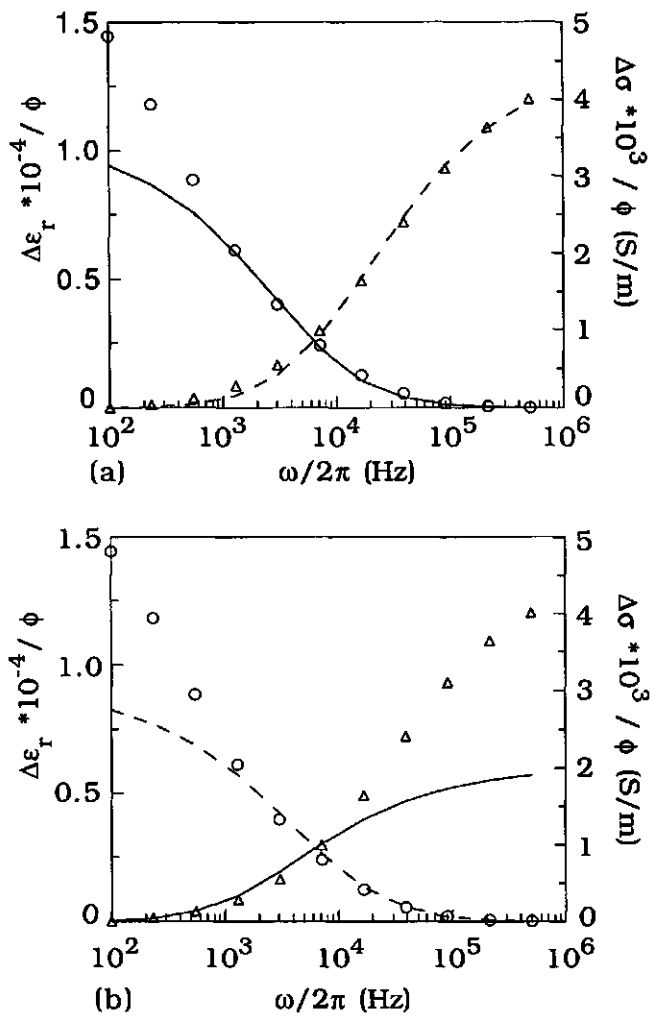


Figure 11. a Computed dispersion of half and half mixture of two sols considered in Fig. 10 with $a=250\text{nm}$ and $a=1\mu\text{m}$. (○) $\Delta\epsilon_r/\phi$, (△) $\Delta\sigma/\phi$. Drawn and dashed lines are fitted curves. b Same as a but (—) $\Delta\sigma(\Delta\epsilon_r)$ and (---) $\Delta\epsilon_r(\Delta\sigma)$. Explanation see text.

Nevertheless, in connection with the observed counterion specificity and the distribution of relaxation times, they mentioned the possibility of slight coagulation. Moreover, they also suggest that it may be invoked to explain the semicircularity of the Cole-Cole plots. However, according to the objections raised in the theoretical section, such a shape of the Cole-Cole plot does not provide sound evidence for slight aggregation.

Comparison with mobilities

The electrophoretic mobility has been measured as a function of the pH for one hematite ($a=257\text{nm}$) and one silica sample ($a=184\text{nm}$). The dielectric response of the hematite sample at pH=5.0 significantly differed from that at pH=4.1. However, the mobility was approximately constant in this pH range, i.e. $u_{el}=3.5\pm0.2*10^{-8}\text{m}^2/\text{Vs}$ at $\kappa a=31$. The same was observed for silica; in the pH range from 7.4 til 8.6 the dielectric response increased while the mobility had reached a plateau value, i.e. $u_{el}=4.0\pm0.2*10^{-8}\text{m}^2/\text{Vs}$ at $\kappa a=19$.

The estimate ζ_{el} is determined from the electrophoretic mobility by using the unmodified thin double layer theory of Fixman. As shown in Table 2, for both silica and hematite and for all pH values, the value for ζ_{el} is much smaller than $\zeta(\Delta\epsilon_r)$ or $\zeta(\Delta\sigma)$. Obviously, the classical theory is also not applicable to these sols. However, these results are typical for sols which exhibit surface conduction (7). Hence, the second fitting procedure is used to determine ζ_{comb} and Θ . The results are listed in Table 2, which also shows the corresponding values for σ_s and σ_d .

The high values obtained for Θ show that the electrokinetic properties are greatly affected by the presence of surface conduction. As surface conduction leads to an increase of the dielectric response and a decrease of the mobility, it is generally found that $\zeta(\Delta\epsilon_r)=\zeta(\Delta\sigma)>\zeta_{comb}>\zeta_{el}$. We observe that ζ_{el} and especially $\zeta(\Delta\epsilon_r)$ and $\zeta(\Delta\sigma)$ provide poor estimates for ζ_{comb} . For silica, the absolute differences between ζ_{el} and ζ_{comb} as well as those between $\zeta(\Delta\epsilon_r)$ and ζ_{comb} are roughly in the order of 25 mV, depending on the pH. For hematite, the differences

Tabel 1. Results of fitting dielectric spectra silica and hematite.Silica: $a=132\text{nm}$, $[\text{KCl}]=1.6 \cdot 10^{-3}\text{M}$, $\kappa a = 17$.

pH	$\zeta(\Delta\epsilon_r)$	$a(\Delta\epsilon_r)^{(1)}$	$\sigma_d(\Delta\epsilon_r)^{(2)}$	$\zeta(\Delta\sigma)$	$a(\Delta\sigma)^{(1)}$	$\sigma_d(\Delta\sigma)^{(2)}$
7.5	2.8	165	0.9	3.0	135	1.0
8.0	3.2	171	1.1	3.5	142	1.3
8.6	3.4	197	1.2	3.8	175	1.6

Silica: $a=184\text{nm}$, $[\text{KCl}]=1.0 \cdot 10^{-3}\text{M}$, $\kappa a = 19$.

pH	$\zeta(\Delta\epsilon_r)$	$a(\Delta\epsilon_r)^{(1)}$	$\sigma_d(\Delta\epsilon_r)^{(2)}$	$\zeta(\Delta\sigma)$	$a(\Delta\sigma)^{(1)}$	$\sigma_d(\Delta\sigma)^{(2)}$
7.5	3.7	205	1.2	3.6	233	1.1
8.2	4.1	215	1.5	4.3	178	1.6
8.6	4.3	241	1.6	4.6	173	1.8

Hematite: $a=184\text{nm}$, $[\text{KCl}]=1.3 \cdot 10^{-3}\text{M}$, $\kappa a = 22$.

pH	$\zeta(\Delta\epsilon_r)$	$a(\Delta\epsilon_r)^{(1)}$	$\sigma_d(\Delta\epsilon_r)^{(2)}$	$\zeta(\Delta\sigma)$	$a(\Delta\sigma)^{(1)}$	$\sigma_d(\Delta\sigma)^{(2)}$
4.3	5.2	254	2.8	6.4	185	5.2
5.2	5.6	193	3.5	5.9	180	4.0
5.7	5.0	198	2.6	5.3	173	3.0

Hematite: $a=257\text{nm}$, $[\text{KCl}]=1.3 \cdot 10^{-3}\text{M}$, $\kappa a = 31$.

pH	$\zeta(\Delta\epsilon_r)$	$a(\Delta\epsilon_r)^{(1)}$	$\sigma_d(\Delta\epsilon_r)^{(2)}$	$\zeta(\Delta\sigma)$	$a(\Delta\sigma)^{(1)}$	$\sigma_d(\Delta\sigma)^{(2)}$
4.1	5.6	393	3.6	6.4	290	5.2
5.0	5.6	282	3.5	5.9	288	4.0

Hematite: $a=336\text{nm}$, $[\text{KCl}]=1.3 \cdot 10^{-3}\text{M}$, $\kappa a = 40$.

pH	$\zeta(\Delta\epsilon_r)$	$a(\Delta\epsilon_r)^{(1)}$	$\sigma_d(\Delta\epsilon_r)^{(2)}$	$\zeta(\Delta\sigma)$	$a(\Delta\sigma)^{(1)}$	$\sigma_d(\Delta\sigma)^{(2)}$
3.7	6.0	565	4.2	6.5	436	5.4
4.7	5.5	446	3.4	5.9	368	4.1
5.0	5.2	437	2.9	5.5	345	3.5

⁽¹⁾ calculated from τ , ⁽²⁾ in $\mu\text{C}/\text{cm}^2$.

Table 2. Surface conduction in silica and hematite sols.2a Silica: $a=184\text{nm}$, $u_{el}=4.0$ ($10^{-8}\text{m}^2/\text{Vs}$), $\kappa a=19$ and $\zeta_{el}=2.3$.

Combination u_{el} and $\Delta\epsilon_r$.							
pH	$\zeta(\Delta\epsilon_r)$	ζ_{comb}	$a^{(1)}$ nm.	Θ	$\sigma_d^{(2)}$	$\sigma_s^{(2)}$	
7.4	3.7	2.7	200	1.2	0.7	0.6	
8.2	4.1	2.9	215	1.6	0.8	1.0	
8.6	4.3	3.0	240	1.7	0.8	1.0	

Combination u_{el} and $\Delta\sigma$.

pH	$\zeta(\Delta\sigma)$	ζ_{comb}	$a^{(1)}$ nm.	Θ	$\sigma_d^{(2)}$	$\sigma_s^{(2)}$	
7.4	3.6	2.7	224	1.2	0.7	0.6	
8.2	4.3	3.0	178	1.7	0.8	1.1	
8.6	4.6	3.1	175	1.9	0.9	1.3	

2b Hematite: $a=257\text{nm}$, $u_{el}=3.5$ ($10^{-8}\text{m}^2/\text{Vs}$) $\kappa a=31$ and $\zeta_{el}=1.8$ Combination u_{el} and $\Delta\epsilon_r$.

pH	$\zeta(\Delta\epsilon_r)$	ζ_{comb}	$a^{(1)}$ nm.	Θ	$\sigma_d^{(2)}$	$\sigma_s^{(2)}$	
5.0	5.6	2.8	282	5.8	0.8	3.8	
4.1	5.6	2.8	393	5.9	0.8	3.9	

Combination u_{el} and $\Delta\sigma$.

pH	$\zeta(\Delta\sigma)$	ζ_{comb}	$a^{(1)}$ nm.	Θ	$\sigma_d^{(2)}$	$\sigma_s^{(2)}$	
5.0	5.9	2.9	288	6.2	0.9	4.4	
4.1	6.4	3.2	290	7.0	1.0	6.0	

⁽¹⁾ calculated from τ , ⁽²⁾ in $\mu\text{C}/\text{cm}^2$.

between ζ_{el} and ζ_{comb} are approximately the same, whereas those between ζ_{comb} and either $\zeta(\Delta\epsilon_r)$ or ζ_{comb} are as large as 75 mV.

The sum of σ_s and σ_d provides an estimate of the titratable surface charge density σ_0 . Values for σ_0 are reported for hematite in the order of $10\mu C/cm^2$ (44), whereas for Stöber silica values of the order of $100\mu C/cm^2$ are obtained (45). These values refer to experimental conditions comparable to those of the samples in Table 2. Hence, the results suggest that $\sigma_s + \sigma_d < \sigma_0$. The most obvious explanation for this discrepancy is the low mobility of counterions within the plane of shear. The lower their mobility, the less they affect the electrokinetic properties.

Remarkable is that the values for Θ of hematite are substantially higher than those of silica, a difference which is not expected on the basis of the titratable surface charge densities. A further explanation of this difference requires a detailed discussion of the mechanism of surface conduction on oxides, which is probably very much different from that for latices. Possible mechanisms could involve particle roughness, porosity and a gel structure on the surface. For the moment our main conclusion is that differences in surface structure can be detected electrokinetically, provided that surface conduction is properly accounted for. Furthermore, it is interesting that charging the particle leads to an increase of Θ . This illustrates a well-known screening feature; with increasing surface charge density screening occurs relatively closer to the surface, i.e. in our case especially within the plane of shear.

Our observation that silica exhibits surface conduction at high pH values does not stand alone. Experiments by Van Der Linde and Bijsterbosch (5) on the electrical conductivity of plugs show that not only for latices but also for silica at pH=8.5 a mechanism of surface conduction appears to be operative. Hence, the picture is emerging that the phenomenon of surface conduction is general rather than exceptional.

Conclusions

From the present study of electrokinetic properties of silica and hematite sols, the following conclusions can be drawn:

- Reliable data on the dielectric response of dilute sols can be obtained by the application of a four-electrode technique. However, the choice of the system parameters, in our case pH and ionic strength, is restricted in order to keep the signal-to-noise ratio sufficiently high.
- The dielectric response of both oxides is a function of pH (surface charge density), κa and the particle radius. In accordance with theory, the dielectric response is an increasing function of the surface charge density at constant ionic strength.
- The frequency dependence of the response of hematite and silica sols is in fair agreement with theoretical prediction.
- The presence of aggregates can be deduced from a comparison between the dielectric increment $\Delta\epsilon$, and the conductivity increment $\Delta\sigma$. If aggregates are present, the latter provides a better estimate of the single particle size than the former.
- For both sols, ζ potentials were estimated from the data by neglecting a possible surface conduction contribution. The resulting values obtained from the dielectric measurements were systematically higher than those obtained from the electrophoretic mobility. This result is typical for sols which exhibit surface conduction.
- An extension of the Fixman model is used to quantify the effects of surface conduction and to obtain better estimates for the ζ potential. These estimates differ markedly from those obtained from either the dielectric response or electrophoretic mobility. For example, the improved estimate ζ_{comb} is typically 25 mV higher than the estimate ζ_{el} obtained from the mobility. Moreover, the surface conductivity increases with growing surface charge density and it is substantial higher for hematite than for silica. This reflects the difference in the surface structure of hematite and silica.

Finally, we may mention that the classical electrokinetic model is devised to interpret electrokinetic measurements only in terms of

diffuse double-layer properties. However, our results and those of others clearly show that this model cannot explain the electrokinetic behaviour of important colloids such as latices and oxides; different sol properties yield different values of ζ . This proves that the electrokinetic properties of sols contain more information than just about the diffuse part of the double layer. Obviously, this information can only be extracted if data are available on various electrokinetic properties. Unless surface conduction has been shown to be unimportant, care has to be taken in interpreting only one single electrokinetic property.

References

- (1) O'Brien, R. W. and Perrins, W. T., *J. Colloid Interface Sci.* **99**, 20 (1984).
- (2) Springer, M. M., Ph. D Thesis, Wageningen University, 1979.
- (3) Springer, M. M., Korteweg, A. and Lyklema, J., *J. Electroanal. Chem.* **153**, 55 (1983).
- (4) Zukoski IV, C. F. and Saville, D. A., *J. Colloid Interface Sci.* **114**, 45 (1986).
- (5) Linde v. d., A. J. and Bijsterbosch, B. H., *Croatica Chem. Acta* **63**, 455 (1990).
- (6) Put v. d., A. G., Ph. D. Thesis, Wageningen University, 1980.
- (7) Kijlstra, J., van Leeuwen, H. P. and Lyklema, J., accepted *J. Chem. Soc., Faraday Trans.* **2** (1992).
- (8) Wiersema, P. H., Loeb, A. L. and Overbeek, J. T. G., *J. Colloid Interface Sci.* **22**, 78 (1966).
- (9) O'Brien, R. W. and White, L. R., *J. Chem. Soc., Faraday Trans.* **274**, 1607 (1978).
- (10) DeLacey, E. H. B. and White, L. R., *J. Chem. Soc., Faraday Trans.* **277**, 2007 (1981).
- (11) Meyers, D. F. and Saville, D. A., *J. Colloid Interface Sci.* **131**, 448 (1989).
- (12) Put v. d., A. G. and Bijsterbosch, B. H., *J. Colloid Interface Sci.* **92**, 499 (1983).
- (13) Zukoski IV, C. F. and Saville, D. A., *J. Colloid Interface Sci.* **107**, 322 (1985).
- (14) Marlow, B. J. and Rowell, R. L., *Langmuir* **7**, 2970 (1991).
- (15) Elimelech, M. and O'Melia, C. R., *Colloids and Surfaces* **44**, 165 (1990).
- (16) Midmore, B. R. and Hunter, R. J., *J. Colloid Interface Sci.* **122**, 521 (1988).
- (17) Lyklema, J., Springer, M. M., Shilov, V. N. and Dukhin, S. S., *J. Electroanal. Chem.* **198**, 19 (1986).

- (18) Rosen, L. A. and Saville, D. A., *J. Colloid Interface Sci.* **140**, 82 (1990).
- (19) Rosen, L. A. and Saville, D. A., *Langmuir* **7**, 36 (1991).
- (20) Rosen, L. A. and Saville, D. A., *J. Colloid Interface Sci.* **149**, 542 (1992).
- (21) Zukoski IV, C. F. and Saville, D. A., *J. Colloid Interface Sci.* **114**, 32 (1986).
- (22) Voegtli, L. P. and Zukoski IV, C. F., *J. Colloid Interface Sci.* **141**, 92 (1991).
- (23) Goff, J. R. and Luner, P., *J. Colloid Interface Sci.* **99**, 468 (1984).
- (24) Stöber, W., Fink, A. and Bohn, E., *J. Colloid Interface Sci.* **26**, 62 (1968).
- (25) Penners, N. H. G. and Koopal, L. K., *Colloids and Surfaces* **19**, 337 (1986).
- (26) Myers, D. F. and Saville, D. A., *J. Colloid Interface Sci.* **131**, 448 (1989).
- (27) "Handbook of Chemistry and Physics", CRC Press, Inc., 1990-1991.
- (28) Kijlstra, J., *Ph. D. Thesis; Chapter 2* (1992).
- (29) Dukhin, S. S. and Shilov, V. N., "Dielectric Phenomena and the Double Layer in Disperse Systems and Polyelectrolytes", Wiley, New York, 1974.
- (30) Saville, D. A., *J. Colloid Interface Sci.* **91**, 34 (1983).
- (31) Böttcher, C. J. F. and Bordewijk, P., "Theory Of Electric Polarization", Elsevier Scientific Publishing Company, Amsterdam, 1978.
- (32) Kramers, H. A., *Atti. Congr. Int. Fysici, Como* **2**, 545 (1927).
- (33) Kronig, R., *J. Opt. Soc. Am.* **12**, 547 (1926).
- (34) O'Brien, R. W., *J. Colloid Interface Sci.* **113**, 81 (1986).
- (35) Shilov, V. N. and Dukhin, S. S., *Kolloidn. Zh.* **32**, 117 (1970).
- (36) Fixman, M., *J. Chem. Phys.* **72**, 5177 (1980).
- (37) Fixman, M., *J. Chem. Phys.* **78**, 1483 (1983).
- (38) O'Konski, C. T., *J. Phys. Chem.* **64**, 605 (1960).
- (39) Dukhin, S. S. and Semenikhin, N. M., *Kolloidn. Zh.* **32**, 360 (1970).
- (40) Dukhin, S. S. and Derjaguin, B. V., in "Surface Colloid Science" (E. Matijevic, Eds.), p. Wiley, New York, 1974.
- (41) Sauer, B. B., Stock, R. S., Lim, K. and Harmon Ray, W., *J. Applied Polymer Sci.* **39**, 2419 (1990).
- (42) Lim, K. and Franses, E. I., *J. Colloid Interface Sci.* **110**, 201 (1986).
- (43) Cole, K. S. and Cole, R. H., *J. Chem. Phys.* **9**, 341 (1941).
- (44) Penners, N. H. G., Koopal, L. K. and Lyklema, J., *Colloids and Surfaces* **21**, 457 (1986).
- (45) Koopal, L. K. and Giatti, A., *unpublished results* (1992).

Chapter 5

Electrokinetic Properties of Bacterial Suspensions *Short Communication*

Introduction

Adhesion of bacteria to surfaces is a common phenomenon in natural environments as well as in bioreactors. In order to understand the adhesion behaviour, it is necessary to study the characteristics of the bacterial cell surface (1). Most bacteria are of colloidal size and, at neutral pH, their surfaces are negatively charged due to the presence of acidic groups in the cell wall. As a result, the bacteria are surrounded by an electrical double layer which affects the adhesion properties. Common colloid chemical techniques to characterize the double layer structure are potentiometric proton titration and electrokinetics, especially microelectrophoresis.

Traditionally, microelectrophoresis is used to determine the electrostatic ζ potential at the slip plane. However, the conversion from mobility to ζ potential is not straightforward. For example, conduction by ions within the slip plane thwarts the interpretation. This phenomenon is called surface conduction. For bacteria, it may occur due to the presence of mobile ions inside the cell wall. Hence, for a correct conversion, the surface conductivity has to be determined. In this respect, we will show that low-frequency dielectric spectroscopy can be of help.

Dielectric spectroscopy involves the measurement of the complex conductivity K^* or complex permittivity ϵ^* as a function of the frequency, given by

$$K^* = \frac{\epsilon^*}{i\omega} = \sigma + i\omega\epsilon_0\epsilon_r$$

with $i = \sqrt{-1}$, ω the angular frequency of the applied electric field, ϵ_0 the permittivity of vacuum and ϵ_r the relative permittivity of the suspension. The conduction σ represents the current in phase with the applied field whereas $\omega\epsilon_0\epsilon_r$ represents the out of phase component. Convenient experimental parameters are the conductivity increment $\Delta\sigma$ and the dielectric increment $\Delta\epsilon_r$, defined by

$$\Delta\sigma(\omega) = \sigma(\omega) - \sigma(\omega^0) \quad \text{and} \quad \Delta\epsilon_r(\omega) = \epsilon_r(\omega) - \epsilon_r(\omega^*),$$

where ω^0 is the minimum frequency in the experimental frequency window and ω^* the maximum.

Already in the sixties, Einolf and Carstensen (2) published data on the low-frequency dielectric response of a concentrated bacterial suspension with a volume fraction ϕ of the suspended bacteria of approximately 50%. They showed that both σ and ϵ_r were strongly frequency dependent in the range of 500Hz-200kHz. At that time, no theory was available to interpret these data adequately. During the last few decades, much progress has been made in understanding the electrokinetic properties of dilute colloids. It is now of interest to apply these new theoretical concepts to bacterial suspensions.

Results and discussion

Figure 1 shows the dielectric response of a dilute suspension of a spherical coryneform bacterium (DSM6685) (3) in $1.5 \cdot 10^{-3}$ M KCl. The radius a of the bacterium is approximately 360 nm (determined by dynamic light scattering) and $\kappa a \approx 45$, with κ^{-1} the Debye length. The measurements have been carried out on suspensions with a volume fraction ϕ of less than 5%, obtained by diluting a concentrated stock suspension. No non-linearities in the dependence on ϕ were observed. A detailed description of the dielectric spectrometer has been given in ref. (4).

We observe the same trends as Einolf and Carstensen did: large values of $\Delta\epsilon_r$ at low frequencies and $\Delta\sigma$ growing with increasing frequency. The drawn lines in Fig. 1 are obtained by fitting the data with the thin double layer theory of Fixman (5), valid if $\kappa a \gg 1$. In this theory,

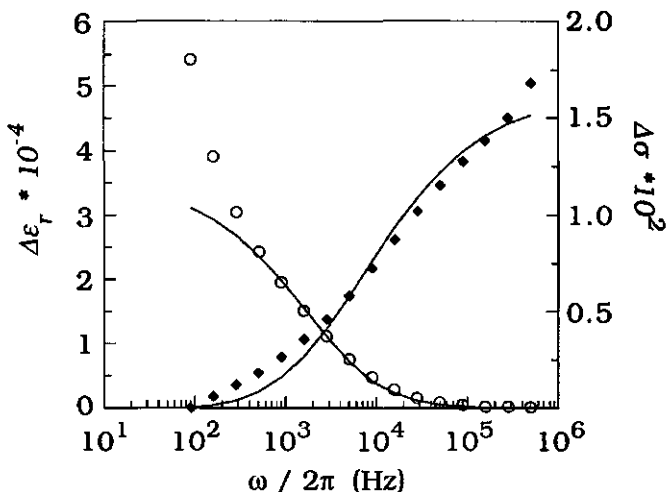


Figure 1. Dielectric response of the bacterial suspension. (○) $\Delta\epsilon_r$, (♦) $\Delta\sigma$ in S/m; the increments are normalized to the volume fraction of the bacterial stock suspension, which was approximately 30%.

particles are considered as solid spheres surrounded by a diffuse double layer. Hence, it neglects a possible surface conduction contribution. Thin double layer theories are also thought to be valid for conducting particles, provided that charge transfer across the particle/solution interface is impossible. Hence, they may be applicable to bacteria. According to Carstensen (6) and as confirmed by own experiments, the cell membrane behaves as an insulator. The fitting procedure provides us with two estimates for the ζ potential: one from $\Delta\epsilon_r$ and one from $\Delta\sigma$. Details about this procedure are given in ref. (7).

Although the two estimates for ζ differ and are dependent on the estimated value for ϕ , they are in any case both remarkably high: in the range of 150-200 mV! Fixman's theory was also used to obtain an estimate for the ζ potential from the electrophoretic mobility u_{el} . The mobility has been measured under the same conditions as the dielectric response: $u_{el} = 3.0 \cdot 10^{-8} m^2/Vs$. The resulting ζ potential is only approximately 40 mV !

In a recent paper (8), we have extended the theory of Fixman to include surface conduction. Moreover, we have shown that the above found inconsistency between the different estimates for the ζ potential is typical for systems in which surface conduction plays a significant role. The extended theory can be used to quantify the surface conductivity and to obtain an improved estimate for the ζ potential from a combination of dielectric response and mobility data. The relevant surface conductivity parameter in this theory is Θ , defined as the ratio of the excess density of (mobile) counterions within the slip plane to that beyond it. It is assumed that the presence of co-ions within the slip plane can be neglected.

Applying the extended theory to our results, we obtain an improved estimate for the ζ potential in the range of 75-100 mV and a value for Θ of approximately 20. This corresponds to (mobile) counter charge densities of approximately $1\text{-}2 \mu\text{C}/\text{cm}^2$ in the diffuse part of the double layer and $20\text{-}30 \mu\text{C}/\text{cm}^2$ within the plane of shear. This shows that most of the charge of the bacterial cell wall is screened within the cell wall itself. At first sight, the high value for Θ may seem unrealistic. However, own experimental work on the potentiometric titrations of isolated cell walls of other coryneform bacteria provides independent support. Comparison of the titratable surface charge density of the cell wall with its value estimated from the electrophoretic mobility indicates that for bacteria values of Θ as high as 30 are realistic.

To illustrate the influence of surface conduction on the electrophoretic mobility, we have calculated u_{el} versus ζ potential for different values of Θ . The results are displayed in Figure 2.

In their theory for the electrophoretic mobility of biological cells, Ohshima and Kondo (9) assume that double layer polarization can be neglected, since in most practical cases the ζ potential is assumed to be low and $\kappa a \gg 1$. Then the thin double layer theory reduces to the Smoluchowski equation, which linearly relates the mobility $u_{el}^{Smol.}$ to the ζ potential. However, in Fig. 2 we see that, for a given κa value, the deviation between u_{el} and $u_{el}^{Smol.}$ increases not only with growing ζ potential, but also with growing Θ . This deviation is caused by the polarization of the double layer which increases with the total counter charge in the double layer; it creates a back-field which partially

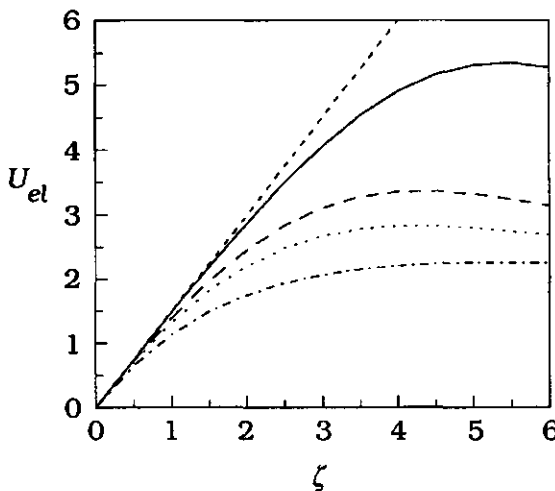


Figure 2. The scaled electrophoretic mobility U_{el} versus scaled ζ potential for different values of Θ . U_{el} is the mobility scaled on $2kT\epsilon_0\epsilon_r/3\eta e$ and potentials are scaled on kT/e , with k the Boltzmann constant, T the absolute temperature, η the solvent viscosity and e the unit charge. $\kappa a = 50$. (----) u_{el}^{Smol} . Results thin double layer theory: (—) $\Theta = 0$, (---) $\Theta = 5$, (···) $\Theta = 20$, (- - -) $\Theta = 30$.

counteracts the applied field and, hence, it retards the electrophoretic mobility. Therefore, even under the restrictions assumed by Ohshima and Kondo, the effect of double layer polarization remains important as long as the surface conductivity is high. For the coryneform bacterium, this is very likely to be the case.

A more complete interpretation of the dielectric measurements of bacterial suspensions is still pending. For example, the difference between the estimates for the ζ potential from $\Delta\epsilon_r$ and $\Delta\sigma$ requires an explanation. Investigations in this area will be pursued. Nevertheless, the present results show clearly that low-frequency dielectric measurements yield additional information about the structure of the electric double layer of suspended bacteria, information which cannot be extracted from electrophoretic data only.

References

- (1) van Loosdrecht, M. C. M., Norde, W., Lyklema, J., Zehnder, A. J. B., *Aquatic Sciences* **52**, 103-114 (1990).
- (2) Einolf, C. W., Carstensen, E. L., *Biochim. Biophys. Acta* **148**, 506-516 (1967).
- (3) Bendinger, B., Kroppenstedt, R. M., Klatte, S., Altendorf, K., *accepted Int. J. Syst. Bacteriol.* (1992).
- (4) Kijlstra, J., Ph. D. Thesis, Wageningen University, 1992.
- (5) Fixman, M., *J. Chem. Phys.* **78**, 1483-1491 (1983).
- (6) Carstensen, E. L., *Biophys. J.* **7**, 493-503 (1967).
- (7) Kijlstra, J., van Leeuwen, H. P., Lyklema, J., *submitted Langmuir; Chapter 4* (1992).
- (8) Kijlstra, J., van Leeuwen, H. P., Lyklema, J., *accepted J. Chem. Soc., Faraday Trans. 2; Chapter 3* (1992).
- (9) Ohshima, H., Kondo, T., *Biophysical Chemistry* **39**, 191-198 (1991).

Chapter 6

Polarizability Effects in the Electrostatic Repulsion between Charged Colloidal Particles

Abstract

The electrostatic interaction between two colloidal spheres with a fixed surface charge density is calculated in order to determine the influence of the polarizability of the spheres on the repulsive electrostatic force. The linearized form of the Poisson-Boltzmann equation is used in combination with the Laplace equation, which enables us to construct an exact solution in terms of a multipole expansion. The calculations show clearly how the electrostatic force decreases with the polarizability of the particle, the decrease becoming larger with stronger double layer overlap, whereas it is relatively insensitive to κa . This insensitivity is a consequence of tangential screening effects inside the particles, as illustrated by a comparison of the exact solution with a Derjaguin-type approximation in which the possibility of tangential screening is not included. It is pointed out that for slowly coagulating dispersions of particles with a fixed surface charge density, the colloid stability ratio W is sensitive to the polarizability of the particle.

Introduction

The stability of hydrophobic colloidal suspensions is determined by the interparticle forces. In the DLVO theory, two types of forces are distinguished, the attractive Van der Waals force and the repulsive electrostatic force. The latter occurs when diffuse double layers overlap. From these forces, the energy of interaction as a function of the interparticle distance can be deduced, which in turn is necessary to compute the colloid stability ratio W (1).

Usually the Poisson-Boltzmann equation is solved to calculate the electrostatic repulsion between two hydrophobic colloidal particles and many papers devoted to this subject have appeared in the literature.

The solution of this equation depends not only on the geometry of the system, to which much attention has been paid (1-4), but also on the distribution of the surface charge density. Regarding this distribution, an assumption has to be made.

Verwey and Overbeek (1) already distinguished two limits of interaction between particles, the constant (surface) charge and the constant (surface) potential case. The first case applies when the time scale of particle interaction is too short for the surface charge to adjust. If, on the other hand, desorption of surface charge is very fast compared to the abovementioned time scale, equilibrium between the surface charge and the ions in solution will be maintained continually. For the latter case Verwey and Overbeek assumed the surface potential to be independent of the interparticle distance. This assumption has been shown to be not very realistic for systems such as oxides. In these systems the potential is determined by a charge regulation mechanism, which, in comparison with either the constant charge or the constant potential case, may give rise to large differences in the colloid stability (5, 6). In the regulation model the double layer is always in equilibrium and the surface charge, as well as the surface potential, is adjusted during particle interaction. The adjustment of both these parameters is caused by the entropic contribution of the surface charge determining ions to the free energy, which generally corresponds to a nonlinear function of the surface charge density. Consequently, both charge and potential may vary along the particle surface. Obviously, this will also be the case if the time scales of interaction and surface charge relaxation are of the same order, resulting in disequilibration of the surface charge during interaction.

Apart from the limiting situation of a constant surface potential, all cases have in common that an electric field will be present inside the particles during interaction. In principle, this field has to be taken into account in calculating the electrostatic repulsion. However, Gauss's law suggests that the influence of this field on the electrostatic force can probably be neglected in the case of low values of the ratio between the dielectric constants of the particle (ϵ_2) and the electrolyte solution (ϵ_1). For many aqueous dispersions this is probably true and therefore the approximation is often applied in the literature (7, 8). An example of a

well-known colloidal system for which this is likely a poor approximation is a TiO_2 rutile sol. Depending on the optic axis, rutile has two dielectric constants, i.e. of 86 and 170 (9). The quality of the approximation does not only depend on ϵ_2/ϵ_1 , but also on the geometry of the system. For the interaction between two parallel plates of finite thickness with constant surface charge density on both sides, Ohshima (10) showed how the correctness of the approximation improves with decreasing value of ϵ_2/ϵ_1 , as well as with increasing value of κd , with κ^{-1} and d being the double layer and plate thickness respectively. In his analytical theory for the interaction between two spherical particles with constant surface charge density (11), he neglects the tangential component of the electric field inside the particle. However, according to Dukhin and Lyklema (12), this component is the most important one and therefore they conclude that the geometrical parameter of importance for spheres is $O(\sqrt{\kappa a})$ instead of $O(\kappa a)$, with a the particle radius. This geometrical parameter and the distance between the two particles, which gives the degree of double layer overlap, determine together primarily the gradient in the surface potential and thus the electric field strength inside the particle.

In this paper, the validity of the approximation of neglecting the electric field inside the particle will be tested for the interaction between two identical spherical particles with a fixed homogeneous surface charge distribution. A simple model is invoked in order to determine in which range of κa and particle-particle distance the influence of the particle polarizability on the electrostatic force is significant. We assume the particles to have one dielectric constant, irrespective of the optic axis. The electrostatic repulsion is calculated by solving the differential equations for the electric field inside and outside the spheres. The linearized form of the Poisson-Boltzmann equation is used in combination with the Laplace equation, which enables us to construct an exact solution in terms of a multipole expansion. Tangential screening effects are therefore all taken into account. The Poisson-Boltzmann equation and the Laplace equation are coupled at the particle surface by Gauss's law. Consequently, a nondiffuse part of the double layer, for example a Stern layer, is assumed to be absent. In systems where the nondiffuse part of the

double layer is important, the model has to be extended for accurate quantitative calculations. The multipole expansion of the linearized Poisson-Boltzmann equation has been used before to check the Derjaguin approximation (7) and to calculate the effect of surface charge relaxation on the force between two particles ($\epsilon_2 = 0$) at fixed distance (8).

Generally, by using the Derjaguin approximation, one neglects the field inside the particle. It is, however, possible to take, on the same level of approximation, the effect of this field into account by using the theory of Ohshima (10) for the interaction between two parallel plates of finite thickness. The results of the exact solution will therefore be compared with the combination of the Derjaguin approximation with Ohshima's theory. In this approach, in contrast to the exact method, tangential screening effects are not incorporated.

Theory

Consider two identical interacting spherical particles (phase 2) in a symmetric electrolyte solution (phase 1). For low potentials the electrostatic potential ψ_1 in the electrolyte solution is governed by the linearized Poisson-Boltzmann equation

$$\nabla^2 \psi_1 = (\kappa a)^2 \psi_1 \quad [1]$$

with κ^{-1} the Debye length. Throughout this section, dimensionless parameters are used, the potential ψ scaled on kT/e and lengths scaled on the particle radius a , with e the elementary charge and kT the Boltzmann temperature. Linearization of the PB equation is justified if $z\psi_1 < 1$, with z the charge of the ions. The potential ψ_2 inside the sphere, where the charge density equals zero, is governed by the Laplace equation

$$\nabla^2 \psi_2 = 0 \quad [2]$$

The general solution of [1] for two identical interacting spherical particles, using polar coordinates, is given by (13)

$$\psi_1 = \sum_{n=0}^{\infty} f_n \left[K_n(kar) P_n(\cos \theta) + \sum_{m=0}^{\infty} B_{nm}(kar_{sep}) (2m+1) I_m(kar) P_m(\cos \theta) \right] \quad [3]$$

with the polar axis $\theta=0$ coinciding with the line connecting the centers of the two spheres, r the radial coordinate, r_{sep} the center-to-center distance, P_n the Legendre polynomials, I_m and K_n the spherical modified Bessel functions of the first and third kind, and f_n the unknown coefficients. The function B_{nm} is defined as

$$B_{nm}(kar_{sep}) = \sum_v A_{nmv} K_{n+m-2v}(kar_{sep}) \quad [4]$$

with

$$A_{nmv} = \frac{\Gamma(n-v+\frac{1}{2})\Gamma(m-v+\frac{1}{2})\Gamma(v+\frac{1}{2})(n+m-v)!(n+m-2v+\frac{1}{2})}{\pi\Gamma(n+m-v+\frac{3}{2})(n-v)!v!(m-v)!} \quad [5]$$

and Γ the gamma function. Solution [3] satisfies the requirements of zero field at the midplane and zero potential at infinity. For a finite potential inside the sphere, the solution of [2] is

$$\psi_2 = \sum_{n=0}^{\infty} g_n r^n P_n(\cos \theta) \quad [6]$$

The coefficients f_n and g_n can be determined from the boundary conditions at the particle surface. For the present case, where space charges inside the particle and nondiffuse double layer effects in the solution are supposed to be absent, the boundary conditions are given by the continuity of the potential

$$\psi_1|_{r=1} = \psi_2|_{r=1} \quad [7]$$

and the law of Gauss

$$\frac{\epsilon_2}{\epsilon_1} \frac{\partial \psi_2}{\partial r} \Big|_{r=1} - \frac{\partial \psi_1}{\partial r} \Big|_{r=1} = \sigma \quad [8]$$

with σ the surface charge scaled on $\epsilon_1 kT/ea$. The importance of the first term on the left hand side of [8], representing the polarizability of the particle, which has been been neglected in the literature, is now point of discussion.

Combining [3] and [6] with the potential continuity equation [7] gives

$$g_j = f_j K_j(\kappa a) + \sum_{n=0}^{\infty} f_n (2j+1) B_{nj}(\kappa a r_{sep}) I_j(\kappa a) \quad [9]$$

By substituting the derivatives of the potentials at the particle surface in Gauss's law, we get

$$\begin{aligned} & \kappa a \sum_{n=0}^{\infty} f_n \{K'_n(\kappa a) P_n(\cos \theta) + \sum_{m=0}^{\infty} (2m+1) B_{nm}(\kappa a r_{sep}) I'_m(\kappa a) P_m(\cos \theta)\} \\ & - \frac{\epsilon_2}{\epsilon_1} \sum_{n=0}^{\infty} g_n n P_n(\cos \theta) = -\sigma \end{aligned} \quad [10]$$

with the derivatives of the Bessel functions taken with respect to the argument.

The method used to calculate the electrostatic interaction between two identical spheres is not restricted to spheres with a constant surface charge density. It is also applicable to two interacting spheres with an inhomogeneous charge distribution, provided that the conditions of symmetry (axial symmetry around the polar axis $\theta=0$ and symmetry plane midway between the spheres) are satisfied. The distribution of the surface charge density can then be written as a series of Legendre polynomials

$$\sigma = \sum_{j=0}^{\infty} \sigma_j P_j(\cos \theta) \quad [11]$$

In our limiting case of constant surface charge density, we have

$$\sigma_0 = \sigma, \sigma_{j>0} = 0 \quad [12]$$

For an isolated sphere with a homogeneous charge distribution, the charge-potential relation $\sigma = \psi_s(1 + \kappa a)$ is valid, with ψ_s the surface

potential. By substituting [9] and [11] into [10] and taking the inner product with $P_j(\cos \theta)$, we end up with the following set of linear equations

$$\begin{aligned} (\kappa a) f_j K'_j(\kappa a) + (\kappa a) \sum_{n=0}^{\infty} f_n (2j+1) B_{nj}(\kappa a r_{sep}) I'_j(\kappa a) \\ - \frac{\epsilon_2}{\epsilon_1} j \{ f_j K_j(\kappa a) + \sum_{n=0}^{\infty} f_n (2j+1) B_{nj}(\kappa a r_{sep}) I_j(\kappa a) \} = -\sigma_j \end{aligned} \quad [13]$$

This set is solved by truncating the multipole expansion and using standard numerical techniques to compute the unknown coefficients f_j .

For low potentials, the interaction force F_e between two identical particles due to the osmotic pressure and the Maxwell stress has been given as [7]

$$F_e = \pi \int_{-1}^1 \{ [(\kappa a)^2 \psi^2 + E_\theta^2 - E_r^2] \mu + 2E_r E_\theta (1-\mu^2)^{1/2} \} d\mu \quad [14a]$$

with the electric field scaled on kT/ae , the force on $\epsilon_1(kT)^2/e^2$, $\mu = \cos \theta$ and the integrand evaluated at any surface enveloping the particle, for example at the particle surface. The polar components of the electric field at the surface E_θ and E_r are given by

$$E_r = \kappa a \sum_{n=0}^{\infty} f_n \left[K'_n(\kappa a) P_n(\cos \theta) + \sum_{m=0}^{\infty} B_{nm}(\kappa a r_{sep}) (2m+1) I'_m(\kappa a) P_m(\cos \theta) \right] \quad [14b]$$

$$E_\theta = -\sin \theta \sum_{n=0}^{\infty} f_n \left[K_n(\kappa a) P'_n(\cos \theta) + \sum_{m=0}^{\infty} B_{nm}(\kappa a r_{sep}) (2m+1) I_m(\kappa a) P'_m(\cos \theta) \right] \quad [14c]$$

with the derivatives of the Bessel and Legendre functions again taken with respect to the arguments. For further details on the expression for the force in terms of Legendre and Bessel functions, the reader is referred to Weaver and Feke (8). For a discussion of the numerical limitations of this method, see Glendinning and Russel (7). The number of terms used in the expansions was chosen in order to converge the force within 0.1%.

Derjaguin approximation

An approximate method to calculate the electrostatic force between two spherical particles from the knowledge of the interaction between two infinitely large parallel plates has been given by Derjaguin (14). According to his approximation, the electrostatic force F_D is expressed for low potentials by the integral

$$F_D = \frac{\pi \kappa a}{2} \int_{H_0}^{\infty} \psi_m^2 dH \quad [15]$$

with ψ_m the potential midway between two parallel plates (of finite thickness) at distance H and H_0 the closest distance between the surfaces of the spheres. For convenience, these lengths are both normalized on κ^{-1} , the latter being related to r_{sep} through $r_{sep} = 2 + H_0/\kappa a$.

Analytical expressions for ψ_m are available for the linearized PB equation. In the case of given surface potential ψ_s , we have

$$\psi_m = \frac{\psi_s}{\cosh(H/2)} \quad [16]$$

and in the case of constant surface density on both sides of the plates, according to Ohshima (10)

$$\psi_m = \sigma^* \frac{1 + \alpha}{\alpha \cosh(H/2) + \sinh(H/2)} \quad [17]$$

and

$$\alpha = \frac{1}{1 + (\epsilon_1/\epsilon_2)\kappa d} \quad [18]$$

with σ^* the surface charge scaled on $\kappa \epsilon_1 kT/e$, and ϵ_2 and d the dielectric constant and the thickness of both plates, respectively. The dimensionless parameter α represents the importance of the electric field inside the plates during interaction, present due to the difference in surface potentials on both sides of each plate. In the limiting case of very low ϵ_2/ϵ_1 and/or very thick plates, the electric field inside the

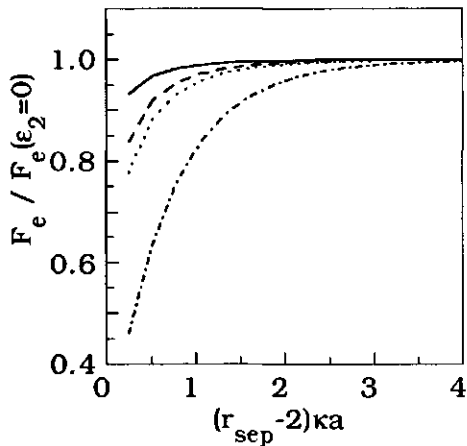


Figure 1. Ratio of exact force to exact force for $\epsilon_2 = 0$. $\kappa a = 1$, $\epsilon_1 = 80$,
 (—) $\epsilon_2 = 10$, (---) $\epsilon_2 = 30$,
 (- · -) $\epsilon_2 = 50$, (- · - ·) $\epsilon_2 = 10^4$.

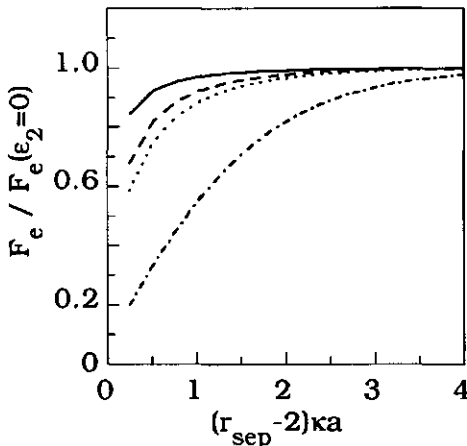


Figure 2. Ratio of exact force to exact force for $\epsilon_2 = 0$. $\kappa a = 10$,
 $\epsilon_1 = 80$, (—) $\epsilon_2 = 10$, (---) $\epsilon_2 = 30$, (- · -) $\epsilon_2 = 50$, (- · - ·) $\epsilon_2 = 10^4$.

plates can be neglected, and α approaches zero. Analytical solutions of the integral in [15] are known for the constant surface potential, as well as for the constant charge case with $\alpha = 0$,

$$F_D = 2\pi\kappa a \psi_s^2(H_0 = \infty) \frac{e^{-H_0}}{1 \pm e^{-H_0}} \quad [19]$$

with the + and - signs referring to the first and second case respectively. If, at a given surface charge density, $\alpha \neq 0$, the integral in [15] can be easily evaluated numerically in combination with [17].

Results and conclusions

Figures 1 and 2 show the ratio $F(\epsilon_2)/F(\epsilon_2 = 0)$ as a function of the interparticle distance for κa values of 1 and 10, calculated by using the exact solution [14]. For all graphs shown, the surface charge density, the surface potential of the isolated particles ($\psi_s(r_{sep} = \infty) = 0.5$) and the dielectric constant of the electrolyte solutions ($\epsilon_1 = 80$) are fixed.

An important feature is that, even for not too high values of ϵ_2/ϵ_1 , the ratio $F_e(\epsilon_2)/F_e(\epsilon_2 = 0)$ decreases with diminishing interparticle

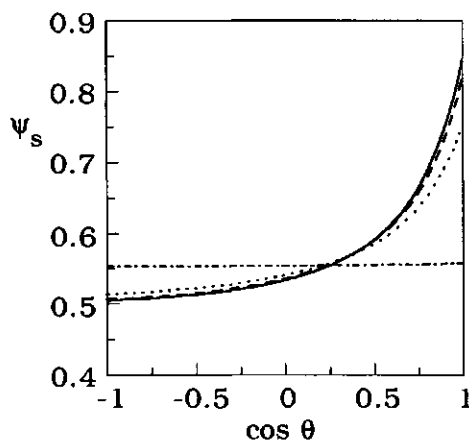


Figure 3. Surface potential distribution for the case of $\kappa a = 1$, $\sigma = 1$, $\psi_s(r_{sep} = \infty) = 0.5$, $\epsilon_1 = 80$ and $(r_{sep} - 2)\kappa a = 1$. (—) $\epsilon_2 = 0$, (---) $\epsilon_2 = 10$, (- · -) $\epsilon_2 = 50$, (· · ·) $\epsilon_2 = 10^4$.

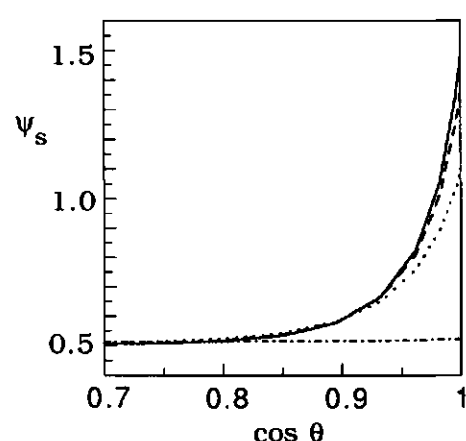


Figure 4. Surface potential distribution for the case of $\kappa a = 10$, $\sigma = 5.5$, $\psi_s(r_{sep} = \infty) = 0.5$, $\epsilon_1 = 80$ and $(r_{sep} - 2)\kappa a = 1$. (—) $\epsilon_2 = 0$, (---) $\epsilon_2 = 10$, (- · -) $\epsilon_2 = 50$, (· · ·) $\epsilon_2 = 10^4$.

distance to values significantly less than 1. This is the immediate consequence of the increase of ψ_s in the interaction regime with decreasing particle-particle distance and the concomitant increase of the electric field strength inside the particle. At constant σ , the ratio $F(\epsilon_2)/F(\epsilon_2 = 0)$ also decreases with increasing ϵ_2 . This is obvious because the higher ϵ_2 , the lower the electric field strength inside the particle. Such a situation can only be accomplished if ψ_s decreases inside the interaction regime, whereas it increases somewhere outside that regime (in comparison with the $\epsilon_2 = 0$ case).

This has been illustrated in Figures 3 and 4, which display results from the exact solution. For $\kappa a = 1$ we see even a slight increase of ψ_s with ϵ_2 at the "back" of the sphere ($\cos \theta = -1$), in contrast to the case of $\kappa a = 10$, where the most significant increase appears just around the interaction regime. From the limited penetration depth of the electric field into the particle for not too low κa values, it can be concluded that its tangential component inside the particle is important.

The deviations of the Derjaguin force from the exact force are shown in Figure 5 for $\kappa a = 20$ and different ϵ_2 values. The poor quality of

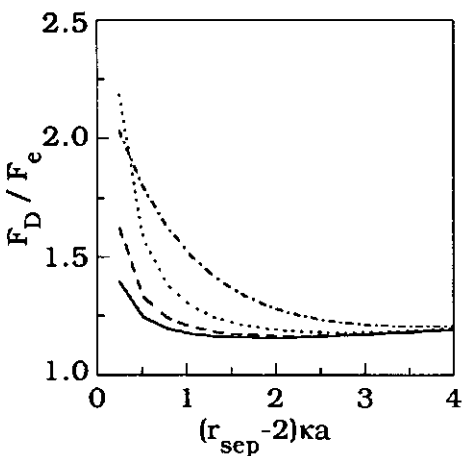


Figure 5. The ratio of the Derjaguin force to the exact force in the case of $\kappa a = 20$, $\epsilon_1 = 80$. (—) $\epsilon_2 = 0$, (---) $\epsilon_2 = 10$, (···) $\epsilon_2 = 50$, (----) $\epsilon_2 = 10^4$.

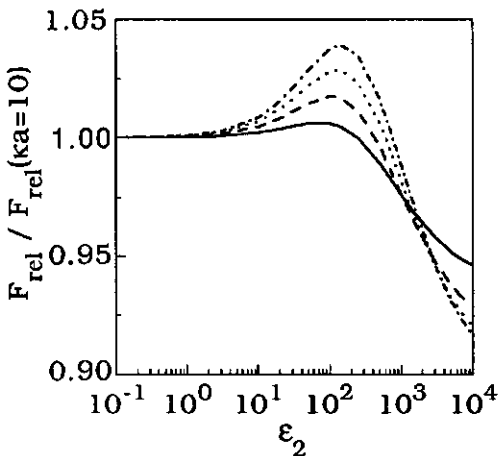


Figure 6. The ratio $F_{\text{rel}}(\kappa a)/F_{\text{rel}}(\kappa a = 10)$ as a function of ϵ_2 , with $\epsilon_1 = 80$, $(r_{\text{sep}} - 2)\kappa a = 1$ and $F_{\text{rel}} = F_e(\epsilon_2)/F_e(\epsilon_2 = 0)$. (—) $\kappa a = 20$, (---) $\kappa a = 30$, (···) $\kappa a = 40$, (----) $\kappa a = 50$.

the Derjaguin approximation for $\epsilon_2 = 0$ has been noted before (7) and is due to the presence of tangential screening effects in the diffuse double layer. Introducing a second possibility of lateral screening, by taking the polarizability of the particle into account, only makes the approximation worse.

In the limit of $\epsilon_2 \rightarrow \infty$, the interior of the particle will behave like a conductor, forcing the potential along the particle surface to be constant during interaction. The value of this potential will exceed the surface potential of an isolated particle, but the difference decreases slightly with increasing κa and thus $F_e(\epsilon_2 = \infty)/F_e(\epsilon_2 = 0)$ does too. However, at not too high values of ϵ_2 , the radial screening effects become relatively less important than the tangential ones. Moreover, the tangential field along the surface diminishes with κa and the combination of these effects cause $F_e(\epsilon_2)/F_e(\epsilon_2 = 0)$ to increase with κa . The calculated sensitivity of $F_e(\epsilon_2)/F_e(\epsilon_2 = 0)$ to κa is however small, providing a solid support for the first order estimate of Dukhin and

Lyklema (12). In most cases, changing κa will have an effect in the order of only a few percent, as is shown in Figure 6.

In general, the approximation of neglecting the electric field inside the particle becomes worse at smaller separation distances and higher ϵ_2/ϵ_1 values. For example, for aqueous suspensions, if $(r_{sep} - 2)\kappa a < 1$ and $\epsilon_2 > 30$ the error in the electrostatic force adds up to more than ten percent. A small change in the electrostatic force, however, can have a large effect on the stability factor W . For slow coagulation, the stability factor W is mainly determined by the net force at distances of $(r_{sep} - 2)\kappa a \approx 1$, a region where the net force is relatively small compared to its repulsive and attractive components. Consequently, a change in the repulsive force of 10% results in a change of W which can be on the order of one magnitude or more. The relative size of the change is more pronounced for large stability factors, for which the maximum in the net force is located at shorter interparticle distances. For suspensions with $\epsilon_2/\epsilon_1 = O(1)$, for example nonaqueous suspensions, it is clear that the electric field inside the particle has to be accounted for. Especially for systems with high κa values, the calculations show that the tangential component of this field is important.

References

1. Verwey, E. J., and Overbeek, J. Th. G., "Theory of the Stability of Lyophobic Colloids" (Elsevier, Amsterdam, 1948).
2. James, A. E., and Williams, D. J. A., *J. Colloid Interface Sci.* **107**, 44 (1985).
3. Bentz, J., *J. Coll. Int. Sci.* **90**, 164 (1982).
4. Ring, T. A., *J. Chem. Soc. Faraday Trans 2*, 78, 1513 (1982).
5. Prieve, D. C. and Ruckenstein, E., *J. Colloid Interface Sci.* **60**, 337 (1977).
6. Healy, T. W., Chan, D., and White, L. R., *Pure Appl. Chem.* **52**, 1207 (1980).
7. Glendinning, A. B., and Russel, W. B., *J. Colloid Interface Sci.* **93**, 95 (1983).
8. Weaver, D. W., and Feke, D. L., *J. Colloid Interface Sci.* **103**, 267 (1985).
9. Weast, R. C. (Ed.), Handbook of Chemistry and Physics 55th ed., E-58, CRC Press, Cleveland, OH, 1974.
10. Ohshima, H., *Colloid Polym. Sci.* **252**, 158 (1974).
11. Ohshima, H., *Colloid Polym. Sci.* **253**, 150 (1975).

12. Dukhin, S. S. and Lyklema, J., *Coll. J. of the USSR Eng. Trans.* **51**, 244 (1989).
13. Marcelja, S., Mitchell, D. J., Ninham, B. W., and Sculey, M. J., *J. Chem. Soc. Faraday Trans. 2* **73**, 630 (1977)
14. Derjaguin, B., *Trans. Faraday Soc.* **36**, 203 (1940).

Chapter 7

Surface Charge Relaxation during Coagulation

Abstract

Transient deviations from the equilibrium surface charge density during the interaction of colloidal particles have been studied. Such deviations cause the process of particle encounter to become a non-first-order Markov process, complicating the analysis of colloid stability. Two methods are presented to calculate a modified colloid stability ratio, taking such deviations into account in an approximate way. These methods differ by their estimates for the time scale of the Brownian encounter and its dependence on the height of the energy barrier. Despite these differences, both methods show that double-layer dynamics can have major consequences for the stability ratio. However, the resulting dependences of the rate of slow coagulation on the particle radius are different for the two methods. This indicates that double-layer dynamics could explain the experimentally found insensitivity of the stability ratio to the particle size, provided the time scale of the encounter is strongly dependent on the height of the energy barrier. However, this proviso is unlikely to be satisfied. A simple statistical analysis indicates that the time scale of any individual encounter slightly decreases with growing barrier height!

Introduction

Slow perikinetic coagulation of hydrophobic colloids is a dynamic process. Only by Brownian motion, particles are able to pass the energy barrier between them and form aggregates. Obviously, the rate of coagulation depends on the height (and shape) of the energy barrier, which, in the DLVO theory (1, 2), is described as the net result of attractive Van der Waals and repulsive electrostatic forces. The calculation of the electrostatic forces is usually based on equilibrium thermodynamics. However, this is justified only when the several

relaxation processes in the double layer, which occur during the particle interaction, are fast compared to the rate of approach.

Usually, the electric double layer associated with the particles is the result of specific interactions of ions with the particle surface. The extent of charge accumulation onto the surface, and hence, the equilibrium structure of the double layer, is determined by a balance of chemical, electrostatic and entropic interactions. If overlap of double layers occurs, for example during a collision, then this balance will be affected, leading to a certain degree of adjustment or complete relaxation of the double layer. This adjustment will be characterized by more than one relaxation time, since rate-determining processes in several parts of the double layer, including diffuse and nondiffuse parts, can be distinguished. Estimates have shown that the relaxation time of the diffuse double layer is short compared to the time scale of a Brownian encounter τ_{int} , the latter being of the order of 10^{-6} – 10^{-4} s, depending on the particle size and the double layer thickness (3, 4). However, estimates for the relaxation time τ_{sc} of the surface charge density vary widely and may well be of the same order as that of the Brownian encounter (3, 4). The Deborah number De can be used to characterize the relative time scales, in our case $De = \tau_{\text{sc}}/\tau_{\text{int}}$.

In many systems, adjustment of the surface charge density may take place via adsorption or desorption of charge determining ions, for example Ag^+ and I^- ions in AgI sols and protons in oxide sols. Polystyrene latices are usually considered as examples where adjustment of the surface charge does not occur. However, to explain electrokinetic data, some people have adopted the idea that co-ion binding on latex particles occurs, contributing to the surface charge density (5, 6). Although this idea is somewhat controversial (7, 8), it illustrates that relaxation processes of the surface charge density might be relevant in a large category of systems.

According to Dukhin and Lyklema (9) a stability theory is "dynamic" if the extent of double layer relaxation is accounted for. The two extremes of such a theory are well-known: $De \ll 1$ and $De \gg 1$. The former refers to the case that the double layer is in full equilibrium at any instant during the encounter and is usually called interaction at constant (surface) potential (cp). In the other extreme case, no surface

charge relaxation takes place during interaction: the so-called interaction at constant (surface) charge (cc). These extreme cases are considered "static" since the surface charge density is independent of the time scale of interaction. Although full equilibrium of the double layer does not necessarily imply that the surface potential stays constant (10, 11), it is, for our purposes, a reasonable assumption; the use of a double layer model with a more advanced equilibrium criterium is not likely to qualitatively affect the dynamic aspects of particle interaction.

The theory of perikinetic coagulation of dilute sols has been developed by Smoluchowski (12, 13) and later extended by Fuchs (14). It applies to sols coagulating under "static" conditions. Calculations have shown that there may be large differences in the stability of sols with interaction at constant potential or at constant charge (15, 16), indicating the sensitivity of the colloid stability to double layer disequilibration. Since transient deviations from equilibrium cannot be generally excluded, the availability of a "dynamic" theory would be desirable. Some experimental motivation for the development of such a theory exists as well. The Smoluchowski-Fuchs theory predicts a pronounced particle size dependence of the colloid stability. Until so far, experiments on a variety of systems, i.e. latices (5, 17) AgI (18) and hematite (19) do not seem to confirm this prediction. If the time scale of an encounter would depend on the particle size, and hence, the extent of the disequilibration of the double layer, then a "dynamic" theory could provide a clue for this problem.

The first "dynamic" theory has been presented by Dukhin and Lyklema (9, 20). They developed a perturbation theory which accounts for small transient deviations from the equilibrium double layer structure due to retarded desorption of charge-determining ions. In a method similar to that of Spielman (21) and Honig et al. (22), who incorporated hydrodynamic interactions into the Smoluchowski-Fuchs theory, they calculated a modified diffusion coefficient. This coefficient has been used to calculate the colloid stability ratio W , which is a measurable quantity. However, this method is valid only in a region of small deviations from equilibrium. Preferably, this restriction should be removed because the perturbations are generally not small, as will be shown.

We want to extend the Smoluchowski-Fuchs theory for systems with $De \approx 1$, systems in which the double-layer dynamics might be important. Further, we are interested in the influence of double layer disequilibration on the particle size dependence of the stability ratio W .

A key issue, as it will appear, is the question whether the time scale of particle interaction is dependent on the height of the energy barrier. If so, then it would be, like the energy barrier itself, a very sensitive function of the particle size. In this paper, two approximate methods will be presented to extend the Smoluchowski-Fuchs theory. Neither method is restricted to small disequilibrations, i.e. the use of a perturbation theory is avoided. In one method, the time scale of interaction is related to the height of the energy barrier, while in the other it is only related to the particle size via the diffusion coefficient. In both cases, the consequences for the particle size dependence of the stability ratio W will be analyzed.

Basic principles

The discussion will be restricted to homodisperse dilute sols of solid spherical particles in a symmetric aqueous 1-1 electrolyte. We assume that $\kappa a \gg 1$, with κ^{-1} and a being the double layer thickness and particle radius, respectively. This condition is true for most colloids under conditions of coagulation. The potential profile of the equilibrium double layer is governed by the Poisson-Boltzmann equation and a Stern-layer is supposed to be absent. The surface charge density σ_0 is determined by adsorption of charge-determining ions and we assume that the equilibrium surface potential ψ_0^{eq} is independent of ionic strength and particle-particle distance. This implies that the equilibrium surface charge density is a variable and a function of these factors.

In the model, disequilibration of the double layer only occurs due to deviations in the surface charge density during the double layer overlap as far as these are transient. The interaction region is determined by the parts of the particles that feel the interaction. For $\kappa a \gg 1$, this region is relatively small in comparison to the entire particle surface and characterized by small values of θ in Fig. 1 (23). We

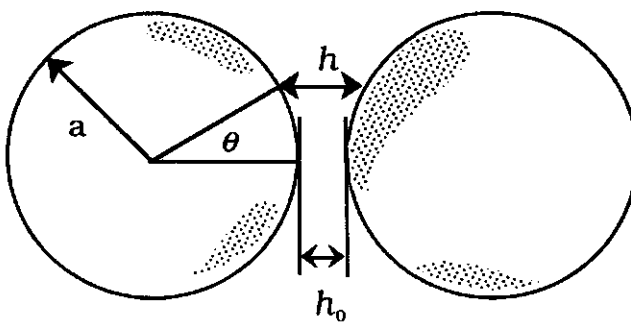


Figure 1. Geometrical parameters, characterizing particle interaction.

shall assume that lateral transport of surface charge is not possible and that relaxation of σ_o takes place only via desorption/adsorption processes of charge-determining ions. The diffuse part of the double layer is thought to be completely relaxed during an encounter. Hence, electro-viscous effects as discussed by Warszynski and Van de Ven (24) are neglected.

Smoluchowski-Fuchs theory

The Smoluchowski-Fuchs' approach of the perikinetic coagulation of dilute sols is based on theory of the Brownian motion of particles under the influence of an external field of force. The starting-point of this theory is the Langevin equation, obtained by balancing the forces acting on a particle

$$m d\mathbf{v}/dt = -f\mathbf{v} + \mathbf{F}_w + \mathbf{F}_{el} + \mathbf{F}_r \quad [1]$$

where $m d\mathbf{v}/dt$ is the acceleration force, m and \mathbf{v} are the particle mass and velocity, respectively, f is the friction coefficient, \mathbf{F}_w and \mathbf{F}_{el} are directional forces due Van Der Waals and electrostatic interactions, respectively. \mathbf{F}_r is a fluctuating random force which is characteristic of Brownian motion. When the forces \mathbf{F}_w and \mathbf{F}_{el} are conservative and when processes are considered with relevant time intervals very large compared to m/f and space intervals much larger than $(mkT/f^2)^{1/2}$, then [1] leads to the diffusion equation (25). This is a differential equation

describing the particle density distribution as a function of the position coordinates and time.

In the Smoluchowski-Fuchs theory, the diffusion equation is used to calculate the initial rate of coagulation, i.e. the rate of the formation of doublets from singlets. The model, in which particle encounters are treated as binary collisions, considers the flux of particles towards a (moving) "central" particle. The latter is assumed to act as a perfect sink; it captures the particles coming in contact with it. The capture frequency or rate of coagulation depends on the interaction force between the particles and it is obtained by solving the diffusion equation under spherical symmetry

$$\frac{\partial n}{\partial t} = \frac{1}{r^2} \frac{\partial}{\partial r} r^2 \left(D_m \frac{\partial n}{\partial r} + \frac{D_m n}{kT} \frac{dV}{dr} \right) \quad (r > 2a) \quad [2]$$

with r the distance from the centre of the central particle to that of the incoming particles, n the number density of particles per unit volume, t the time, D_m the mutual particle diffusion coefficient, i.e. the diffusion coefficient with respect to another, V the conservative free energy of interaction, k the Boltzmann constant and T the temperature. Ignoring hydrodynamic interactions, D_m just equals twice the diffusion coefficient D of an isolated particle, i.e. $D_m = 2D$. However, at separation distances comparable to the particle dimensions hydrodynamic interactions do become important. A simplified expression for D_m as a function of the relative separation distance has been given by Honig et al. (22)

$$D_m \approx 2 \frac{6(s-2)^2 + 4(s-2)}{6(s-2)^2 + 13(s-2) + 2} D \quad [3]$$

where $D = kT/f = kT/6\pi a\eta$ and $s = r/a$. The mentioned restrictions on the time and space intervals for the applicability of the diffusion equation are usually satisfied in sols; $\tau_{coag} \gg m/f$ and $(mkT/f^2)^{1/2} \ll \kappa^{-1}$, with κ^{-1} the Debye length.

Obviously, the solution of [2] depends on the boundary conditions. The first one is the abovementioned perfect sink approximation, i.e. $n(2a) = 0$, whereas the number density at infinity is kept at a constant value n^∞ . Furthermore, Smoluchowski and Fuchs assumed the

attainment of a steady state, in which case the left hand side of [2] becomes zero. According to Roebersen and Wiersema (26) this is a reasonable assumption, since transients effects have largely disappeared on time scales of approximately 10^{-2} seconds, too short to detect in classical coagulation experiments. The resulting solution is well-known

$$\frac{n(s)}{n^\infty} = \frac{e^{-V/kT} \int_2^s D_m^{-1} e^{V/kT} d\chi / \chi^2}{\int_2^\infty D_m^{-1} e^{V/kT} d\chi / \chi^2} \quad [4]$$

and

$$J = \frac{D_m^\infty n^\infty}{as^2} \frac{1}{\int_2^\infty (D_m^\infty / D_m) e^{V/kT} d\chi / \chi^2} \quad [5]$$

Here χ is a dummy normalized distance variable ($\chi = r/a$). From [5] it is clear that $4\pi r^2 J$ is a constant, representing the total flux of particles across a spherical envelope at r towards the central sphere, i.e. the rate of coagulation. The colloid stability ratio W is defined by

$$W = 2 \int_2^\infty (D_m^\infty / D_m) e^{V/kT} ds / s^2 \quad [6]$$

Interaction Energy

In the DLVO-theory, the interaction energy V of two spheres is described as the sum of the attractive Van der Waals interaction energy V_w and the repulsive electrostatic interaction energy V_{el} , i.e. $V = V_w + V_{el}$. A convenient expression for V_w under conditions of no retardation has been proposed by Hamaker (27)

$$\frac{V_w}{kT} = -\frac{A}{6kT} \left(\frac{2}{s^2 - 4} + \frac{2}{s^2} + \ln \frac{s^2 - 4}{s^2} \right) \quad [7]$$

where A is the Hamaker constant.

For our purposes, we need an expression for the electrostatic force between two identical particles which is valid irrespective of the boundary conditions for the charge or potential applied at the particle

surface. A suitable expression, valid if $\kappa a \gg 1$, has been introduced by Derjaguin (28). According to his approximation, the electrostatic force F_{el} can be calculated from the interaction between two identical parallel flat plates with given surface charge or surface potential. Accordingly,

$$F_{el} = \pi \kappa a \int_{H_0}^{\infty} (\cosh \psi_m - 1) dH \quad [8]$$

with ψ_m the potential midway between two parallel plates (of finite thickness) at distance $H = \kappa h$, whereas $H_0 = \kappa h_0$ is the shortest distance between the surfaces of the spheres, see Fig. 1. Moreover, the force is scaled on $\epsilon_0 \epsilon_r (kT)^2 / e^2$ and the potential on kT/e , with ϵ_0 the permittivity of vacuum, ϵ_r the relative solvent permittivity and e the elementary charge. Eq. [8] can be used regardless of the charge or potential distribution along the particle surface, provided that the diffuse part of the double layer is always in equilibrium.

If coagulation occurs under the conditions of full equilibrium of the double layer, i.e. if $De \gg 1$, [8] also shows how improvements in the equilibrium double layer model, for example by incorporating dissociation equilibria, affect the particle size dependence of W . When the double layer is completely relaxed, the potential ψ_m is only determined by equilibrium criteria. Therefore, the integral in [8] is independent of the particle size and F_{el} scales with κa , irrespective of the type of equilibrium criteria. Consequently, within the Derjaguin approximation, improvements in the equilibrium double layer model do not affect the particle size dependence of F_{el} and, consequently, neither that of W .

By integration of F_D from infinity to a certain distance s , the electrostatic interaction energy V_{el} can be obtained by

$$\frac{V_{el}}{kT} = \frac{a \epsilon_0 \epsilon_r kT}{e^2} \int_{\infty}^s F_{el} d\chi \quad [9]$$

where χ is again a dummy distance variable.

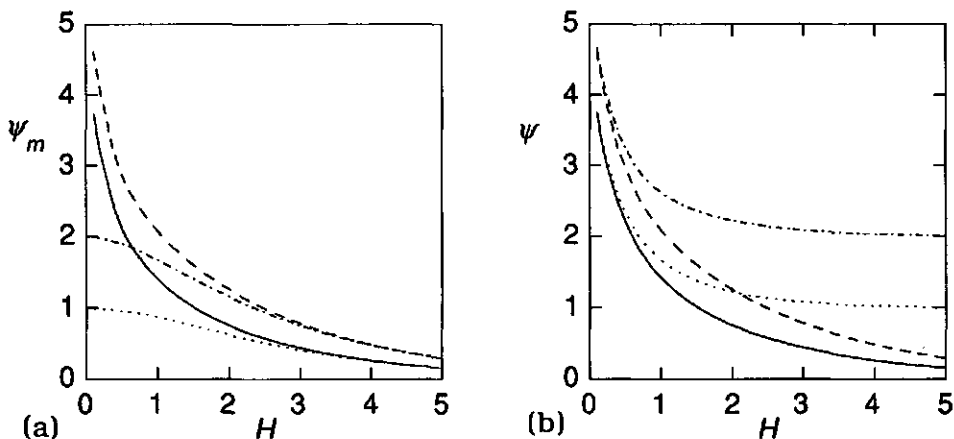


Figure 2. Interaction between two parallel plates: ψ_m and ψ_o versus H . In both figures, ψ_m : (—) $\psi_o^{\text{eq}} = 1$, constant surface charge (cc), (---) $\psi_o^{\text{eq}} = 2$, cc. In (a), ψ_m : (· · · ·) $\psi_o^{\text{eq}} = 1$, constant surface potential (cp), (· · · · ·) $\psi_o^{\text{eq}} = 2$, cp. In (b), ψ_o : (· · · ·) $\psi_o^{\text{eq}} = 1$, cc, (· · · · ·) $\psi_o^{\text{eq}} = 2$, cc.

The potential ψ_m can be (numerically) determined from the non-linearized Poisson-Boltzmann equation for the two parallel flat-plate geometry

$$\frac{\partial^2 \psi}{\partial x^2} = \sinh \psi \quad [10]$$

with x the distance (normalized on the Debye length) from one of the plates. The first boundary condition required to solve this equation is given by the fact that both plates are identical and hence, the electric field strength vanishes midway between both plates. The second is provided by the surface potential ψ_o or the surface charge density. The latter is related to the electric field strength at the surface

$$\sigma_o = -\left. \frac{\partial \psi}{\partial x} \right|_{x=0} \quad [11]$$

with σ_o the surface charge density scaled on $\epsilon_0 \epsilon_r \kappa kT/e$. By writing [11], we have implicitly assumed that any effect of an electric field inside the sphere on the electrostatic force is negligible. For most practical cases where the permittivity of the particle is much smaller than that of

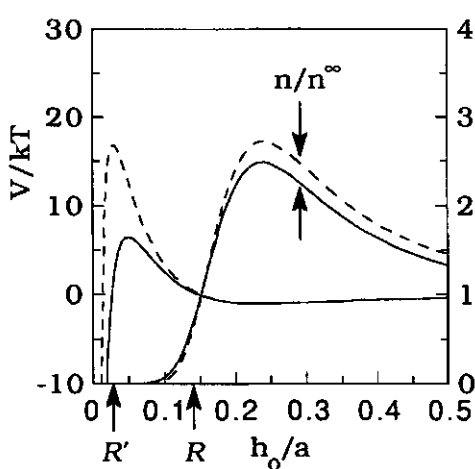


Figure 3. V_d and stationary state value of n/n^∞ as a function of distance. $\psi_o^{eq} = 1$, $A/6kT = 2$. (—) cp, (---) cc.

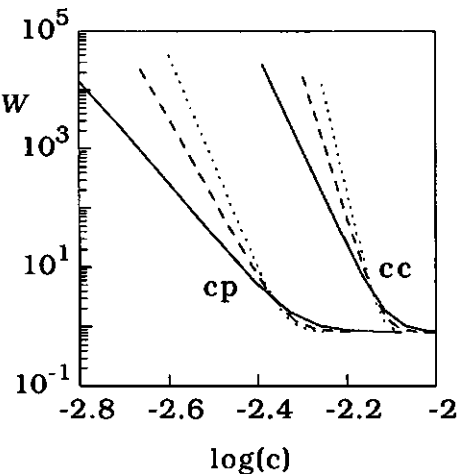


Figure 4. $\log W/\log c$ curve for interaction at cp and cc for different particle radii. $\psi_o^{eq} = 1$, $A/6kT = 2$, radii in nm: (—) 100, (---) 150, (····) 200.

water, this is a good approximation (29). For an isolated surface, σ_o^* follows simply from ψ_o^{eq} according to $\sigma_o^* = -2 \sinh \psi_o^{eq}/2$. For details about the numerical procedure to evaluate [8], [9] and finally [4]-[6], see appendix A.

Some results are displayed in Figs. 2-4. The potential ψ_m versus separation distance for two flat plates interacting at constant potential and at constant charge is shown in Fig. 2. For the latter case, ψ_o is also displayed. For both types of interaction, ψ_o^{eq} is chosen the same. Clearly, major differences between the two mechanisms occur at $H \approx 1$, where approximately the maximum in the interaction energy curve V is located. This is shown in Fig. 3. The same figure also shows that, in comparison with the constant potential mechanism, the maximum of V for the constant charge mechanism is much larger and that its position is shifted towards a lower value of H . This has substantial consequences for the calculated stability, as is shown in Fig. 4, where the stability ratio W is plotted as function of the electrolyte concentration for three

different particle sizes. No hydrodynamic interactions are taken into account; they are known not to affect the results qualitatively (21). Clearly, W is very sensitive to the type of interaction and the particle radius. In the domain of slow coagulation, the stability of a sol interacting at constant surface charge exceeds that of a sol at constant surface potential and it increases with particle size.

Double layer dynamics

As mentioned in the introduction, the basic difference between the two limiting mechanisms of interaction, the constant charge and the constant potential cases, reduces to different values of De . In the intermediate case of $De \approx 1$, transient disequilibrations of the surface charge density occur. Formally, the electrostatic force F_{el} can then be written as the sum of an equilibrium component F_{el}^{eq} , i.e. the force which would be experienced if $De \ll 1$, and a correction ΔF due to the disequilibrium of the double layer, i.e.

$$F_{el} = F_{el}^{eq} + \Delta F \quad [12]$$

The maximum value of ΔF is given by $F_{el}^{cc} - F_{el}^{eq}$, with F_{el}^{cc} the force at constant surface charge density. Its value can be substantial, which follows immediately, in combination with [8], from the differences between ψ_m for the interaction at constant charge and that at constant potential, as shown in Fig. 2.

In general, ΔF will depend on the relative velocity and the path of approach of the two interacting particles. Hence, what happens at a given instant of time t depends on what has already happened during all time preceding t . Therefore, the Brownian movement is not a first-order Markov process anymore. This complicates theoretical progress because the value of ΔF is not a priori known and, at the same time, the diffusion equation does not hold anymore since it is only valid for first-order Markov processes.

We observe that the rate of slow coagulation J strongly depends on the height of the interaction energy barrier V_{max} (see [5] and [6]). For systems with $De \approx 1$, the electrostatic force depends on the rate of

approach, and hence, the height of the energy barrier as well. Probably, the rate of approach will vary during the encounter and the corresponding interaction time will differ from one encounter to another. Our analysis is now aimed at finding an expression for an average rate of approach, representing the dynamics of all the two-particle encounters. Using this average rate of approach, we can calculate $F_{el} = F_{el}^{eq} + \langle \Delta F \rangle$ as a function of the separation distance and consequently V_{el} by using [9]. Here, $\langle \Delta F \rangle$ represents an ensemble average of ΔF . However, in this particular case, V_{el} is a "dynamic electrostatic energy", i.e. the energy barrier which the particles create when they approach each other with a given velocity profile. Despite this change in the interpretation of V_{el} , we use, as a first approximation, the same procedure as described in the previous section ([4]-[6]) to calculate the rate of coagulation. Although the correctness of this procedure is difficult to assess, it can be useful. It enables us to investigate the influence of the particle size on the rate of coagulation under conditions of double layer disequilibration, as will be shown.

If double-layer dynamics are important, then a distribution of interaction times leads to a distribution of ΔF_{el} and V_{el} . According to Adamczyk et al. (30) and Prieve and Lim (31), the neglection of a distribution in the energy barrier could introduce errors in the calculated flux. These errors are more pronounced for larger particles, thus changing the particle size dependence of the $\log W/\log c$ curve. However, for convenience, we will neglect these effects for the moment.

Two methods will be proposed now to derive an expression for the average rate of approach, which is needed to calculate $\langle \Delta F \rangle$ and finally W . In this section, only a description of these methods will be given. Both methods neglect the effect of rotational diffusion. The reasonability of this approximation will be discussed in Appendix B.

Method 1

Formally, it is possible to define an average velocity $\langle v_1 \rangle$ by

$$\langle v_1 \rangle \equiv \frac{J}{n} \quad [13]$$

Both the flux J and the number density n are functions of the separation distance s and so is $\langle v_1 \rangle$. Moreover, $\langle v_1 \rangle$ is also sensitively related to the colloid stability, since it is dependent on J . J and $\langle v_1 \rangle$ are both counted positive for particles approaching each other.

Obviously, the concept of an average velocity can be used to define a characteristic time of interaction $\tau_{int}(1)$ as

$$\tau_{int}(1) = \frac{1}{\kappa} \int_2^0 \langle v_1 \rangle^{-1} dH_0 \quad [14]$$

where, for convenience, the lower integration border is set to zero. Note that $\tau_{int}(1)$ is dominated by the time for the particles to move from $H_0 = 2$ towards the maximum of the energy barrier, since $\langle v_1 \rangle$ strongly increases beyond it. As described in a previous section, we will calculate the "dynamic electrostatic energy" V_{el} , i.e. the energy required to bring the particles together with a known velocity $\langle v_1 \rangle$. To do so, we have to calculate also the relaxation of the surface charge density during the approach. Therefore, we require a model for the desorption/adsorption rate of the surface charge density. In the simple model used, we assume that this rate is linearly dependent on the relative overpotential

$$\frac{\partial \sigma_o}{\partial t_{red}} = -k \frac{\psi_o - \psi_o^{eq}}{\psi_o^{eq}} \quad [15]$$

where k is a dimensionless rate constant and $t_{red} = t/\tau_{int}(1)$. At any point on the particle surface, the charge density $\sigma_o(H)$ can be calculated by the following integral

$$\sigma_o(H) = \sigma_o^\infty + \int_\infty^H \frac{\partial \sigma_o}{\partial \chi} d\chi \quad [16]$$

where χ is a dummy (normalized) distance variable and

$$\frac{\partial \sigma_o}{\partial \chi} = -\frac{k}{\kappa \tau_{int}(1)} \frac{1}{\langle v_1 \rangle} \frac{\psi_o - \psi_o^{eq}}{\psi_o^{eq}} \quad [17]$$

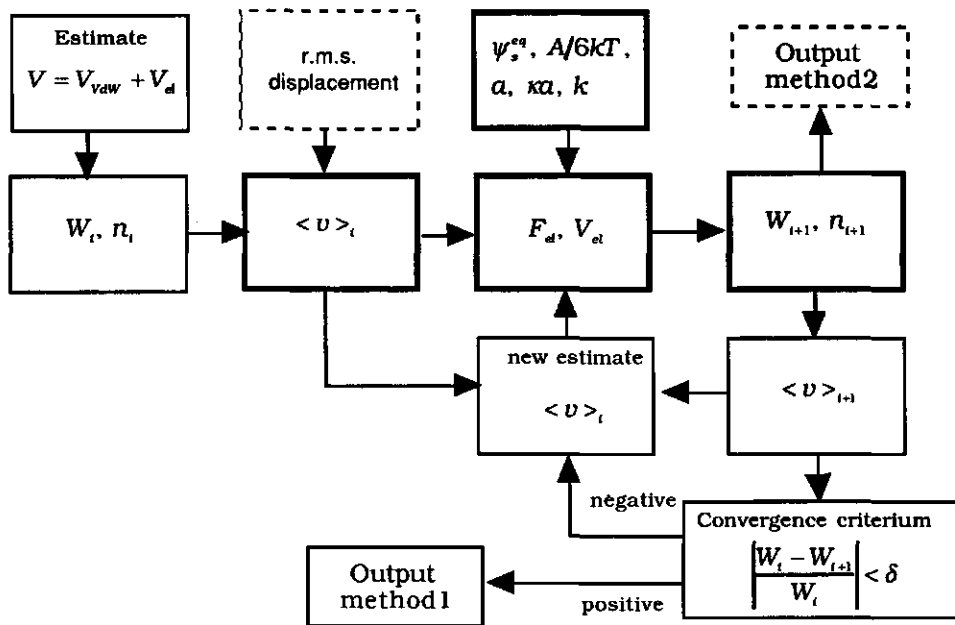


Figure 5. Flow diagram computation method. Bold squares are used in both methods, plain squares only in method 1 and dashed squares only in method 2.

since $\partial\chi = \kappa\tau_{int}(1)\langle v_1 \rangle \partial t_{red}$. Obviously, the transient deviations occur only at positions inside the interaction regime where double layers overlap. Given $\sigma_o(H)$, the potential distribution in the double layer (i.a. ψ_o and ψ_m) follows from the solution of the Poisson-Boltzmann equation [10] and, subsequently, F_{el} from [8].

One of our final aims is to calculate the stability ratio W . Therefore, we have written a computer program which solves simultaneously the integrals in the Eqns. [4]-[10] and [13]-[17] if the average velocity $\langle v_1 \rangle$ is known. However, since $\langle v_1 \rangle$ depends on the colloid stability via [13], which of course is a priori unknown, we have an implicit set of equations. This set can be solved by an iterative procedure, as shown in the flow diagram of the computer program in Fig. 5. Details about the computing procedure are described in Appendix A.

Method 2

It can be argued (see discussion) that the relative mobility of the particles in an encounter is better represented by the root mean square displacement $\langle \Delta x^2 \rangle$ in time than by the average velocity $\langle v_1 \rangle$. In the absence of any interaction, we have

$$\langle \Delta x^2 \rangle = 2D_m t \quad [18]$$

This is Einstein's result, which can be used to obtain an alternative estimate of the interaction time $\tau_{int}(2)$. During an encounter, let the relevant r.m.s. displacement of one particle relative to the other be κ^{-1} , then according to Einstein's equation

$$\tau_{int}(2) = \frac{\kappa^{-2}}{2D_m} \quad [19]$$

Moreover, we can define an average displacement velocity $\langle v_2 \rangle$ by

$$\langle v_2 \rangle = \frac{\kappa^{-1}}{\tau_{int}(2)} = 2D_m \kappa \quad [20]$$

In this approximation, $\langle v_2 \rangle$ is independent of s . Its value is used to calculate the stability ratio W according to approximately the same procedure as in method 1. The major difference is that, because of the simplification considered, no iteration is required, because $\langle v_2 \rangle$ is a priori known and constant. Obviously, the estimate $\tau_{int}(2)$ for τ_{int} will be used instead of $\tau_{int}(1)$, see also Fig. 5.

Results and discussion

The effect of double-layer dynamics on the stability ratio W is illustrated by Figs. 6-8. The system parameters are the same as in Fig. 4, the only exception being the desorption rate constant k . In each graph, the absolute rate constant k/τ_{int} is identical for the 3 curves, corresponding to 3 different particle sizes. Again, hydrodynamic interactions are neglected.

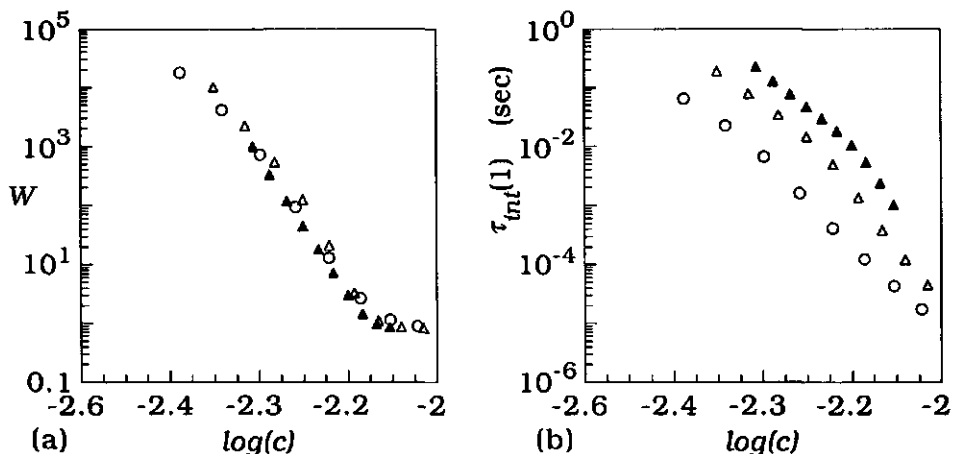


Figure 6. Results of method 1. $k=0.01$, $\psi_0^{eq}=1$, $A/6kT=2$, radii in nm: (○) 100 (Δ) 150, (\blacktriangle) 200. (a) $\log W/\log c$ curve. (b) $\tau_{int}(1)/\log(c)$ curve. Absolute desorption rate constant k/τ_{int} for all cases the same, $k=0.01$ belongs to $a=100$ and lowest electrolyte concentration shown in the graph.

According to method 1, W becomes nearly independent of the particle size for a suitable choice of the rate constant k , see fig. 6a. As shown in Figs. 7 and 8, this result cannot be obtained with method 2, no matter the choice of k . This result is directly related to the particle size dependence of $\langle v \rangle$ and, consequently, to that of τ_{int} . If De becomes strongly particle size dependent, then the extent of disequilibration of the double layer during an encounter does so too. This is what happens, to a certain extent, according to method 1. By combining Eqns. [4], [5] and [13] it follows that $\langle v_i \rangle$ and $\tau_{int}(1)$ are very sensitive to the height of the energy barrier and, hence, to the particle size. Consequently, $\tau_{int}(1)$ is relatively large and grows with increasing a , as is demonstrated in Fig. 6b. In limiting cases, it could be possible that small particles coagulate under conditions of constant charge, whereas bigger ones would coagulate under conditions of constant potential.

In method 2, the interaction time $\tau_2(2)$ is inversely proportional to the particle radius a , since $D \propto a^{-1}$. Apparently, this relation is not strong enough to make W independent of the particle size. Summarizing, the present results indicate that the experimentally found insensitivity of W to the particle size could be explained by double-layer

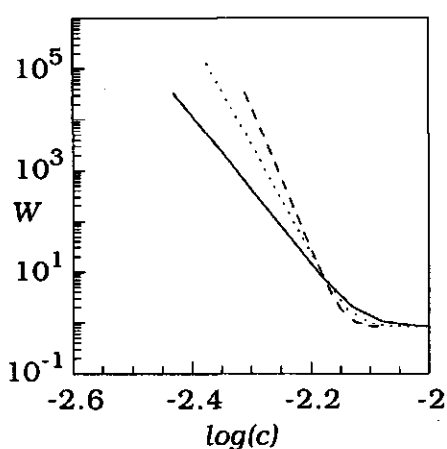


Figure 7. Results of method 2. $\log W/\log c$ curve for "dynamic" interactions. $k=0.1$, radii in nm: (—) 100, (---) 150, (- - -) 200, other parameters and criterium choice k identical as in Fig 6.

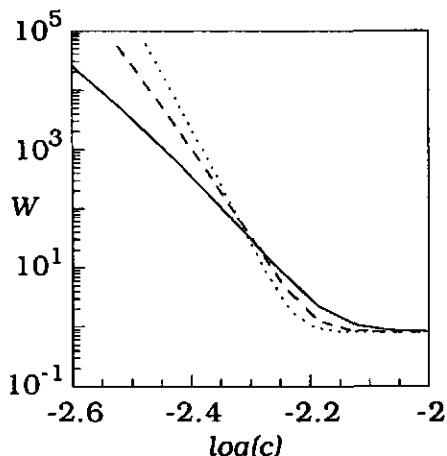


Figure 8. As Fig. 7 but $k=1.0$.

dynamics, provided that the time scale of an Brownian encounter is dependent on the height of the energy barrier.

Still, the question has to be answered which model more realistically describes the interaction time between two particles. The dynamics of an encounter is determined by the relative motion of one single particle with respect to the other. Usually, in the absence of any force field and any particle sink or source, the motion of a single particle is characterized by its r.m.s. displacement. The average displacement of such a particle obviously equals zero; displacements in any direction are equally probable and a net flux of particles does not exist. In this particular case, the average displacement in time, or, in other words, the average velocity $\langle v_i \rangle$, equals therefore zero. Hence, $\langle v_i \rangle$ is a very poor estimate for the motion of single particles because, in this case, it completely neglects Brownian motion. In cases where a force field is present but where the flux is still low, for example in slowly coagulating sols where $W \gg 1$, similar objections can be raised

against the use of $\langle v_t \rangle$ to estimate the motion of single particles. Despite these objections, method 1 shows what kind of effects could be expected if the time scale of interaction is sensitive to the height of the energy barrier.

The discussion above illustrates that the Brownian motion of the particles has to be taken into account by estimating the time scale of interaction. For a single isolated particle in the absence of any force field, the r.m.s. displacement of the particle best characterizes its random motion. This displacement is used in method 2 to estimate the interaction time. However, inherent in the interaction is that each particle feels a force during the encounter. Hence, $\tau_{int}(2)$ can only be a first approximation for the interaction time since the influence of directional forces is neglected.

One way to get an idea on how the particle interaction affects the interaction time τ_{int} is to study transient states of the concentration profile according to the diffusion equation [2]. These transient states occur if the time derivative $\partial n / \partial t$ in [2] cannot be neglected, see for example ref. (26). However, does the solution of a transient state really give us the time scale of an encounter between two particles? In order to answer this question, we consider a transient state of the diffusion according to [2]. Assume that at $t=0$, $n=0$ for $r < R$ and $n=\text{constant}$ for $r > R$, with R a point just before the energy barrier, see Fig 4. We consider a particle to have successfully passed the barrier once it has arrived at $r=R'$. At $t>0$, particles start to penetrate the energy barrier from R towards R' .

Obviously, the penetration depth of the majority of the particles is only limited, after which they move out of the barrier towards R again. Nevertheless, despite the presence of the energy barrier, a certain fraction of the particles will succeed to arrive at R' . The transient solution of the diffusion equation is able to tell us how many particles arrive at R' in time and the time scale to reach a stationary flux. However, since this time scale is probably mainly determined by the fraction of successful attempts to pass the barrier, it does not tell us (except for $W=1$) much about the time scale for an successful attempt to diffuse from R to R' . This is probably the time scale which is most characteristic for the interaction between two particles.

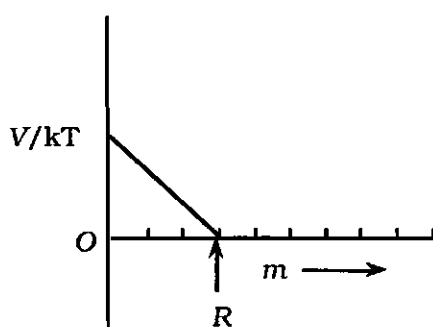


Figure 9. model for diffusion through energy barrier along straight line, see text.

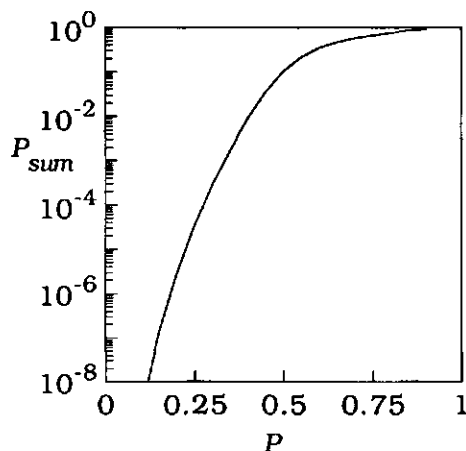


Figure 10. P_{sun} versus P for $R=10$, see text.

Hence, in order to determine whether double-layer dynamics can significantly affect the particle size dependence of W , we have to investigate the dependence of the time scale of a successful attempt on the height (and shape) of the energy barrier. In such an investigation, it is necessary to distinguish between successful and unsuccessful attempts and therefore to keep track of the trajectories of the particles and their probabilities. Within this frame, the following simple analysis has been carried out.

Simple statistical analysis

It is well-known that diffusion can be simulated by solving the problem of (weighted) random flights, where each displacement is of a certain constant length l (25). This principle will be applied to the diffusion of particles along a straight line through a (linear) conservative energy barrier, see Figure 9. We are interested in the probability $P_{R,o}(N)$ that a particle diffuses from R to the origin O in N steps given that its first step from R is towards O and that the particle does not return meanwhile to R . In our context of particle interaction, we regard the average number of N as a measure of the interaction time.

The external force field is reflected in the probability P that a particle between O and R does a step towards the origin; an energy barrier exists if $P < 0.5$, a energy well if $P > 0.5$. Since the energy barrier is linear, the external force is a constant and, hence, P too. We assume that first-order Markov statistics apply. This assumption determines together with the requirement that, under equilibrium conditions, the position probability of a particle satisfies the Boltzmann distribution, the relation between V/kT and P . In our case, we find

$$\frac{V}{kT} = (R - m) \ln\left(\frac{1-P}{P}\right) \quad (m \leq R) \quad [21]$$

A one-dimensional diffusion coefficient D can be defined by $D = nl^2/2$, with n the number of displacements per unit time (25).

The calculation of the probability $P_{R,O}(N)$ runs as follows. We assume that the first step of the particle is from R towards O , i.e.

$$P(R-1,1) = 1; \quad P(m \neq R-1,1) = 0 \quad [22]$$

Next, the particle diffuses according to Markov statistics; the probability $P(m,N)$ that a particle arrives at position m after N steps can be written as

$$P(m,N) = P(m+1,N-1)P + P(m-1,N-1)(1-P) \quad (N > 1) \quad [23]$$

For the calculation of $P_{R,O}(N)$, we do not want to consider those particles which arrive at either O or R and which consequently turn to diffuse back into the energy barrier. Therefore, we put

$$P(O,N) = 0, \quad P(R,N) = 0 \quad (N > 1) \quad [24]$$

which forces the boundaries O or R to act as a sink. Hence, $P_{R,O}(N)$ can be calculated by a matrix procedure according to [23] with the boundary conditions [22] and [24].

The probability P_{sum} that a particle arrives at O without diffusing out of the barrier at R is given by

$$P_{sum} = \sum_N P_{R,O}(N) \quad [25]$$

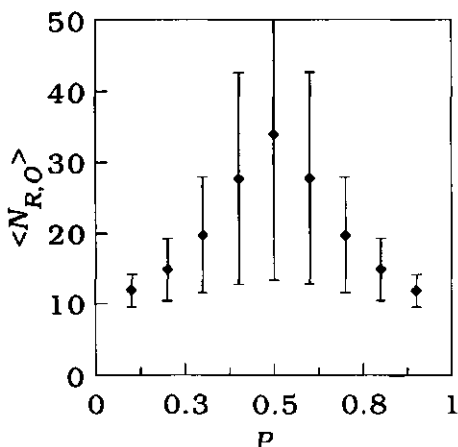


Figure 11. $\langle N_{R,O} \rangle$ versus P for $R=10$, error bars indicate standard deviation.

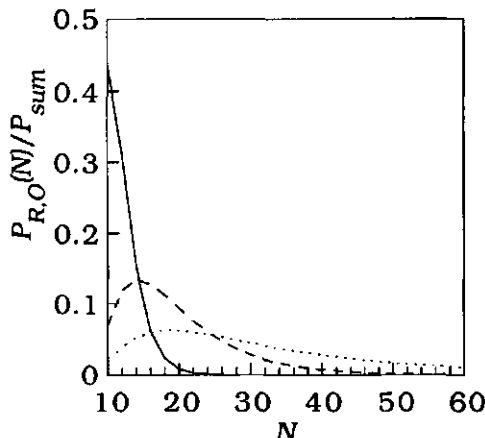


Figure 12. $P_{R,O}(N)$ versus N for $R=10$. (—) $P=0.1$, (---) $P=0.3$, (····) $P=0.5$.

and the corresponding average number of steps $\langle N_{R,O} \rangle$ to get there follows from

$$\langle N_{R,O} \rangle = \sum_N N P_{R,O}(N) / P_{sum} \quad [26]$$

Some results are shown in Figures 10-12 for $R=10^*$. Clearly, P_{sum} is a strongly increasing function of P , see Fig. 10. However, the graph of $\langle N_{R,O} \rangle$ (including its standard deviation) versus P (Fig. 11) is completely symmetric around its maximum at $P=0.5$! This shows that in the presence of any force field, either an attractive or a repulsive one, combinations of many forward and backward movements of particles are suppressed. The pertaining distribution of $P_{R,O}(N)$ is displayed in Fig. 12 (only for even values of N , otherwise $P_{R,O}(N)=0$ since with R chosen even, the total number of steps to get to O is even too). It can be shown that the normalized probability $P_{R,O}(N)/P_{sum}$ also is a symmetric function

* For example, this number may be of the right order for particles of 100nm and $\kappa\alpha>10$. In the absence of Brownian motion, particles with an initial velocity corresponding to an energy of several kT travel approximately only 0.5 nm or less due to the hydrodynamic friction (2).

of P around $P=0.5$. Hence, the present results indicate that the time scale τ_{int} of any individual encounter between colloidal particles (slightly) decreases with growing barrier height. It is quite clear that this τ_{int} for individual particle interaction is basically different from the $\tau_{int}(l)$ in method 1 (which is based on the average velocity as derived from [13] and [14]).

Conclusions

We have presented two approaches to incorporate transient deviations from the equilibrium surface charge density during particle interaction into the theory for colloid stability. A key issue appeared to be the dependence of the time scale of interaction between two particles on the height of the energy barrier. The two different approaches correspond to two different approximations about this dependence. The obtained results indicate that double-layer dynamics could explain the experimentally found insensitivity of the stability ratio to the particle size, provided the time scale of the encounter is strongly dependent on the height of the energy barrier. However, this proviso is unlikely to be satisfied. A simple statistical analysis indicates that the time scale of any individual encounter (slightly) decreases with growing barrier height!

Appendix A

According to [9], V_{el} should be calculated by integrating the force F_{el} , which is expressed as an integral with ψ_m in the integrand, see [8]. Furthermore, the rate of change of σ_o depends on ψ_o , see [15]. Hence, the calculation of the potentials ψ_m and ψ_o has to be repeated a very large number of times for varying values of σ_o and the electrolyte strength. However, the solution of the Poisson-Boltzmann equation [10], which is written in dimensionless parameters, is independent of the electrolyte strength. This enables us to reduce computing time by storing these solutions, i.e. values of ψ_m and ψ_o , in matrices as function of normalized distance H and normalized surface charge density σ_o . For calculations of interactions at constant surface potential, similar matrices are made. By interpolation methods, the desired solution of

the Poisson-Boltzmann can be quickly retrieved. The data in the matrices follow from numerical solutions obtained with a fourth-order Runge-Kutta method.

The integration variable of most integrals of interest, i.e those in Eqns. [4-6], [9] and [16], is the centre-to-centre distance s or it can be transformed to s . These integrals are simultaneously solved by a fourth-order Runge-Kutta method for coupled differential equations.

The derivation of F_D starts with an integration over θ , which can be transformed to an integration over H . Therefore, a particular value of H in [8] corresponds to a point on the surface with a certain value of θ . Hence, an equidistant net of points H_i corresponds to a set of points on the particle surface. Eq. [16] is used now to calculate the surface charge densities σ_o in each of these points during the approach. Once these densities are known, the force is obtained by a Simpson's method of convenient order (usually 11th), while the upper boundary of the integral in [8] is chosen (arbitrarily) $10\kappa^{-1}$. A number of 40 points was usually more than sufficient.

The numerical procedure could be tested only to a limited extent. However, by using the linearized form of the Poisson-Boltzmann equation instead of [10], we obtained perfect agreement with the results of Spielman for the constant potential case. The accuracy of the integrations is chosen such that the calculated stability ratio W is accurate up to 4 significant figures.

Appendix B

In the computations, we have neglected rotational diffusion of the particles during the interaction. In principle, if $De \approx 1$, rotational diffusion could interfere with the force calculations, because then the force would change by rotation of the particle. The pertaining contribution depends on the ratio of the angle of rotation during the interaction to the characteristic angle θ_{int} of the region of interaction, i.e. the region where significant double layer overlap occurs. An estimate of this ratio will be made now.

Arbitrarily, we define the angle θ_{int} as shown in Fig. 1, where $h_0 = \kappa^{-1}$ and $h = 2\kappa^{-1}$. Assuming that θ_{int} is small, i.e. that $\cos \theta_{\text{int}} \approx 1 - \theta_{\text{int}}^2/2$, we find

$$\theta_{\text{int}}^2 \approx \frac{1}{\kappa a + 1} \quad [\text{B.1}]$$

The angle of rotation can be estimated from the mean square angle $\langle \theta^2 \rangle$, defined by

$$\langle \theta^2 \rangle = 4D_r t \quad [\text{B.2}]$$

with $D_r = kT/8\pi\eta a^3$ the rotational diffusion coefficient. By using $\tau_{\text{int}}(2)$ of method 2 as estimate for the characteristic interaction time, we obtain for the $\langle \theta^2 \rangle$ after one encounter

$$\langle \theta^2 \rangle = \frac{3}{4} \frac{1}{(\kappa a)^2} \quad [\text{B.3}]$$

Hence, we get

$$\frac{\langle \theta_r^2 \rangle^{1/2}}{\theta_{\text{int}}} = \sqrt{\frac{3}{4}} \sqrt{\frac{1 + \kappa a}{(\kappa a)^2}} \approx \sqrt{\frac{1}{\kappa a}} \quad [\text{B.4}]$$

Consequently, for $\kappa a \gg 1$, the neglection of the rotational diffusion is a good approximation. On the other hand, for smaller κa values rotation could be significant. Note however that rotation will be hampered under conditions of disequilibration of the double layer when particles interact. Disequilibration occurs only inside the interaction region. Hence, rotation of the particle will introduce "fresh" surface into the interaction region, which is energetically unfavourable. Hence, [B.4] overestimates the ratio $\langle \theta_r^2 \rangle^{1/2}/\theta_{\text{int}}$.

Obviously, a similar estimate for $\langle \theta_r^2 \rangle^{1/2}/\theta_{\text{int}}$ with $\tau_{\text{int}}(1)$ of method 1 would lead to a less positive conclusion, since $\tau_{\text{int}}(1) > \tau_{\text{int}}(2)$. Nevertheless, it is expected that the qualitative conclusions regarding particle size effect still hold, since incorporating of rotation diffusion can be probably simulated by rescaling the desorption rate constant k .

References

- (1) Derjaguin, B. V. and Landau, L. D., *Acta Physicochim. URSS* **14**, 633 (1941).
- (2) Verwey, E. J. W. and Overbeek, J. T. G., "Theory of the Stability of Lyophobic Colloids", Elsevier, Amsterdam, 1948.
- (3) Overbeek, J. T. G., *J. Colloid Interface Sci.* **58**, 408 (1977).
- (4) Lyklema, J., *Pure & Appl. Chem.* **52**, 1221 (1980).
- (5) Elimelech, M. and O'Melia, C. R., *Langmuir* **6**, 1153 (1990).
- (6) Voegtli, L. P. and Zukoski IV, C. F., *J. Colloid Interface Sci.* **141**, 92 (1990).
- (7) Put v. d., A. G., Ph. D Thesis, 1980.
- (8) Midmore, B. R. and Hunter, R. J., *J. Colloid Interface Sci.* **122**, 521 (1988).
- (9) Dukhin, S. S. and Lyklema, J., *Langmuir* **3**, 94 (1987).
- (10) Chan, D., Perram, J. W., White, L. R. and Healy, T. W., *J. Chem. Soc. Farad. Trans. I* **71**, 1046 (1975).
- (11) Healy, T. W., *Pure & Appl. Chem.* **52**, 1207 (1980).
- (12) von Smoluchowski, M., *Physik. Z.* **17**, 557 (1916).
- (13) von Smoluchowski, M., *Z. physik. Chem.* **17**, 129 (1917).
- (14) Fuchs, N., *Z. Physik* **89**, 736 (1934).
- (15) Frens, G. and Overbeek, J. T. G., *J. Colloid Interface Sci.* **38**, 376 (1972).
- (16) Joseph-Petit, A. M., Dumont, F. and Watillon, A., *J. Colloid Interface Sci.* **43**, 649 (1973).
- (17) Ottewil, R. H. and Shaw, J. N., *Discuss. Faraday Soc.* **42**, 154 (1966).
- (18) Reerink, H. and Overbeek, J. T. G., *Discuss. Faraday Soc.* **18**, 74 (1954).
- (19) Penners, N. H. G. and Koopal, L. K., *Colloids and Surfaces* **28**, 67 (1987).
- (20) Dukhin, S. S. and Lyklema, J., *Faraday Discuss. Chem. Soc.* **90**, 261 (1990).
- (21) Spielman, L. A., *J. Colloid Interface Sci.* **33**, 562 (1970).
- (22) Honig, E. P., Roebersen, G. J. and Wiersema, P. H., *J. Colloid Interface Sci.* **36**, 97 (1971).
- (23) van Leeuwen, H. P. and Lyklema, J., *Ber. Bunsenges. Phys. Chem.* **91**, 288 (1987).
- (24) Warszynski, P. and van de Ven, T. G. M., *Adv. Colloid Interface Sci.* **36**, 33 (1991).
- (25) Chandrasekhar, S., *Rev. Mod. Phys.* **15**, 1 (1943).
- (26) Roebersen, G. J. and Wiersema, P. H., *J. Colloid Interface Sci.* **49**, 98 (1974).
- (27) Hamaker, C. *Physica* **4**, 1058 (1937).
- (28) Derjaguin, B., *Trans. Faraday Soc.* **36**, 203 (1940).
- (29) Kijlstra, J., accepted *J. Colloid Interface Sci.*; see chapter 6 (1992).

- (30) Adamczyk, Z., Czarnecki, J. and Warszynski, P., *J. Colloid Interface Sci.* **106**, 299 (1985).
- (31) Prieve, D. C. and Lin, M. M., *J. Colloid Interface Sci.* **86**, 17 (1982).

Summary

The purpose of the present study is to improve our insight into the relaxation of the electrical double layer around particles in hydrophobic sols. A detailed knowledge of the relaxation mechanisms is required to explain the behaviour of sols under conditions where the double layer is perturbed. Such conditions are frequently encountered in colloid science; for instance when colloidal particles coagulate or when they are subjected to an external field as in electrokinetics.

One of the appropriate electrokinetic methods to experimentally study the dynamic properties of double layers is low-frequency dielectric spectroscopy. Previous studies have shown that latices exhibit a large dielectric response. However, these results could not be quantitatively reconciled with either electrophoresis data or existing theory. To discriminate whether the disagreements were due to theoretical or experimental imperfections, dielectric data on inorganic sols were highly desirable. The major aim of this study is to provide such data and, where necessary, to improve the existing theory. The results are described and discussed in chapters 2-5.

The stability of sols against coagulation is of crucial importance for their applications. In principle, hydrophobic sols are thermodynamically unstable; they tend to form aggregates due to the attractive Van der Waals forces. However, in many cases the rate of coagulation is slowed down by the presence repulsive electrostatic forces. These occur if double layers overlap.

Coagulation is a dynamic process. Particles interact on a certain time scale during which the extent of double layer overlap varies. Consequently, the equilibrium double layer structure will be perturbed, inducing relaxation processes. In principle, the colloid stability depends on the relaxation time of the double layer, which may be well of the same order as the typical time scale of a particle collision. However, the knowledge about the influence of the relaxation processes on the coagulation rate was limited. Therefore, the second aim of this study is to improve that situation. We focussed our attention on those cases

where the relaxation rate of the double layer is determined by the adjustment of the surface charge density, see chapter 7. Chapter 6 discusses a related topic.

A short summary of the results and main conclusions of each chapter is given below.

Chapter 2 gives a description of a newly constructed four-electrode dielectric spectrometer, designed to measure the dielectric response (or complex admittance) of sols in the frequency range of approximately 500 Hz to 500 kHz. A four-electrode design is developed to avoid problems related to electrode polarization and, at the same time, to enable the use of an automatic frequency response analyzer. The device is suitable for fast and accurate data acquisition, the measurement of one complete spectrum taking a few minutes only. Furthermore, it is especially designed to measure frequency-difference spectra.

In **chapter 3** it is shown that the thin double layer theory for the electrokinetic properties of dilute colloids can be extended to include surface conduction, i.e. a conduction contribution by ions *behind* the plane of shear. The calculations show that the occurrence of surface conduction leads to a reduction of the electrophoretic mobility and to an increase of the static sol conductivity and the dielectric response. Moreover, it also follows from the theory that an unambiguous interpretation of only one type of experimental data, for example the electrophoretic mobility, is impossible if surface conduction occurs. To assess whether this is the case, one is bound to also measure either the static conductivity or the dielectric response of the sol. The comparison between theory and experiment has been made for literature data on latices. For polystyrene latices, the mobility and static conductivity can be well explained if surface conduction is taken into account. However, the extended theory is not able to provide a quantitative explanation of the extreme dielectric increment of latices.

Chapter 4 provides experimental data on the low-frequency dielectric response of dilute aqueous hematite and silica sols of spherical particles as a function of pH, ionic strength and particle size. The pH-sensitivity of the dielectric responses of the two sols shows that this response is a function of the surface charge density. The particle size dependence of the characteristic relaxation frequency is in fair agreement with theoretical predictions. In contrast to the case of latices, the dielectric behaviour of both hematite and silica can be well explained by classical electrokinetic theory yielding reasonable values for the ζ potentials. However, these values are systematically higher than those obtained electrophoretically. This inconsistency indicates the occurrence of surface conduction within the plane of shear, a type of conduction not included into the classical theory. By using the theory as developed in chapter 3, a distinction can be made between the (mobile) counter charge within and that beyond the plane of shear. Application to the hematite and silica data shows that a large fraction of the (mobile) counter charge is located inside this plane. This fraction increases with increasing surface charge density.

The experimental and theoretical framework developed in the previous chapters has been applied to a spherical coryneform bacterium suspension in **Chapter 5**. According to the preliminary results, approximately 95% of the total (mobile) counter charge in the double layer of the bacterium is located behind the plane of shear, i.e. probably within the cell wall itself. Such a large surface conduction contribution inhibits the possibility to determine the ζ potential of bacteria by electrophoretic measurements only. In this respect, additional information is necessary. The present investigation shows that dielectric spectroscopy is a useful technique to obtain that information.

Chapter 6 presents a model to calculate the electrostatic interaction between two colloidal spheres, accounting for their polarizabilities. Under conditions where the potential along the surface varies during interaction, for example under those as discussed in chapter 7, the polarizability of a particle affects the electrostatic repulsion. Results are presented for spheres interacting at constant

surface charge density. The calculations clearly show how the electrostatic force decreases with the polarizability of the particle. The decrease becomes larger with stronger double layer overlap, whereas it is relatively insensitive to κa . This insensitivity is a consequence of tangential screening effects inside the particles. It is pointed out that for slowly coagulating sols of particles with a fixed surface charge density, the stability ratio W is sensitive to the polarizability of the particle.

Transient deviations from the equilibrium surface charge density during the interaction of colloidal particles and their influence on colloid stability are discussed in **chapter 7**. Such deviations cause the process of particle encounter to become a non-first-order Markov process, which complicates the analysis of colloid stability. Two methods are presented to calculate a modified colloid stability ratio, taking such deviations into account in an approximate way. These methods differ by their estimates for the time scale of the Brownian encounter and its dependence on the height of the energy barrier. Despite these differences, both methods show that double-layer dynamics can have major consequences for the stability ratio. However, the predicted dependences of the rate of slow coagulation on the particle radius of the two methods are different. This indicates that double-layer dynamics could explain the experimentally found insensitivity of the stability ratio to the particle size, provided the time scale of the encounter strongly increases with growing height of the energy barrier. However, this proviso is unlikely to be satisfied. A simple statistical analysis indicates that the time scale of any individual encounter should decrease with growing barrier height!

This thesis presents experimental and theoretical work related to double layer relaxation of colloids. It is not only of academic interest but also of significant practical importance. The results provide an encouraging basis for further research in the field of electrokinetics and stability of hydrophobic colloids.

Samenvatting

Kolloiden zijn mengsels van twee fasen waarbij de ene fase in de vorm van mikroskopisch kleine deeltjes homogeen is verdeeld in de andere. De grootte van deze deeltjes ligt in de orde van 10^{-9} – 10^{-6} m. Zo'n systeem wordt ook wel een sol genoemd als de continue fase een oplosmiddel is. Kolloiden vinden een lange reeks aan praktische toepassingen; ze worden o.a. gebruikt bij de produktie van medische tests (b.v. zwangerschapstests), verven en fotografische film.

Van nature zijn kolloiden vaak niet stabiel. Er bestaat een aantrekkende kracht tussen de deeltjes onderling, de Van der Waals kracht, die ervoor zorgt dat de deeltjes de neiging hebben om te aggregeren. Hierdoor kunnen vlokken ontstaan die mogelijk een neerslag vormen. Men noemt zulke kolloiden ook wel thermodynamisch instabiel. Echter, er kunnen ook afstotende krachten aanwezig zijn die het vlokproces vertragen. Met name in waterige kolloiden speelt ladingsophoping op de deeltjes daarbij een belangrijke rol. Stoffen als oxiden hebben zure en/of basische groepen op het oppervlak die (afhankelijk van de zuurgraad) dissociëren als het oppervlak bevochtigd wordt. In andere gevallen hebben bepaalde soorten ionen in de oplossing een affiniteit voor het oppervlak waardoor ze in meerdere of mindere mate zullen adsorberen. Meestal is de resulterende netto lading voornamelijk gelokaliseerd op het deeltjesoppervlak en leidt dan tot de zgn. oppervlaktelading. Het verschijnsel dat gelijke ladingen elkaar afstoten (elektrostatische afstoting) verklaart waardoor in aanwezigheid van oppervlaktelading het vlokproces wordt vertraagd. De balans van aantrekkende en afstotende krachten bepaalt uiteindelijk de weerstand tegen het vlokken. Om die reden kunnen kolloiden stabiel zijn.

Voor het kwantificeren van de elektrostatische afstoting tussen kolloïdale deeltjes is het verschijnsel dat ongelijke ladingen elkaar aantrekken ook van belang. Het geheel van deeltje plus omgeving heeft nl. een netto lading van nul. Dit houdt in dat eenzelfde hoeveelheid lading als op het oppervlak, maar dan van tegengesteld teken, zich in de

oplossing bevindt. Deze vormt een wolk van tegenlading om het deeltje. Oppervlaktelading en tegenlading tezamen vormen de zgn. elektrische dubbellaag, waarvan de structuur de elektrostatische afstoting tussen de deeltjes bepaalt. Deze structuur hangt af van de eigenschappen van het oplosmiddel; zo neemt b.v. de dikte van de dubbellaag af bij toenemende zoutsterkte. De verhouding tussen de deeltjesstraal (a) en de maat voor de dikte van de dubbellaag (κ^{-1}) speelt vaak een belangrijke rol bij de theoretische beschrijvingen.

Het in dit proefschrift beschreven onderzoek heeft zich voornamelijk gericht op de relaxatie van de elektrische dubbellaag in relatie tot de dynamische eigenschappen van het kolloïd. Relaxatie van de dubbellaag treedt op wanneer zijn evenwichtsstructuur wordt verstoord, waarna het systeem weer terug naar evenwicht kan gaan. Zulke storingen komen vaak voor in de kolloïdchemie; o.a. bij vlokking als dubbellagen van verschillende deeltjes elkaar overlappen en bij toepassing van elektrokinetische technieken, waarbij een storing kunstmatig aan het kolloïd wordt opgelegd in de vorm van een elektrisch veld. Daar de respons van het kolloïd op het elektrisch veld (het elektrokinetisch gedrag) bepaald wordt door de structuur van de dubbellaag, worden deze technieken vaak gebruikt om het ladingsgedrag van de deeltjes te bestuderen. Onderzoek is verricht naar beide bovengenoemde voorbeelden.

Een belangrijke term in de elektrokinetiek is het 'afschuifvlak'. Bij een oppervlakteladingsdichtheid ongelijk aan nul ondergaan kolloïdale deeltjes een gerichte beweging onder invloed van een aangelegd elektrisch veld, de zgn. elektroforese. Vanwege hydrodynamische interactie zal een bewegend deeltje een gedeelte van zijn omringende vloeistof met zich meesleuren. Het afschuifvlak is nu gedefinieerd als het denkbeeldige vlak dat op een zekere afstand van het deeltjesoppervlak ligt en waar buiten vloeistofstroming t.o.v. het deeltje mogelijk is. De afstand van dit vlak tot de wand is meestal veel kleiner dan de dikte van de dubbellaag. De elektrische potentiaal in het afschuifvlak wordt de ζ (zeta) potentiaal genoemd. Op basis van elektroforese metingen worden vaak schattingen van deze potentiaal gemaakt.

De aangewezen elektrokinetische techniek om de relaxatie van dubbellaag om kolloïdale deeltjes experimenteel te bestuderen is laagfrequente diëlektrische relaxatie van solen in het gebied van ongeveer $10^2 - 10^5$ Hz. Simpelweg komt deze techniek er op neer dat men het verband bepaalt tussen de gemiddelde stroom- en veldsterktes in een sol als functie van de wisselveldfrequentie. Vorige onderzoeken hebben aangetoond dat latices, dit zijn solen van polymeerbolletjes, een zeer grote diëlektrische respons geven; veel groter dan men op basis van de elektroforese en theoretische overwegingen had verwacht. Het was echter niet duidelijk of de slechte overeenkomsten het gevolg waren van gebrekkige theoretische interpretaties of van de mogelijkheid dat latices, in tegenstelling tot de verwachtingen, niet zulke ideale modelsystemen vormen. Om uitsluitsel te geven waren nieuwe diëlektrische experimenten aan andere type kolloiden wenselijk. Het belangrijkste doel van dit onderzoek is om deze experimenten te verrichten en, indien noodzakelijk, de bestaande theorie verder te ontwikkelen. In de hoofdstukken 2-5 worden de behaalde resultaten beschreven.

Het tweede doel van het onderzoek is beter inzicht te verkrijgen in de relatie tussen de relaxatieprocessen in de dubbellaag en de kolloïdale stabiliteit. Hierover was nog weinig bekend, met name wanneer de relaxatietijd van de dubbellaag van dezelfde grootte orde is als de tijdschaal van interactie tussen twee kolloïdale deeltjes. Onze aandacht heeft zich toegespitst op die gevallen waarbij de relaxatietijd van de dubbellaag wordt bepaald door de snelheid van aanpassing van de oppervlakteladingsdichtheid. Dit onderwerp wordt besproken in hoofdstuk 7. In hoofdstuk 6 wordt een aan kolloïdale stabiliteit gerelateerd onderwerp behandeld.

Hieronder wordt van elk hoofdstuk een korte samenvatting van de belangrijkste resultaten en konklusies gegeven.

Hoofdstuk 2 geeft een beschrijving van een nieuw ontwikkelde 4-elektrode diëlektrische spektrometer, geschikt om de diëlektrische respons (of complexe impedantie) van solen te meten in een frequentiegebied van ongeveer 500 Hz tot 500 kHz. De 4-elektrode konstructie is

ontworpen om problemen t.g.v. elektrodepolarisatie te omzeilen en, tegelijkertijd, gebruik te kunnen maken een automatische impedantiemeter. Het instrument is met name geschikt om verschil-spektra op te nemen en het maakt het mogelijk om nauwkeurig en snel metingen te verrichten; het opnemen van een compleet spektrum kost slechts enkele minuten.

In **hoofdstuk 3** wordt beschreven hoe de dunne-dubbellaag theorie ($ka \gg 1$) voor de elektrokinetische eigenschappen van verdunde solen met bolvormige deeltjes kan worden uitgebreid met het verschijnsel 'oppervlaktegeleiding'. Met deze term wordt de bijdrage van beweeglijke ionen, gelokaliseerd binnen het afschuifvlak, aan de geleiding van het sol aangeduid. De berekeningen laten zien dat oppervlaktegeleiding leidt tot een verminderde elektroforetische beweeglijkheid en tot een verhoging van de statische geleiding en de diëlektrische respons van het sol. Bovendien blijkt het dat een eenduidige interpretatie van één elektrokinetische eigenschap van een sol, bv. de elektroforese, niet mogelijk is als oppervlaktegeleiding optreedt. Of dit het geval is zal moeten blijken uit aanvullende metingen van andere elektrokinetische eigenschappen. Experimentele gegevens uit de literatuur over latices zijn vergeleken met de uitgebreide theorie. De elektroforese en statische geleiding van polystyreen latices kunnen kwantitatief en consistent worden verklaard als oppervlaktegeleiding in rekening wordt gebracht. Voor de extreme diëlektrische toename van zulke latices is dit echter niet het geval.

In **hoofdstuk 4** worden experimentele gegevens gepresenteerd over de laag-frequente diëlektrische respons van waterige silica en hematiet (ijzeroxide) solen als functie van de zoutsterkte, pH en deeltjesstraal. De deeltjes in alle solen zijn bolvormig. De pH-afhankelijkheid van de diëlektrische respons van beide typen solen bewijst dat deze een functie is van de oppervlakteladingsdichtheid. Vergelijking met de theorie, zonder rekening te houden met eventuele oppervlaktegeleiding, geeft redelijke resultaten. De afhankelijkheid van de karakteristieke relaxatiefrequentie van de deeltjesgrootte komt redelijk goed overeen met theoretische verwachtingen. Tevens kan, in

tegenstelling tot wat voor latices geldt, het diëlektrische gedrag van zowel silica als hematiet kwantitatief worden verklaard door redelijke waarden voor de ζ potentiaal aan te nemen. Echter, deze waarden zijn systematisch hoger dan die welke werden geschat op basis van elektroforese metingen. Volgens de theorie uit hoofdstuk 3 duidt dit op de aanwezigheid van oppervlaktegeleiding. Bovengenoemde theorie is vervolgens gebruikt om de oppervlaktegeleiding te bepalen uit de combinatie van elektroforese en diëlektrische gegevens. Het blijkt dat een vrij grote fractie van de totale (beweeglijke) tegenlading binnen het afschuifvlak is gelokaliseerd, een fractie die toeneemt met de oppervlakteladingsdichtheid.

De methoden ontwikkeld in de vorige hoofdstukken zijn toegepast op een suspensie van bolvormige (corynevormige) bacteriën in **hoofdstuk 5**. De eerste resultaten tonen aan dat ongeveer 95% van de totale (beweeglijke) tegenlading in de dubbel-laag gelokaliseerd is binnen het afschuifvlak, d.w.z. waarschijnlijk in de celwand zelf. De oppervlaktegeleiding is dus erg groot waardoor het maken van schattingen van de ζ potentiaal op basis van enkel de elektroforese wordt verhinderd. Dit onderzoek laat zien dat ook bij de kolloidchemische karakterisering van bacteriën diëlektrische spektroskopie een zeer waardevolle techniek kan zijn.

Hoofdstuk 6 is gedeeltelijk een vreemde eend in de bijt: het behandelt het een onderwerp dat niet direct te maken heeft met de relaxatie van dubbellagen. Een model wordt gepresenteerd voor de berekening van de elektrostatische afstoting tussen twee kolloidale bollen waarbij rekening wordt gehouden met de polariseerbaarheid van die bollen zelf. In principe is deze polariseerbaarheid van invloed als de potentiaal langs het oppervlak varieert tijdens de interactie, b.v. onder de omstandigheden welke worden besproken in hoofdstuk 7. Resultaten worden gegeven voor de wisselwerking tussen bollen met een constante oppervlakteladingsdichtheid. De berekeningen laten zien dat de elektrostatische afstoting afneemt als de polariseerbaarheid toeneemt; de afname wordt sterker met afnemende onderlinge afstand en is relatief ongevoelig is voor de waarde van κ_a . Deze ongevoeligheid wordt

veroorzaakt door zijdelingse afscherming in het deeltje zelf. Tevens wordt er op gewezen dat voor langzaam vlokkende solen met deeltjes met een constante oppervlaktelading de kolloidale stabiliteitsfactor W gevoelig is voor deze vorm van polarisatie.

Kortstondige afwijkingen van de oppervlakteladingsdichtheid uit evenwicht tijdens de wisselwerking tussen kolloidale deeltjes en hun invloed op de stabiliteit van kolloiden worden besproken in hoofdstuk 7. Door het optreden van zulke afwijkingen kan het vlokproces niet meer worden beschreven als een eerste-orde Markov proces. Dit bemoeilijkt de berekening van de kolloidale stabiliteit. Twee modellen worden beschreven die, binnen een zekere benadering, een gemodificeerde kolloidale stabiliteitsfactor uitrekenen waarbij met bovengenoemde afwijkingen rekening wordt gehouden. Het wezenlijke verschil tussen beide modellen ligt in de gemaakte aanname voor de tijdschaal τ_{int} van interaktie tussen twee kolloidale deeltjes en zijn afhankelijkheid van de hoogte van de energiebarrièrē. Berekeningen met beide modellen laten zien dat de dynamika van de elektrische dubbellaag sterk van invloed kan zijn op de stabiliteit. Echter, de modellen verschillen sterk in hun voorspellingen t.a.v. de invloed van de deeltjesstraal op de stabiliteitsfactor van langzaam vlokkende solen. Dit duidt er op dat dubbellaag-dynamika de experimenteel gevonden ongevoeligheid van de stabiliteitsfactor voor de deeltjesstraal zou kunnen verklaren, op voorwaarde dat τ_{int} een sterk stijgende functie is van de hoogte van de energiebarrièrē. Aan deze voorwaarde wordt in de praktijk waarschijnlijk niet voldaan. Volgens een eenvoudige statistische analyse zou de tijdschaal van interaktie een (zwak) dalende functie van de barrièrehogte moeten zijn!

Samenvattend kan gekonkludeerd worden dat het in dit proefschrift beschreven experimentele en theoretische onderzoek aan dubbellaagrelaxatie van kolloiden niet alleen van academische maar ook van praktische betekenis is. De verkregen resultaten vormen een bemoedigend uitgangspunt voor verder onderzoek op het gebied van elektrokinetiek en stabiliteit van kolloiden.

Curriculum Vitae

De auteur werd op 8 januari 1963 in Enschede geboren. In 1981 behaalde hij het Atheneum diploma aan de Rijksscholengemeenschap te Lochem. In hetzelfde jaar begon hij aan de studie Molekulaire Wetenschappen aan de toenmalige Landbouwhogeschool te Wageningen. Na het volgen van de fysisch-chemische oriëntatie studeerde hij af in januari 1988. Het doktoraalpakket bestond uit een hoofdvak fysische chemie en de bijvakken molekulaire fysika en wiskunde. De stage werd vervuld bij het onderzoekslaboratorium van "Eastman Kodak Company" te Rochester, New York. Van maart 1988 tot maart 1992 werkte hij als onderzoeker in opleiding (o.i.o.) in dienst van N.W.O. (S.O.N.) bij de vakgroep Fysische en Kolloidchemie van de Landbouwuniversiteit te Wageningen. In deze periode is het in dit proefschrift beschreven onderzoek uitgevoerd. Vanaf 1 oktober 1992 is hij werkzaam bij Bayer AG te Leverkusen, Duitsland.

Nawoord

Een engelse collega zei eens dat een goede onderzoeker zich eenzaam voelt op zijn vakgebied. Als kritische lezer zal u de algemeenheid van deze uitspraak wel in twijfel trekken. Anderen zullen zich wellicht afvragen in hoeverre deze van toepassing is op ondergetekende. Daarom het volgende. Wat betreft de kwalifikatie "goed" laat ik het antwoord aan u, tenslotte is dit pagina 137 en heeft u inmiddels het hele proefschrift doorgeworsteld. Ongeacht uw oordeel heb ik me echter bij het verrichten van dit onderzoek op meerdere momenten eenzaam gevoeld: o.a. bij het oplossen van sommige problemen, bij het uitblijven van resultaten en als een goed idee toch niet zo goed bleek te zijn. Gevoelens zijn echt maar niet altijd gegrond. Eenzaam ben ik niet geweest. Integendeel, veel mensen hebben in meerdere of mindere mate enthousiast bijgedragen aan de totstandkoming van dit boekje, zowel in wetenschappelijke als in niet-wetenschappelijke zin. Enkelen wil ik hier met name noemen.

Mijn promotor en co-promotor hebben mij een grote speelruimte gegeven waar ik dankbaar gebruik van heb gemaakt. Herman stond altijd open voor mijn gedachtenkronkels, om er uiteindelijk in de vorm van een woordgrapje er nog één aan toe te voegen. Hans heeft vooral in de afrondingsfase zijn vakmanschap getoond door snel en kritisch mijn werk te bekomenntariëren. Met plezier kijk ik terug op de samenwerking met hen in de afgelopen leerzame jaren.

Op experimenteel gebied heb ik met name veel steun gehad aan Ronald Wegh. Hij heeft me laten zien hoe je complexe stromen kunt meten, stromen waarvan ik, in den beginne, nauwelijks wist dat ze bestonden. De ontwikkeling van de diëlektrische cel is voornamelijk aan hem te danken, waarvoor hij, met de hulp van Rob Vullings, ook de elektronika heeft verzorgd. Hennie van Beek en Louis Verhagen van de werkplaats hebben, naast vele andere klusjes, het huis van de cel gemaakt.

Zonder solen geen experimenten. De synthese van met name de hematiet-solen ging niet zonder problemen. Gelukkig heeft Wim

Threels me daarbij uit de brand geholpen. Ab van der Linde heeft me o.a. bij de elektroforese-metingen ondersteund.

Ondersteuning op het gebied van computers werd verkregen vanuit de polymeerhoek. Peter Barneveld is hiervoor nu de verantwoordelijke en, volgens mij, met succes. Zonder zo'n persoon vaart geen "computer-gestuurde" vakgroep wel.

Binnen de vakgroep vervulden een aantal andere personen voor mij een speciale rol. De interaktie met doktoraalstudent Adri Minnaard is zeer nuttig gebleken en dankzij Bert van der Wal noem ik mezelf (als het me uitkomt) biotechnoloog. Van mijn plezierige kamergenoot Klaas Besseling stak ik veel op als hij zijn heldere gedachten ventileerde. Luuk Koopal ben ik niet alleen dankbaar voor de wetenschappelijke discussies. De snelle levering van een deugdelijke bureaustoel verdient bewondering en ook zijn internationale wetenschappelijke kontakten waardeer ik zeer.

I am indebted to many persons outside our department for helpful discussions and suggestions or to those who made my wanderings in the scientific world more pleasant. Some of them I want to mention personally: J. Dhont, S. S. Dukhin, R. W. O'Brien, T. Odijk, J. P. M. van der Ploeg, D. A. Saville and L. R. White.

Wat betreft het niet-wetenschappelijke vlak: de prettige sfeer op het lab zorgde ervoor dat er weinig dagen waren dat ik met tegenzin de berg op fietste. Die fiets was slechts één onderdeel van het pakket dat ik heb meegekregen van mijn familie en welke mij in staat stelt steeds nieuwe wegen in te slaan. Zij kijken echter wel (op afstand) toe en zijn niet te beroerd om onverhullend commentaar te leveren. Zo oefenden zij een relativerende invloed uit met hun gezond gebrek aan "respekt" voor het wetenschappelijke wereldje.

Geniet er van,

Johan